DISSERTATIONES
MEDICINAE
UNIVERSITATIS
TARTUENSIS
360

CELIA TERESA POZO RAMOS

Preparation and assessment of antimicrobial electrospun matrices for prospective applications in wound healing

DISSERTATIONES MEDICINAE UNIVERSITATIS TARTUENSIS
360

DISSERTATIONES MEDICINAE UNIVERSITATIS TARTUENSIS
360

CELIA TERESA POZO RAMOS

Preparation and assessment of antimicrobial electrospun matrices for prospective applications in wound healing

UNIVERSITY OF TARTU
Press
1632

Institute of Pharmacy, Faculty of Medicine, University of Tartu, Estonia

Dissertation is accepted for the commencement of the degree of Doctor of Philosophy (in Pharmacy) on 20.03.2024 by the Council of the Faculty of Medicine, University of Tartu, Estonia.

Supervisors: Professor Karin Kogermann, PhD
Institute of Pharmacy, Faculty of Medicine
University of Tartu, Estonia

Professor Tanel Tenson, PhD
Institute of Technology, Faculty of Science and Technology
University of Tartu, Estonia

Associate Professor Ivo Laidmäe, PhD
Institute of Pharmacy, Faculty of Medicine
University of Tartu, Estonia

Marta Putrinš, PhD
Institute of Pharmacy, Faculty of Medicine
University of Tartu, Estonia

Reviewed by: Professor Angela Ivask
Institute of Molecular and Cell Biology,
Faculty of Science and Technology
University of Tartu, Estonia

Professor Reet Mändar
Institute of Biomedicine and Translational Medicine,
Faculty of Medicine
University of Tartu, Estonia

Opponent: Professor Hanne Mørck Nielsen
Center for Biopharmaceuticals and Biobarriers in Drug Delivery
Department of Pharmacy
University of Conpenhagen, Denmark

Commencement: May 10, 2024

ISSN 1024-395X (print) ISSN 2806-240X (pdf)
ISBN 978-9916-27-493-4 (print) ISBN 978-9916-27-494-1 (pdf)

University of Tartu Press
www.tyk.ee

“There’s plenty of room
at the bottom”

Richard Feynman

CONTENTS

LIST OF ORIGINAL PUBLICATIONS

This thesis is based on the following original publications referred to in the text by Roman numerals (I–III):

I. **Celia Ramos***, Georg-Marten* Lanno, Ivo Laidmäe, Andres Meos, Riinu Härmas and Karin Kogermann. 2020. High humidity electrospinning of porous fibers for tuning the release of drug delivery systems. *International Journal of Polymeric Materials and Polymeric Biomaterials*. 70, 880–892.
https://doi.org/10.1080/00914037.2020.1765361
* Equal contribution to this publication.

II. Georg-Marten Lanno, **Celia Ramos**, Liis Preem, Marta Putrinš, Ivo Laidmäe, Tanel Tenson and Karin Kogermann. 2020. Antibacterial Porous Electrospun Fiber as Skin Scaffolds for Wound Healing Applications. *ACS Omega* 5, 30011–30022.
https://doi.org/10.1021/acsomega.0c04402

III. **Celia Ramos**, Kairi Lorenz, Marta Putrinš, Charlotte K. Hind, Andres Meos, Ivo Laidmäe, Tanel Tenson, J. Mark Sutton, A. James Mason and Karin Kogermann. 2024. Fibrous matrices facilitate pleurocidin killing of wound associated bacterial pathogens. *European Journal of Pharmaceutical Sciences*. 192, 106648.
https://doi.org/10.1016/j.ejps.2023.106648.

Contribution of Celia Ramos to original publications (I–III):

I. Electrospinning of the fibers, determination of diameter and surface topography, attenuated total reflection Fourier transformed infrared spectroscopy, and thermal analysis. Participation in data analysis and cowriting the article.

II. Participation in study design, electrospinning of the fibers, determination of diameter and surface topography, fibroblast cell attachment and growth, and bacterial and biofilm studies. Participation in data analysis and cowriting the article.

III. Participation in study design, peptides purification, and bacterial studies (pleurocidin activity in solution and within fiber matrices, biocides activity, synergism behaviour between pleurocidin and biocides). Participation in data analysis and cowriting the article.

ABBREVIATIONS

AA	Acetic Acid
ACE	Acetone
AFM	Atomic Force Microscope
AIC	Akaike Informative Criterion
AMP	Antimicrobial Peptide
AMR	Antimicrobial Resistance
ASAP	Accelerated Surface Area and Porosimetry System
ATR	Attenuated Total Reflection
ATR-FTIR	Attenuated Total Reflection Fourier Transformed Infrared Spectroscopy
BHK	Baby Hamster Kidney
CAM	Chloramphenicol
CF	Chloroform
CFM	Confocal Fluorescence Microscopy
CFU	Colony Forming Unit
DCM	Dichloromethane
DMEM	Dulbecco's Modified Eagle's Medium
DMSO	Dimethyl Sulfoxide
DSC	Differential Scanning Calorimetry
ECM	Extracellular Matrix
EPS	Extracellular Polymeric Substances
ESBL	Extended Spectrum Beta-Lactamase
ESKAPE	*Enterococcus faecium, Staphylococcus aureus, Klebsiella pneumoniae, Acinetobacter baumannii, Pseudomonas aeruginosa* and *Enterobacter* species.
FA	Formic Acid
FBS	Fetal Bovine Serum
FDA	Food and Drug Administration
FIC	Fractional Inhibitory Concentration
FTIR	Fourier Transformed Infrared Spectroscopy
GBD	Global Burden of Disease
GMEM	Glasgow Minimal Essential Medium
GMP	Good Manufacturing Practice
HEPES	4-(2-hydroxyethyl)-1-piperazineethanesulfonic acid
HPLC	High Performance Liquid Chromatography

IC_{50}	Half-maximal Inhibitory Concentration
ISO	International Organization for Standardization
IR	Infrared Spectroscopy
LB	Lysogeny Broth
MHB	Mueller-Hinton Broth
MIC	Minimum Inhibitory Concentration
NCTC	British National Collection of Type Cultures
OD_{600}	Optical Density at 600nm
PBS	Phosphate Buffered Saline
PCL	Polycaprolactone
PCR	Polymerase Chain Reaction
PVA	Polyvinyl Alcohol
PVP	Polyvinyl Pyrrolidone/ Povidone
PVP-iodine	Povidone iodine
QAC	Quaternary Ammonium Compound
R&D	Research and Development
RH	Relative Humidity
RT	Room Temperature
S_{BET}	Specific Surface Area
SD	Standard Deviation
SEM	Scanning Electron Microscopy
TEM	Transmission Electron Microscopy
TFA	Trifluoroacetic Acid
T_g	Transition Temperature
THF	Tetrahydrofuran
T_m	Melting Temperature
TPS	Tryptose Phosphate Broth
V/V	Volume per volume
w/V	Weight per volume
w/w	Weight per weight
XRD	X-Ray Diffraction

1. INTRODUCTION

The incidence of acute and chronic wounds is high and progressively escalating (Martinengo et al., 2019). Living with non-healing wounds constitutes an important burden to patients as well as to the healthcare systems, which earmark many funds to cover their treatment expenses (Lindholm and Searle, 2016).

Probably the main pillar for the treatment of wounds is the control of the infection that occurs or may occur when the skin barrier is broken. Debridement is the cornerstone of wound care; it involves the cleaning of the wound preparing it for the administration of topical drugs (Anghel et al., 2016). However, conventional topical therapeutic formulations (creams, gels, solutions, etc.) encounter many efficacy problems due to the presence of wound exudate. Systemic antibiotics are also employed; nonetheless, this administration route comes with toxicity issues which may restrain its use (Eriksson et al., 2022). Besides the drug formulation, another critical challenge for wound healing therapeutics is the development of antimicrobial resistance (AMR) (Probst et al., 2022). In recent years, the availability of antimicrobial drugs has diminished as AMR is exponentially growing. This dissertation was aimed to address both issues by proposing a novel drug delivery system to enhance the efficacy of antimicrobial substances.

An antibiotic, chloramphenicol (CAM), and various antimicrobial peptides (AMPs) were selected to investigate their action against different wound pathogens. Besides, AMP combinations with biocides, widely used for wound cleaning, were assessed. Pleurocidin was selected as a relatively novel AMP with a broad mechanism of action, making it a promising alternative to antibiotics against multiresistant bacteria and potentially hindering the development of AMR.

Moreover, CAM and pleurocidin have been separately incorporated into a novel drug delivery system as an approach to overcome current low efficacy and toxicity issues encountered by conventional therapies. Wound dressings, developed using electrospinning, are defined by their nanotechnology approach, where fibers on the nanoscale are collected together in a nonwoven matrix. This fabrication method allows the incorporation of active drug substances, improving their stability and controlling their release (Yarin, 2011). Moreover, the physicochemical features of electrospun matrices such as their high surface area to volume ratio, mechanical properties, and high porosity contribute to and sustain a good moisture balance, absorbability, and gas-exchange in the wound, promoting its healing (Leaper et al., 2014; Muthukrishnan, 2022).

In the present thesis, antimicrobial matrices have been developed and characterised using *in vitro* experiments as an initial step in understanding their fabrication and their ability to combat wound pathogens. This dissertation identifies certain limitations but also introduces a new strategy that will be studied further, with the hope of ultimately incorporating these matrices as a new therapeutic option for wound healing applications.

2. LITERATURE REVIEW

2.1. Wounds

The incidence of chronic wounds and other skin diseases is high and increasing (Vos et al., 2016). A recent study has defined the prevalence of chronic wounds of mixed aetiologies in the general population as 2.21 per 1000 population (Martinengo et al., 2019). Including chronic and acute wounds, it is estimated that 1.5–2 million people in Europe suffer their consequences (Lindholm and Searle, 2016).

Living with chronic wounds profoundly affects the quality of life of a person, causing pain, distress, social isolation, anxiety, chronic morbidity, and even mortality. This is an enormous burden that is added to the economic strain on healthcare systems to cover their treatment expenses (Lindholm and Searle, 2016).

This section delineates the physiology of healthy skin to understand wound formation, identifies key microorganisms involved in wound infections, discusses factors contributing to the development of non-healing wounds, and outlines current treatment options.

2.1.1. Wound healing physiology

The skin, being the largest organ in the body, serves as a huge physical and chemical barrier, preventing the entry of pathogens and noxious chemicals while also regulating the loss of water and other substances. Besides, it performs other functions such as temperature regulation, sensory perception, vitamin D synthesis, and the release of nitric oxide (Weller et al., 2015).

The outermost layer of the skin, the epidermis, is impermeable. Keratinocytes make up about 85% of cells in the epidermis. Their life cycle and relation with the environment create different layers or strata. Additionally, the epidermis also contains sebaceous glands, sweat glands, and hair follicles. Supporting the epidermis structurally, the dermis provides nutrients to the skin. Fibroblasts are the predominant cells found in the dermis, a layer rich in extracellular matrix (ECM) where collagen makes up to 70–80% of its dry weight. Beneath the dermis lies the subcutaneous adipose tissue, serving as an energy reserve. In addition, each layer contains immune cells that play a vital role in protecting against infection (Habif, 2015; Rodrigues et al., 2019; Weller et al., 2015).

A wound occurs when the structural and functional integrity of the skin and/or its underlying tissues is compromised. When this occurs, different physiological pathways activate wound healing. Haemostasis, inflammation, proliferation, and remodelling are the phases that a wound must overcome in order to heal completely. However, in certain instances, wound progression deviates from the norm, resulting in a cessation of the healing process, often during the inflammatory phase. Should a wound persist without healing for a duration exceeding 4 weeks, it may be classified as chronic (Eriksson et al., 2022).

The first stage of wound healing is haemostasis. It begins with vasoconstriction which reduces bleeding from injured vasculature. Afterwards, the exposed thrombogenic endothelial matrix binds platelets and causes integrin activation and attachment to other platelets and surrounding ECM. The activated platelet plug mechanically seals the blood vessel and establishes the so-called primary haemostasis. Secondary haemostasis begins with the activation of factor X through an intrinsic or extrinsic pathway. This leads to a molecular cascade that ends with the formation of fibrin, which binds the aggregated platelet plug forming a thrombus (Rodrigues et al., 2019).

The second phase of wound healing is inflammation. During this phase, the recruitment and activation of different cells occur. Neutrophils, macrophages, and other cells such as mast cells and dendritic cells, migrate to the wound and release chemokines, growth factors, and other molecules that modulate inflammation and combat pathogens (Rodrigues et al., 2019).

The proliferation and re-epithelization stage begins concurrently with inflammation. This stage involves a migration and activation loop that enhances angiogenesis, as well as the recruitment and proliferation of fibroblasts and keratinocytes. Initially, fibroblasts synthesize ECM to form granulation tissue, which is gradually replaced by normal connective tissue during re-epithelization (Rodrigues et al., 2019).

Regeneration of the skin is a gradual but interconnected process that includes many molecules and pathways. One of the most common reasons for the development of non-healing wounds is a pathogenic infection that disturbs the normal process. The longer a wound persists, the greater the likelihood of contamination, colonization, and subsequent infection development.

2.1.2. Wound infection

The skin harbors a multitude of bacteria, collectively forming a complex ecosystem. Major phyla found on the skin include Actinobacteria (36-51%), Firmicutes (24–34%), Proteobacteria (11-16%), and Bacteroidetes (6-9%). Dry areas of the skin exhibit the highest diversity, with a varied colonization of these phyla. Conversely, moist and oily areas tend to have elevated levels of specific bacteria. *Staphylococcus* (Firmicutes) and *Corynebacterium* (Actinobacteria) are prevalent in moist areas, while oily regions are dominated by *Cutibacterium* (Actinobacteria) species (Carmona-Cruz et al., 2022).

Under normal conditions of the skin these bacteria should not cause skin infections, although this is possible and fairly common in some cases, e.g., acne caused by *Cutibacterium* (Mayslich et al., 2021; Weller et al., 2015).

The majority of chronic wounds are infected by more than a single microbe, usually by groups of bacteria (both aerobes and anaerobes (Brook, 1992)), and/or fungi (Dowd et al., 2011). All these microorganisms frequently establish a biofilm, regulated via quorum sensing, where the bacteria interact to coordinate different parameters such as microbial growth rates, enzyme and toxin production, and even AMR. This communication and successful evasion of the

immune system ultimately promotes a chronic inflammatory state and delays wound healing (Percival et al., 2014). Therefore, the variety of microorganisms found in a wound is usually higher the longer the wound has been present. The most common species in wound infection are Gram-negative bacteria: *Pseudomonas aeruginosa, Escherichia coli, Proteus mirabilis, Klebsiella pneumoniae,* and *Acinetobacter baumannii;* and *Staphylococcus aureus* as the main representative of Gram-positive bacteria (Puca et al., 2021).

2.1.3. Wound treatment

The cornerstone of effective wound care is debridement, a process vital for removing necrotic tissue, slough, and bioburden. By cleaning the wound through debridement, angiogenesis and re-epithelialization are promoted, topical drug formulations become more effective, and the risk of sepsis is reduced. Debridement plays a crucial role in disrupting biofilms, maintaining bacterial cells in a metabolically active state during the reformation after debridement, and preventing them from maturing into a more resilient biofilm. This process increases the effectiveness of antibiotics, as many of them target metabolic machinery or cell wall synthesis directly associated with bacterial growth and metabolism. A window of increased antibiotic sensitivity lasting 24-48 hours post-debridement has been observed for wound biofilms. Surgical debridement is commonly employed, although alternative techniques such as larval therapy can also be utilized (Anghel et al., 2016; Wolcott et al., 2010).

In addition to debridement, other treatments are usually necessary to control infections and promote wound healing. Bioburden presents a clinically significant barrier to healing in all chronic wounds (Cadogan et al., 2011). To plan an optimal treatment approach, the use of molecular diagnostics such as polymerase chain reaction (PCR) is highly recommended for identifying and addressing all different microorganisms present in the wound. This strategy can increase the healing odds up to 200 % (Dowd et al., 2011). While systemic antibiotics and topical antimicrobials remain the main pharmaceutical formulations used to treat wound infections, they have limitations such as toxicity to humans and low efficacy that will need to be addressed in future formulations (Eriksson et al., 2022).

Wounds need to be protected from contamination and provided with physical support while promoting healing, and this can be performed using dressings. For effective healing, the dressing should have appropriate moisture management and fulfil a list of requisites depending on the wound (Eriksson et al., 2022).

Chronic wounds or other wounds that are difficult to heal may be eligible for alternative treatment strategies. Negative pressure wound therapy, grafting, and hyperbaric oxygen are among those that aim to speed up wound healing and reduce the number of complications (Eriksson et al., 2022). However, each wound requires specific treatment, and no ideal single treatment is usually possible.

2.2. Antimicrobial resistance

The treatment of wounds and many other diseases has become arduous in recent years due to the development of AMR. AMR is a natural phenomenon that occurs when microorganisms are exposed to antimicrobial drugs. Under this stress, susceptible bacteria are inhibited or killed, while other bacteria are resistant and the stress does not, or barely, affect them. The resistance mechanisms may be intrinsic or may have been acquired (Prestinaci et al., 2015). AMR mechanisms can be classified into several categories, including drug inactivation, modification of drug binding targets, changes in cell permeability, and biofilm formation (Santajit and Indrawattana, 2016). The spread of AMR within different bacteria frustrates traditional treatments, increasing mortality and aggravating many diseases.

2.2.1. General perspective

A quite comprehensive article has recently been published in The Lancet analysing the global burden of AMR (Murray et al., 2022). This analysis shows that, in 2019, there were a total of 1.27 million deaths directly attributable to AMR and 4.95 million deaths associated with AMR. Being the third leading Global Burden of Disease (GBD) Level 3 cause of death, only ischaemic heart disease and stroke accounted for more deaths that year.

The variety of bacteria that present AMR is expanding, causing attributable and associated deaths that are shown in **Figure 1**. The leading pathogens, identified as priority pathogens by the World Health Organisation (WHO) are *Escherichia coli, Staphylococcus aureus, Klebsiella pneumoniae, Streptococcus pneumoniae, Acinetobacter baumannii,* and *Pseudomonas aeruginosa* (Murray et al., 2022).

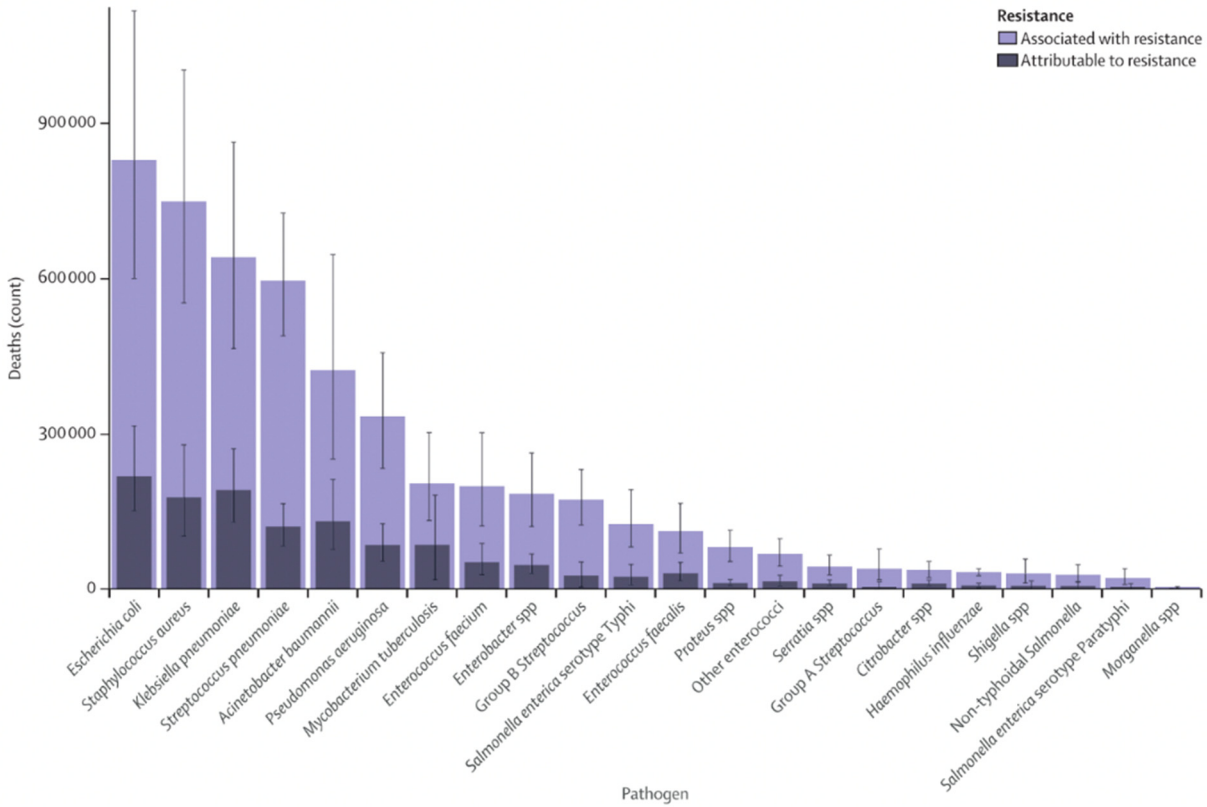

Figure 1. Global deaths (counts) attributable to and associated with bacterial AMR by pathogens, 2019. Estimates were aggregated across drugs, accounting for the co-occurrence of resistance to multiple drugs. Error bars show 95% uncertainty intervals. Figure from Murray et al., 2022 (open access permitting reproduction).

A considerable amount of information has been published regarding AMR and its causes and consequences, which are beyond the scope of this work (Abushaheen et al., 2020; Michael et al., 2014; Prestinaci et al., 2015). Moreover, many guidelines on how to treat these bacteria have been written and need to be updated frequently while levels of AMR keep increasing (Paul et al., 2022; Terreni, 2021).

The future perspective for AMR is complicated but an improvement is possible. The solutions need to be based on a combination of prevention measures and an increase in research and development (R&D) of new antimicrobial molecules. In order to spur governments to put policies in place to incentivize R&D, WHO has published a list of bacteria for which new antibiotics are urgently needed (World Health Organization, 2017). This list is adapted and shown in **Table 1**.

Table 1. Resistant bacteria in urgent need of new antibiotic development. Key: !!! = Critical, !! = High, ! = Medium. ESBL = Extended Spectrum Beta-Lactamase.

Priority	Pathogen	Resistance
!!!	*Acinetobacter baumannii*	Carbapenem-resistant
!!!	*Pseudomonas aeruginosa*	Carbapenem-resistant
!!!	*Enterobacteriaceae*	Carbapenem-resistant, ESBL-producing
!!	*Enterococcus faecium*	Vancomycin-resistant
!!	*Staphylococcus aureus*	Methicillin-resistant, Vancomycin-intermediate and resistant
!!	*Helicobacter pylori*	Clarithromycin-resistant
!!	*Campylobacter* spp.	Fluoroquinolone-resistant
!!	*Salmonella*	Fluoroquinolone-resistant
!!	*Neisseria gonorrhoeae*	Cephalosporin-resistant, Fluoroquinolone-resistant
!	*Streptococcus pneumoniae*	Penicillin-non-susceptible
!	*Haemophilus influenzae*	Ampicillin-resistant
!	*Shigella* spp.	Fluoroquinolone-resistant

2.2.2. AMR found in wounds

Unfortunately, most of the pathogens found in wounds belong to the so called "ESKAPE" cluster, composed by *Enterococcus faecium, S. aureus, K. pneumoniae, A. baumannii, P. aeruginosa* and *Enterobacter* species. These microorganisms originally identified in hospital settings are notorious for their frequent occurrence and association with AMR (Rice, 2008). The specific antibiotic resistances commonly observed in each of these pathogens are detailed in **Table 1**.

As mentioned above, chronic wounds are usually infected by these bacteria, which are able to form a biofilm. This environment is ideal for the development of AMR due to the difficulty of drug penetration caused by the extracellular polymeric substances (EPS) that form the biofilm matrix. This lowers the therapeutical concentration of drugs interacting with bacteria, allowing for bacterial adaptation. Moreover, the biofilm permits the accumulation of genetic elements through the lysis of heterogeneous species, which facilitates the transmission of AMR genes through horizontal gene transfer (Goel et al., 2021).

Fortunately, there are still some therapeutic options: amikacin and meropenem are the most effective antibiotics against Gram-negative bacteria, whereas vancomycin appears to be the most effective antibiotic for Gram-positive ones (Puca et al., 2021). However, it is important to continue the R&D of new antibacterial molecules and find novel local drug delivery approaches to improve the efficacy of antimicrobial substances.

2.3. Antimicrobial agents for the treatment of wound infections used in this dissertation

2.3.1. Antibiotics

From very early years, ancient civilizations have used many remedies to overcome bacterial wound infections. Honey, herbs, mouldy bread and even animal faeces were the substances that were used in ancient Egypt, China, Serbia, Greece and Rome (Gould, 2016). Since then, many important discoveries in microbiology have led to the development of more effective and defined antibacterial molecules named as antibiotics.

The choice of antibiotic treatment for wound infection highly depends on the specific pathogens present in the wound and their AMR profiles. Current guidelines, which account for the prevalence of AMR (including pathogens resistant to third-generation cephalosporins and carbapenems) recommend the use of the latest antibiotics or antimicrobial molecules developed and the use of combination treatments (Paul et al., 2022). However, it is expected that new AMR will develop against these novel treatments. In the meantime, further R&D efforts are necessary for antimicrobial molecules, including the reevaluation of molecules that were used in the past but where their application was reduced due to issues

such as toxicity (World Health Organization, 2017). Modifying drug formulations can mitigate systemic toxicity concerns when applied topically, as demonstrated by chloramphenicol which has also been retrieved (Drago, 2019).

2.3.1.1. Chloramphenicol

Chloramphenicol (D-(-)-threo-1-*p*-nitrophenyl-2-dichloroacetamido 1,3-propanediol, CAM) is a broad-spectrum antibiotic originally isolated from *Streptomyces venezuelae* in 1947 (**Figure 2**). This molecule binds to the 50S ribosomal subunit of the 70S ribosome, interfering with peptidyl transferase and thus, inhibiting peptide bond synthesis and the formation of bacterial ribosomes (Shen et al., 2018; Yunis, 1988).

Its biological activity is closely related to its chemical structure. The primary alcohol at carbon 3 of the propanediol chain, the dichloroacetyl moiety and the *p*-NO2 group are responsible for the correct binding to its target, although some of them can be replaced by functional groups with similar characteristics (Yunis, 1988).

The clinical use of CAM was reduced due to its association with toxic effects when administrated systemically (i.e. hematotoxicity). However, in recent years, enhanced by strategies on AMR, CAM has been reconsidered as an antibacterial therapy (Drago, 2019). Besides, using this drug topically, it is possible to reduce its toxicity while ensuring high concentrations at the infection site. A single dose of CAM produces a relative reduction in wound infection rate of 40% (Heal et al., 2009).

This molecule has been proven to be of great potential for topical wound and ocular treatment, although special care must be taken as hypersensitivity reactions have been described (Drago, 2019; Livingston et al., 2013).

CAM remains active against a variety of bacterial pathogens, including those resistant to multiple antimicrobial agents. However, the most prevalent mechanisms of CAM resistance involve well-documented functions such as enzymatic inactivation, efflux pumps, and ribosome protection (Crofts et al., 2019).

2.3.2. Antimicrobial peptides

Antimicrobial peptides (AMPs) are natural molecules, found in different organisms that present antimicrobial properties. Furthermore, not only are they able to directly fight pathogens, but they are also involved in other processes such as immune response, inflammation, and angiogenesis. For this reason, they are often referred to as host defence peptides (Gera et al., 2021; Patel and Akhtar, 2017).

Based on their amino acid composition, AMPs have an amphiphilic nature, with hydrophobic and hydrophilic moieties. Most of them are cationic and can vary in size up to 600 amino acids (Patel and Akhtar, 2017).

AMPs have aroused huge interest in recent years due to their potential ability to overcome AMR. AMPs have a broad mechanism of action, mainly involving

membrane disruption and genetic material damage. This unspecific target prevents bacteria from adapting and resisting the stress caused by AMPs. Besides, AMPs are potent but fragile killing molecules that are rapidly effective in a small dose but are degraded in contact with the environment (e.g. temperature, humidity, pH) thus, their spread in water and soils is rare, while common antibiotics reach different environments, spreading AMR (Miao et al., 2021). Thus, AMPs are good alternatives to antibiotics. Besides, their antimicrobial, anti-inflammatory, angiogenesis, cell migration, and proliferation promotion, provide a great combination of mechanisms useful to fight against infections and promote wound healing (De Souza et al., 2022).

In this dissertation, different AMPs were selected and tested for their antimicrobial properties and their potential to be formulated into electrospun fibrous dressings for wound healing applications. Namely, pleurocidin, D-pleurocidin-KR and temporin B L1FK (**Table 2**).

2.3.2.1. Pleurocidin and analogues

Pleurocidin was first characterised in 1997, isolated from the winter flounder fish (*Pleuronectes americanus*). It is 25 amino acids long and presents an alpha-helical conformation (Cole et al., 1997). This peptide binds and disrupts bacterial membranes and also penetrates them to interact with intracellular targets, inhibiting the synthesis of DNA, RNA, and proteins (Patrzykat et al., 2002). Its enantiomer, D-pleurocidin, has been created to overcome the enzymatic degradation produced by proteases and it has been proven to have lower haemolytic activity than the L-form, although its antibacterial activity may diminish. Fortunately, D-pleurocidin is still a potent antibacterial agent (Lee and Lee, 2008).

D-pleurocidin-KR is another synthetic AMP obtained by modifying pleurocidin (Manzo et al., 2020). It is the result of substituting all four lysine residues with arginines. These lysine residues in pleurocidin are crucial for forming an extended alpha-helix, and their absence in D-pleurocidin-KR results in greater conformational flexibility. Besides, arginine residues promote increased hydrogen bonding between the peptide and the lipid headgroups. Both factors contribute to a much higher penetration of the hydrophobic core, inducing greater disorder compared to pleurocidin (Manzo et al., 2020).

2.3.2.2. Temporins

Temporins were initially isolated from the skin mucus of the European common frog *Rana temporaria*. Temporin B L1FK is an analogue of temporin B that was synthesised on the basis of retaining the features that could infer in the membrane interaction, however, this peptide has proven to be more potent against bacterial pathogens, specifically Gram-negative bacteria, than its parent peptide (Grassi et al., 2017).

Table 2. The amino acid sequence of antimicrobial peptides (AMPs) used. Key: Bold and underlined letters indicate the substitutions compared to the parent peptide.

Peptide	Sequence
Pleurocidin	GWGSFFKKAAHVGKHVGKAALTHYL
Pleurocidin-KR	GWGSFF**RR**AAHVG**R**HVG**R**AALTHYL
Temporin B L1FK	FLPIVGLLKSLLK

2.3.3. Biocides

Biocides are antimicrobial molecules widely used in disinfectants and antiseptics. These chemical agents are distinguished from antibiotics by the fact that they act on a broad spectrum of microorganisms and their cellular targets usually are not as specific, acting on multiple sites (Mcdonnell and Russell, 1999). Their wider activity prevents the development of AMR, or at least limits resistance to a narrower range compared to antibiotics. However, resistance mechanisms to biocides may occur and they must be investigated as these molecules may stop being effective or, even worse, cause cross-resistance with antibiotics (Meade et al., 2021). All biocides used in this work (chlorhexidine digluconate, benzalkonium chloride, silver nitrate, silver sulfadiazine, octenidine dichloride, and povidone iodine) are used for wound infection as a conventional topical treatment (European Wound Management Association (EWMA), 2006). A summary of these biocides, including their chemical structure and antimicrobial action mechanisms, are given in the following paragraphs.

2.3.3.1. Chlorhexidine digluconate

1,6-*bis*(4'-chlorophenylbiguanide) hexane or chlorhexidine is a bisbiguanide introduced in 1954 as an antiseptic hand scrub and wounds irrigator (J.-Y. Maillard et al., 2021). It carries two cationic groups, separated by a hydrophobic structure, which reacts with the negatively charged microbial cell surface, thereby destroying the integrity of the cell membrane (**Figure 2**). The hydrophobic moiety is six carbons long and somewhat inflexible thus it is not able to interdigitate through the bilayer. Their mechanism of action is based on the bridges formed between each biguanide and pairs of adjacent phospholipid headgroups (Gilbert and Moore, 2005).

Resistance mechanisms against chlorhexidine based on efflux pumps have been described to cause cross-tolerance and cross-resistance to relatively new antibiotics such as imipenem or cefepime (J.-Y. Maillard et al., 2021).

2.3.3.2. Benzalkonium chloride

Benzalkonium chloride is always a mixture of n-alkyldimethylbenzyl ammonium chlorides where the n-alkyl groups can be of variable length within a specified range (**Figure 2**). It is a monocationic antimicrobial agent, specifically a mono-quaternary ammonium compound (QAC). These molecules have their mechanism of action on the interaction of their positive charge with the negatively charged cell membrane. The hydrophobic tail then interdigitates into the membrane core, losing its integrity and releasing all the cell contents, hence explaining their designation as biological detergents (Gilbert and Moore, 2005).

The QACs have been actively deployed since the 1930s, although their effectiveness is still good due to the high doses used. Different mechanisms of resistance against these compounds have been described such as efflux pumps and changes in the acidic phospholipid content on the membrane. *P. aeruginosa* for example, is relatively insensitive to QAC biocides due to a molecule penetration failure (Gilbert and Moore, 2005).

2.3.3.3. Silver biocides

There are different silver products used for the treatment of wounds, including hydrocolloids, and dressings containing nanocrystals of Ag or as bound cationic Ag^+ (Silver et al., 2006). Two different silver biocides, namely silver nitrate and silver sulfadiazine were used in the present dissertation.

Silver nitrate is an inorganic salt (**Figure 2**) that was introduced for the treatment of burns in 1965 as a 0.5% solution, being a considerate advance at that time, shortening the hospitalization time and decreasing mortality (Moyer et al., 1965). Although its photosensitivity dyes the skin black (argyria) and it may produce skin irritation, it is generally recognised as safe (White and Cooper, 2005).

On the other hand, silver sulphadiazine is a more complex silver salt (**Figure 2**). Silver sulphadiazine is formed by the reaction between sulphadiazine and silver nitrate.

The silver moiety found in both molecules is crucial for their antibacterial activity. Silver is only active in its ionic state. Ag^+ is a highly reactive ion that interacts with key biological components such as thiols, present in enzymes, DNA, surface components, etc. Being able to bind to all these targets, silver has a broad antimicrobial spectrum. Besides, theoretically, silver has benefits to the wound healing process having a potential effect on inflammatory cytokines and interacting with metalloproteins and metallothionines (White and Cooper, 2005).

However, it is unclear where the activity of silver sulphadiazine comes from: it may be a synergistic action from both molecules (silver and sulfadiazine) (Richards et al., 1991). Sulfadiazine is a sulfonamide antibacterial agent. This broad-spectrum bacteriostatic antibiotic inhibits the folate pathway by hindering the formation of dihydropteroic acid (White and Cooper, 2005). However, after silver sulphadiazine molecular dissociation, only the binding of silver to

intracellular target (DNA) has been found (Modak and Fox, 1973), leading to the belief that most, if not all, of its activity is caused by Ag^{+}. It is thought that sulfadiazine does not act via the described route but rather acts as a stable reservoir for silver ions (Fox and Modak, 1974; Modak et al., 1988).

2.3.3.4. Octenidine dichloride

Octenidine is a bispyridine separated by ten methylene groups and a terminal octanyl group from both sides (**Figure 2**) that has been used widely for more than 20 years as an antiseptic for wounds (Hübner et al., 2010). Octenidine differs from other QACs because of the lack of an amide and ester component within the structure. Therefore, it is less toxic (Rzycki et al., 2021). This structure gives the molecule an amphipathic character that resembles features of AMPs, including their mechanism of action.

Octenidine binds and penetrates the bacterial outer membrane; initially, due to electrostatic interactions and then, interfering with the fatty acyl chains through its hydrocarbon chains. Being detergent-like, it destroys the packing order of bacterial phospholipids, breaking the bacterial membrane (Malanovic et al., 2020). Additionally, octenidine is stable over the whole pH range of 1.6–12.2, which is particularly important considering varying conditions in wound healing (Hübner et al., 2010; Schneider et al., 2007).

A resistance mechanism has been described for *P. aeruginosa*, which is based on mutations in *smvR* (increasing the expression of efflux pumps), as well as in the *pssA* and *pgsA* genes (phospholipid synthases), causing membrane remodelling. This leads to a 256-fold increase in octenidine tolerance (Bock et al., 2021).

2.3.3.5. Povidone iodine

Although the activity of iodine as an antiseptic has been known since 1829, its poor solubility and stability caused serious difficulties in its application and wider use. It was not until 1956 when povidone iodine (PVP-iodine) was introduced, solving the aforementioned problems (J.-Y. Maillard et al., 2021; Williamson et al., 2017).

Povidone (polyvinyl pyrrolidone, PVP) is a synthetic polymer that forms a complex with iodine, being its carrier and reservoir (**Figure 2**). Thus, an equilibrium between PVP-bound iodine and free iodine is formed, enhancing the solubility of this molecule and improving its safety (Bigliardi et al., 2017).

The antimicrobial activity of this molecule is caused by the iodine moiety, however, PVP presents a certain degree of affinity to the bacterial cell surface that brings the iodine closer to its target and promotes bacterial killing (Zamora, 1986). Once separated from the complex, free iodine oxidizes the bacterial cell membrane and penetrates into the cytoplasm oxidizing other molecules such as enzymes, amino acids, and nucleotides. It rapidly kills microorganisms by

inhibiting essential cellular processes, including cellular respiration, electron transport, and protein synthesis (Williamson et al., 2017).

PVP-iodine is an antiseptic with a broad antibacterial spectrum. Moreover, the absence of bacterial resistance mechanisms and the low cytotoxicity exhibited by this molecule endow it with favourable properties for the treatment of wound infections (Bigliardi et al., 2017).

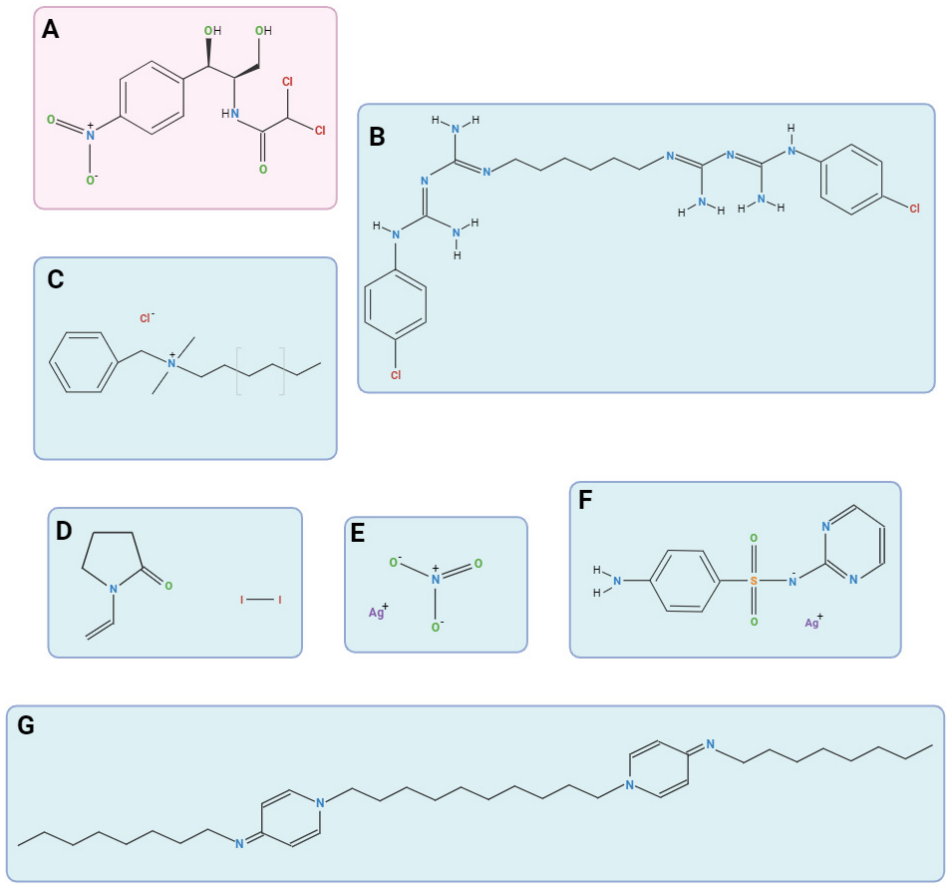

Figure 2. Chemical structure of antibiotic and biocides used in this dissertation. **A.** Chloramphenicol. **B.** Chlorhexidine. **C.** Benzalkonium chloride. **D.** PVP-iodine. **E.** Silver nitrate. **F.** Silver sulphadiazine. **G.** Octenidine. Created with BioRender.com.

2.4. Electrospun matrices as wound dressings

Traditional dressings, made of woven and non-woven cotton, rayon, or polyester fibres, may be useful on dry wounds. However, where there is slight drainage or bigger exudating wounds, these materials are associated with maceration of healthy tissues and adhesion to the wound, resulting in delayed healing and painful removal (Piaggesi et al., 2018). Therefore, new wound dressings, such as films, foams, hydrogels, hydrocolloids, and nanofiber matrices have been formulated to promote wound healing (Kaiser et al., 2021).

Nanofibrous electrospun matrices are very good wound dressing candidates due to their outstanding physicochemical features. Their high surface area to volume ratio, flexibility, mechanical strength, high porosity, their ability to be highly tuneable in terms of drug delivery – adjusting the hydrophobicity of the fibers – and their great biocompatibility with biological tissues make these dressings one of the most investigated at the moment (Muthukrishnan, 2022). They resemble the natural ECM, allowing a sufficient absorbability and gas-exchange that control and maintain an appropriate moisture balance, avoiding maceration and desiccation of the wound bed (Leaper et al., 2014). All these properties enhance good haemostasis and promote wound healing.

When electrospun matrices are loaded with different molecules that facilitate the healing process (i.e. antimicrobial agents), further characterisation needs to be conducted. The drug content and release from the matrix into the environment and the activity of the drug need to be assessed. Moreover, all matrices used for wound treatment should be proven safe and biocompatible.

2.4.1. Electrospinning technology

In order to develop electrospun dressings, it is crucial to understand the method. Electrospinning is a versatile and straightforward technique used for the fabrication of fibers on the micro to nanoscale. It involves the application of a high-voltage electric field to a polymer solution, causing the formation of a thin jet from a small nozzle (Syed et al., 2023).

The electric field accumulates on the solution inside the nozzle until the solution reaches the same polarity charge as the applied electric field. Then, electrical repulsion occurs between the like charges. This repulsive force overcomes the surface tension of the solution, leading to the formation of a conical shape known as the Taylor cone and the ejection of a polymer jet from the nozzle. This jet stretches and elongates due to the electrostatic repulsion between the charged jet and the grounded collector. As the solvent in the jet evaporates, the charged polymer fibers solidify and these solid fibers are collected on a grounded collector as a nonwoven matrix (Huang et al., 2003). A schematic representation of electrospinning is provided in **Figure 3**.

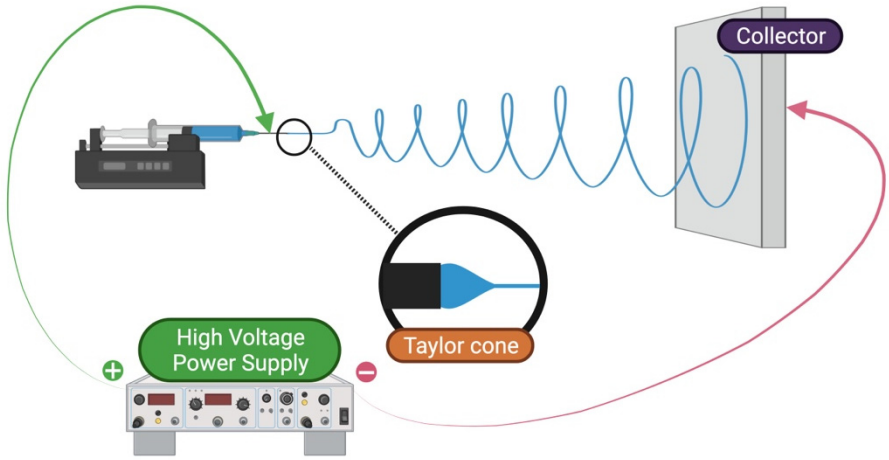

Figure 3. Schematic diagram of the electrospinning process. Created with BioRender.com.

2.4.2. Parameters

The electrospinning technique relies on different parameters that require optimisation and influence the physicochemical properties and behaviour of the fibrous matrix. These parameters come from different variables that are summarised in **Table 3**.

Table 3. List of variables affecting the electrospinning process and their subsequent effects.

General variable	Parameter	Effect	References
Solution properties	Polymer concentration	An increase in polymer concentration reduces the number of beads and increases fiber diameter	(Luraghi et al., 2021)
	Solvent volatility	Increased solvent volatility results in higher chances of pore formation and increased surface area	(Thakkar and Misra, 2017)
	Viscosity	Increased viscosity results in larger diameters	(Huang et al., 2003)
	Conductivity	An increase in solvent conductivity results in finer nanofibers, reducing bead formation and obtaining lower diameter	(Thakkar and Misra, 2017)
	Surface tension	Reduction of surface tension results in avoidance of bead formation and lower fiber diameter	(Thakkar and Misra, 2017)
Electrospinning parameters	Flow rate	An increase in flow rate increases fiber diameter	(Thakkar and Misra, 2017)
	Voltage	Increase in voltage results in a higher diameter	(Refate et al., 2023)
	Distance tip-collector	Diameter increases with a decrease in distance	(Huang et al., 2003)
Ambient parameters	Temperature	An increase in temperature is associated with an increase in nanofiber diameter	(Refate et al., 2023)
	Humidity	An increase in humidity increases fiber diameter and enables the formation of pores	(Luraghi et al., 2021; Refate et al., 2023)

2.4.3. Loading techniques

Although a final product may consist solely of an electrospun matrix formed by the employed polymer (e.g. polymeric matrices or scaffolds for tissue engineering (Oztemur et al., 2023)), many applications require loading other molecules into the electrospun matrix. As part of the pharmaceutical technology approach, different drugs have been incorporated using different loading techniques (**Figure 4**).

Post-loading techniques
This approach involves surface immobilization of the bioactive molecule after the electrospinning process. This method has various advantages: it prevents the need for contact between the drug and solvents that may degrade the molecule, and it allows an easier development of the matrix to preserve its original degradation and mechanical properties (Luraghi et al., 2021). One method to achieve this is the physical adsorption technique, however, the bonds formed are often weak, thus releasing the drug very fast when the matrix gets in contact with the aqueous environment (Karge and Weitkamp, 2008). To mitigate this issue, other stronger non-covalent interactions and cross-linking processes are needed.

Drug blending
This methodology relies on the dissolution of both the drug and polymer in a suitable solvent. When achieved, it is probably the simplest approach and the one with the highest drug loading capacities. However, it is not always feasible. Sometimes it is difficult to find a solvent that dissolves both molecules and even so, many organic solvents can degrade the active molecule. Besides, the drug release obtained from these fibers usually starts with a burst release (Luraghi et al., 2021).

Emulsion electrospinning
The drug can be encapsulated using an emulsion technique. In this case, the drug is usually prepared in a water solution and the polymer is dissolved in an oily one. Afterwards, both solutions are mixed vigorously, and micelles are formed. This method allows to form core-shell nanofibers without the use of a concentric needle that prevents a close contact between the drug and a potential organic solvent that could degrade it (Luraghi et al., 2021).

Coaxial electrospinning
Unlike all other methods mentioned above, whose matrices are electrospun using a monoaxial nozzle, this technique is based on the preparation of different solutions for the polymer and the drug that afterwards are combined into a concentric needle to form core-shell nanofibers. Similar to the emulsion technique, it prevents contact between the drug and a potential organic solvent. Moreover, the polymeric shell functions as a physical barrier that hinders burst release (Luraghi et al., 2021).

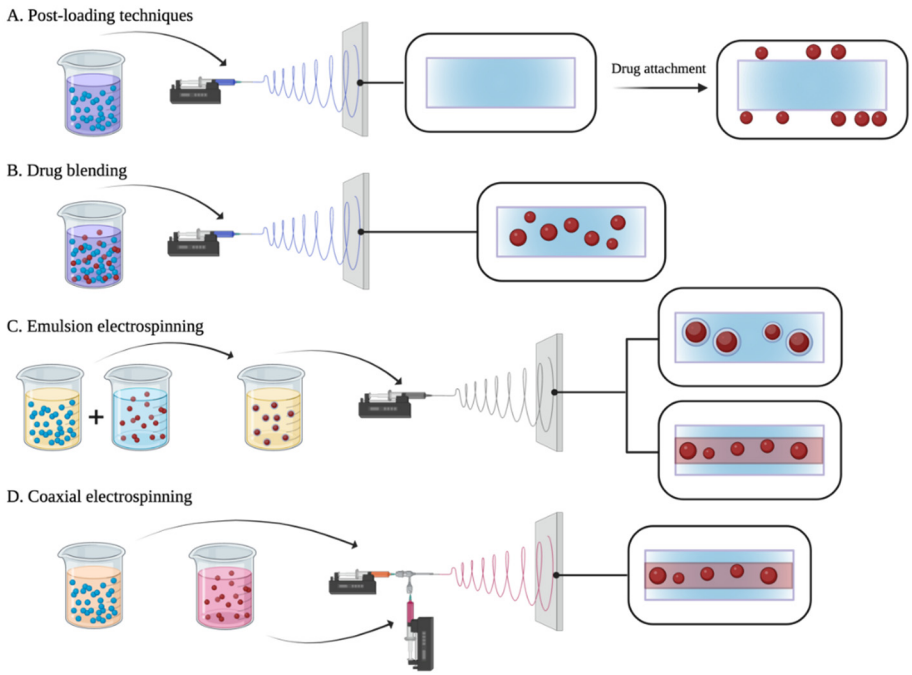

Figure 4. Various strategies used for drug incorporation into the electrospun fibers. Created with BioRender.com.

Although the techniques mentioned above are the most common, there are various other electrospinning methods and setups available. Some of them are triaxial electrospinning (Yang et al., 2023), side-by-side electrospinning (Cai et al., 2019), and needleless electrospinning (Elsherbiny et al., 2023). Moreover, a high-intensity ultrasound electrospinning method (USES) (patent available) (Laidmäe et al., 2016) and a microfluidic electrospinning method (patent pending) (Lanno et al., 2022) have been developed in our research group.

2.4.4. Characterization of electrospun matrices

Polymeric nanofibers are attracting great interest due to their wide applications in numerous fields. They have been used for the fabrication of membranes (Mizan et al., 2023), textiles (Sanchaniya et al., 2023), nanosensors (Oh et al., 2023), and biomedical applications (Yan et al., 2022), among others. However, in order to fulfil the parameters needed in each one of these usages, the electrospun matrices need to be carefully analysed. Some of these characterization methods are described below (Haider et al., 2018).

2.4.4.1. Morphology

Electrospinning is a method that enables to develop very small fibers, nonetheless, their diameter may vary widely from micro to nanoscale. Some parameters affecting this size distribution are mentioned in **Table 3**.

Besides the various fiber diameter sizes, different types of fiber surfaces can also be found on the fibers, namely smooth (Xia et al., 2023), pitted (D'Amato et al., 2019), grooved (Wu et al., 2020), wrinkled (Pai et al., 2009), rough (Haridas et al., 2014) and porous (Huang and Thomas, 2018) surfaces. These different morphologies give the matrix different properties, for instance, highly influencing the drug release. Porous fibers are known to have valuable properties for some applications such as filtration, tissue engineering, and drug delivery (Agarwal et al., 2008; Gopal et al., 2006). Diverse mechanisms have been described for the preparation of pristine porous fibers, including phase separation and breath figure process or a combination of both (Casper et al., 2004; Natarajan et al., 2014). The breath figure process requires the presence of humidity as the water droplets from atmospheric water are formed on fibers due to the evaporative cooling of the polymer solution. As the jet dries, the water droplets leave an imprint on the fiber surface in the form of pores (Megelski et al., 2002). However, the preparation of porous fibers as drug delivery systems is not yet fully understood and there is still a lack of information about the characterization of these matrices.

Furthermore, the structure of the fiber matrix is crucial, including how the fibers are arranged on the collector plate. A homogeneous matrix must be formed to ensure consistent drug release and mechanical properties throughout the entire matrix. Besides, matrix pores impact cell attachment and infiltration (Farooque et al., 2014). All these factors can be tuned in order to obtain the desired properties, making the matrix optimised for each specific application.

The morphology of the fibers can be studied using different methods. Optical microscopy is the easiest and fastest tool to observe fibers, however, it does not enable to measure pore structures and, depending on the fiber diameter, its measurement may not be reliable and accurate enough. In order to study the pore structures, atomic force microscopy (AFM) or scanning electron microscopy (SEM) are used (Agarwal et al., 2016).

SEM is probably the most frequently used method for studying fiber morphology. In contrast to optical microscopy, where a photon (with no mass) is the source of radiation, in SEM an electron is used (mass equal to 9.109×10^{-31} kg) (Agarwal et al., 2016). Electrons are charged particles and they are able to be accelerated and precisely focused by electromagnetic fields. The scattered beams are then collected and refocused to form an image in the manner of an optical microscope (Pennycook, 2005). Besides, SEM enables to distinguish very small wavelengths based on the assigned acceleration voltage for an electron, and thus, it is possible to observe fibers with very small diameters. Nonetheless, the energy exerted on the fiber matrix using SEM may damage the sample (Agarwal et al., 2016).

Transmission electron microscopy (TEM) enables to study the morphology inside the fiber. This is possible because, in this case, the electron beam is passing through the sample (transmission mode), whereas using SEM only the reflected electrons are measured. This is very useful to identify and study core-shell structures (Ghasemvand et al., 2023) or the presence of metal nanoparticles (Razouq et al., 2023). TEM is also used for the study of the cross-section of a fiber. For this purpose, oriented free-standing fibers are required and subsequently sectioned. Liquid nitrogen is sometimes utilized to enhance the stiffness of softer samples (Agarwal et al., 2016). In order to use TEM, the sample needs to be collected onto copper grids that serve as specimen holders. **Figure 5** shows a core-shell structure visualised using TEM.

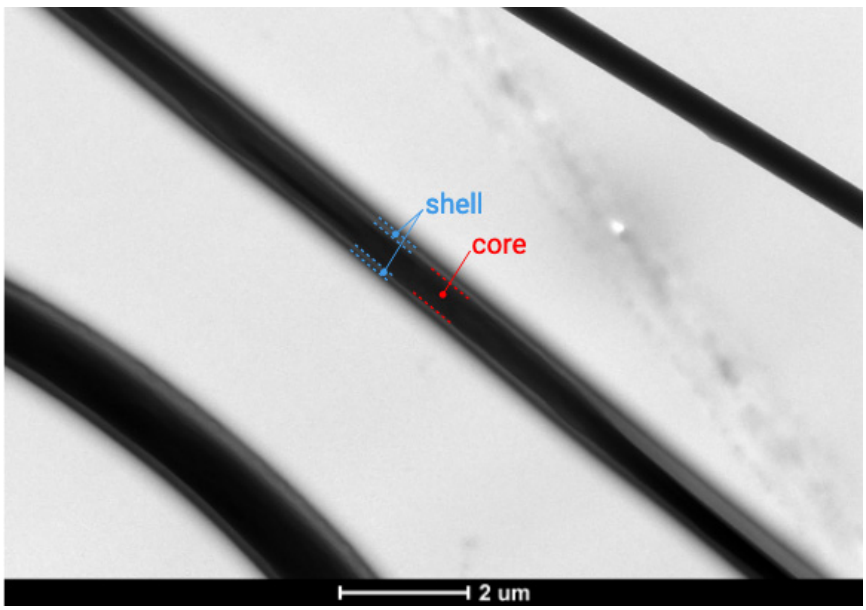

Figure 5. Electrospun fibers with the core-shell morphology observed by TEM.

2.4.4.2. Mechanical properties

The morphology of the fibers described above highly influences their mechanical properties. For the electrospun matrix to accomplish its function, it needs to resist the stresses suffered from the environment and thus, its mechanical properties need to be studied. The mechanical properties of electrospun fibers can be investigated for individual fibers or for their combination forming matrices. However, the measurement of the mechanical properties of materials with such small diameters is challenging and the vast majority of studies are performed for matrices rather than for individual fibers (Neugirg et al., 2016). The mechanical

properties of electrospun matrices are mainly presented as tensile strength, elongation at break, and Young's modulus (Rashid et al., 2021).

The tensile strength is defined as the maximum load that a material can support without fracture when being stretched. Elongation at break is defined as the maximum elongation a material can withstand before breaking, and Young's modulus measures the quantity of elasticity, meaning resistance against elastic deformations. Young's modulus can be calculated from the linear elastic region, which is the first slope of a tensile test, by applying Hooke's law (Jones and Ashby, 2019).

Factors such as diameter (Stachewicz et al., 2012), fiber orientation (Huang et al., 2003), and matrix porosity (Rashid et al., 2021) directly affect their mechanical properties. For example, nonwoven fiber matrices randomly oriented show lower tensile strengths than those oriented in the direction of the stress, and the same occurs with matrices with a high percentage of porosity. Smaller fiber diameters show nonlinear increments in Young's moduli, and thus, in tensile strengths (Rashid et al., 2021). Nonetheless, the development and effect of porous fibers (pores on the surface of individual fibers, distinct from matrix porosity) on mechanical properties, and thus, on the drug contained within the matrix, are not yet fully understood. Exploring these aspects is one of the aims of this dissertation.

2.4.4.3. Contact angle, swelling and weight loss

In order to understand the relationship between the fiber matrix and the aqueous environment, three main methods are used that enable to understand the hydrophilic/hydrophobic nature and wettability of the fibrous matrices.

The contact angle is based on the sessile drop method, measuring the angle that is formed by the application of a single drop of phosphate buffered saline (PBS) and/or water on the matrix. Hydrophilic materials have a lower contact angle (Ph. Eur, 2024)

Swelling capacity is measured by weighing matrices before and after being immersed in a biorelevant buffer solution (usually PBS) after 24 h. A controlled swelling causes an increase in the pore size and porosity of the polymeric matrix, which is ideal for the supply of nutrients and oxygen to the wound, considering the final application of these electrospun matrices (Peter et al., 2010).

Weight loss over time, also referred as degradation behaviour, is measured weighing the matrices before and after immersion in biorelevant medium (e.g. PBS at 37ºC) for longer periods (up to 1 month or even longer if the matrix is planned to be used for longer time-periods). In this particular instance, the sample needs to be freeze-dried prior to conducting the measurement (Nazemi et al., 2014). This procedural step is undertaken to obtain the dry weight of the sample before and after the degradation experiment.

2.4.4.4. Solid state properties

The solid-state characterisation of the antimicrobial drug-loaded and pristine polymer fiber matrices can be achieved through various methods, enabling the investigation of material properties at the molecular level.

One option is the use of infrared spectroscopy (IR). IR is a well-established non-invasive and non-destructive tool that permits the assessment of the chemical composition of a wide range of sample types. It is based on the absorbance capacity of different molecular moieties in the IR range (near-IR: 750–2500 nm, mid-IR: 4000 – 400 cm^{-1} and far-IR: 400-10 cm^{-1}) (Johnson et al., 2023). The absorption of energy occurs when the vibration caused by IR changes the dipole moment, resulting in a change in the vibrational energy level (Larkin, 2011). There are two types of IR spectrometers: dispersive IR and Fourier-transformed infrared spectroscopy (FTIR). The difference is in the spectral device (monochromator or interferometer) that in the case of the interferometer usually gives a single-section beam path and is located between the IR radiation source and the sample, improving the signal-to-noise ratio and enabling fast acquisition (Larkin, 2011). To enhance the precision of measurements and mitigate the inadvertent inclusion of the fiber holder in the analysis, the employment of the attenuated total reflection (ATR) approach is highly recommended. When a sample makes direct contact with the surface, given that the penetration depth is only a few micrometers, which is commensurate to fiber matrices, some wavelengths may be absorbed. This absorption leads to a decrease in the intensity at these wavelengths, thereby facilitating a direct and accurate measurement. The most suitable IR techniques for fiber measurement are combined in the ATR-FTIR spectroscopy, which has been used in this dissertation. The IR spectrum is obtained by plotting the intensity (absorbance) versus the wavenumber, being proportional to the energy difference between the ground and the excited vibrational states (Larkin, 2011). Since the vibrational frequencies of a given functional group correspond to the absorption at a certain frequency, the absorption spectra of the sample are compared with the reference tables containing absorbances of functional groups. This way it is possible to analyse the chemical composition of the sample.

X-ray diffraction (XRD) is a non-destructive technique for characterizing crystalline materials. XRD is based on the production of constructive interference (and a diffracted ray) produced by the interaction between monochromatic X-rays and a crystalline sample. This interaction is defined by Bragg's law (**Equation 1**):

$$n\lambda = 2d\sin\theta \quad (\boldsymbol{Equation\ 1})$$

where n is an integer, λ is the wavelength of the X-rays, d is the interplanar spacing generating the diffraction, and θ is the diffraction angle. The diffracted X-rays are then detected, counted, and conversed into d-spacings, allowing the identification of the compound, as each compound has a unique set of d-spacings

(Bunaciu et al., 2015). Using this method, it is possible to study the crystallinity of the molecules in the fibers (polymer and drug).

Thermal analysis is usually performed using differential scanning calorimetry (DSC). This method is based on the comparison between the heat flow of a sample and a reference, allowing the measurement of the glass transition temperature (T_g), (re)crystallization temperatures, and melting temperatures (T_m) (Laye et al., 2002). Besides, using DSC it is possible to calculate the change of crystallinity due to electrospinning (comparing electrospun fiber samples with control films).

2.4.4.5. Drug content and release

Once the physicochemical characterisation of the matrix has been successfully achieved, the focus should be placed on the drug that was loaded into the matrix. This molecule is the key active compound, and thus, the drug loading efficiency, its distribution within the fiber matrix, and its release into the environment are crucial for successful treatment.

The drug content and release can be measured using different methods, such as UV-Vis spectrophotometry (Mianehro, 2022; Morais et al., 2023), mass spectrometry (Pinheiro Bruni et al., 2020), mass spectrometry imaging (Clitherow et al., 2019) or high performance liquid chromatography (HPLC) (Park et al., 2015). During the electrospinning process, the application of high voltage and exposure to harsh solvents or other molecules may lead to the degradation of the drug. Therefore, the final drug content that has been successfully incorporated within the matrices is measured and can be compared with the theoretical concentration used for the preparation of the electrospun polymer solution. The relation between drug content and theoretical concentration defines the loading efficacy of the method.

Nonetheless, the drug incorporation within electrospun matrices does not necessarily mean that the molecule is able to be released into the environment and thus, is available to reach its target. The drug release mechanism can be attributed to different processes: diffusion, polymer degradation, drug partitioning in polymers, and drug dissolution (Chou et al., 2015). Consequently, often drug molecules that have been incorporated on the surface of fibers are released faster (often causing a burst release) than the molecules that are located deeper inside the fibers. Multiple approaches can be used to tune the drug release such as selecting an appropriate polymer (Chou et al., 2015), using coaxial vs. monoaxial electrospinning (Hu et al., 2014), modifying the thickness (Kim et al., 2010) and the porosity of the matrix (Luong-Van et al., 2006) or modifying the diameter of fibers (Xie and Buschle-Diller, 2010), among others.

2.4.4.6. Antimicrobial activity

There are different electrospun matrices available for wound healing applications, containing growth factors, haemostatic compounds, or other molecules that promote wound closure (Abdulmalik et al., 2023; Tottoli et al., 2023). However, the

need to control potential or concomitant wound infections leads to the preparation of matrices with antibacterial and/or antibiofilm activity.

As mentioned before, wound infections are a major burden in wounds, inhibiting the correct development of the physiological wound healing process. Besides, the most common bacteria that colonize wounds are also the ones presenting the highest AMR rates – the ESKAPE pathogens (Rice, 2008). Therefore, it is crucial to use a drug delivery system that enables to incorporate different novel molecules with diverse characteristics, preserving their antimicrobial activity and also enabling an adequate release to prevent the development of resistance. For this reason, electrospun matrices are a perfect match.

The antimicrobial activity of electrospun matrices should be first studied *in vitro.* This can be achieved using basic microbiological techniques such as disk diffusion (Sheet et al., 2018) or other elaborated methods such as the ones used in this dissertation that will be explained in the Methods section. *Ex vivo* models are a good alternative to test the antibacterial and antibiofilm properties of the matrices before stepping into *in vivo* models. Porcine or murine tissues are typically used (Lorenz et al., 2023), which provide a more physiologically relevant and accurate representation of the biological environment than *in vitro* assays. Despite the fact that *in vivo* animal models are the closest imitation of human skin wounds, the predominantly used rodent models significantly differ in the immune response and wound healing mechanisms compared to humans (Mestas and Hughes, 2004). For this purpose, pig models are preferred, although their use is limited due to the high costs (Summerfield et al., 2015).

Electrospun matrices mimic the ECM, consequently, pristine polymeric matrices could be an appropriate scaffold and/or surface for bacterial attachment and growth. Interactions between electrospun matrices and bacterial cells are known to be incredibly complex, affecting bacterial attachment and spread within nanofibers (Abrigo et al., 2015). These interactions are mainly defined by the surface chemistry features of the matrix, hence, hydrophobic matrices are expected to be better substrates for bacterial attachment and growth (Cerca et al., 2005).

In order to provide an effective antibacterial activity, electrospun matrices should have an appropriate drug release behaviour. For instance, it has been observed that a biphasic extended release profile (an initial burst release followed by a sustained release) sufficient to kill the pathogen is needed to reach antibiofilm efficacy (Sin Cheow et al., 2010).

In order to understand the antibacterial activity of electrospun matrices, the efficacy of the drugs against tested pathogens should be investigated prior to their incorporation into electrospun matrices. This way, it is possible to predict the concentration of drug needed within the matrix, which would need to reach minimum inhibitory concentration (MIC) levels when released into the environment. The "gold standard" method to investigate the antibacterial activity of molecules in solution is to conduct a MIC assay (Andrews, 2001). Here the drug is diluted following a two-fold series in a 96-well plate, where bacteria will then be added. The first well without bacterial growth gives information regarding the

lowest concentration of drug needed to cause inhibition. Thus, this should be the minimal concentration released from the matrix in order to achieve antibacterial activity.

Furthermore, wound healing guidelines often recommend the use of concomitant treatment (European Wound Management Association (EWMA), 2006; Probst et al., 2022). However, the interaction between molecules may not be as beneficial as expected, even when both compounds have antibacterial activity. Different phenotypical effects can be obtained when two antibacterial drugs are used in combination: synergy, additive behaviour or antagonistic effect. These mechanisms are often investigated using the checkerboard microdilution assay, where one antibacterial drug is diluted across rows and the other is diluted across columns, thus obtaining different combinations of these molecules at different concentrations. Afterwards, a known number of bacteria will be added to study their growth. The interactions between these molecules are then calculated using the fractional inhibitory concentration (FIC), which is defined by **Equation 2**.

$$FIC = \frac{MIC\ A_{\ A+B}}{MIC\ A} + \frac{MIC\ B_{\ A+B}}{MIC\ B} \quad (\boldsymbol{Equation\ 2})$$

where A corresponds to the compound A alone, B corresponds to the compound B alone and A+B corresponds to both compounds in combination.

There is an ongoing discussion regarding the analysis of the checkerboard microdilution assay, and breakpoints for the interpretation of the FIC vary from study to study. This variance leads to different interpretations and conclusions drawn from the same results.

Synergy is better understood if the additivity definition is clear. Agents that act additively are no more and no less effective in combination than they are separately, represented by a FIC equal to 1. The perfect example of additivity is the combination of any agent with itself, known as a "sham mixture" based on the Loewe Additivity model (Berenbaum, 1978). Any variation from additivity is classified as synergism or antagonism (Roell et al., 2017).

Synergistic behaviour is defined when two or more agents are more effective in combination than they are separate. This relation is defined theoretically by **Equation 2** when the sum of the fractions is therefore <1. Antagonism, on the other hand, is present when any agents are less effective in combination than they are on their own, in this case, the sum of the fractions is >1 (Berenbaum, 1978; Chou and Talalay, 1984). Although these old definitions are clearly and widely accepted, there are several critical factors in this protocol that lead some authors to consider a more restrictive interpretation of synergistic behaviour.

In MIC testing, there is a widely accepted norm that variation in a single result places a MIC in a three-dilution range (mode ± 1 dilution), therefore the variation and reproducibility in a MIC checkerboard, and thus in FIC values, are considerable (Odds, 2003). For this reason, synergy is defined as FIC < 0.5, encouraging conservative interpretation (Odds, 2003). However, a recent re-evaluation of FIC that stressed the importance of also measuring the MIC in the same

plate, enables to consider values of 0.5 to <1 as weak synergism (Fratini et al., 2017). Other authors have also defended the idea of weak synergism (Hall et al., 1983). While others define the same range for additive behaviour (EUCAST, 2000; Saiman, 2007). There are also differences in the definition of indifference and antagonism. Odds defines indifference with a wider range, from 0.5 to 4, and only above 4 he defends antagonism (antagonism definition that is also claimed by Saiman). Fratini, in this case, follows an idea similar to EUCAST guidelines, where indifference is in the range $1 < FIC \leq 2$ and antagonism above 2.

There are many authors that defend the synergistic breakpoint as FIC <1 (Van Vuuren et al., 2009; Van Zyl et al., 2010), others that use the "weakly synergistic" concept for values in an FIC range from 0.5 to 1 (Arras and Fraser, 2016; Di Blasio et al., 2022) and others that only define synergy when $FIC \leq 0.5$ (Doern, 2014; Saiman, 2007).

In this dissertation, MICs were determined on the same plates as the FICs to increase reproducibility, as explained by Fratini (Fratini et al., 2017) which allows to avoid the issue commented by Odds (Odds, 2003). This way, we consider synergism for FIC values below 1, which conforms to the theoretical definition of synergism proposed by Berenbaum (Berenbaum, 1978). Besides, as we understand that FIC values below 0.5 should be treated as more synergistic than the ones closer to 1, we define different ranges within synergism where 0.5 is the breakpoint between weak and strong synergism. Following EUCAST and Fratini guidelines, indifference effects are defined when $1 < FIC < 2$ and antagonism behaviour for FIC values ≥ 2.

Clearly, it is essential to develop this assay with an extraordinarily careful technique and use replicates to avoid discrepancies due to technical errors. Besides, including the MIC of each agent alone in parallel to the MIC in combination increases reproducibility. These measures should be sufficient to instill confidence in the methodology and allow adherence to the theoretical definition of synergy. Neglecting this definition could result in overlooking essential data. Therefore, this is the strategy followed during this dissertation.

2.4.4.7. Safety

The most important feature of any drug and drug carrier is their safety. Wound dressings need to be biocompatible with the organism. For this reason, only biocompatible polymers approved by a regulatory agency (FDA, European Medicines Agency, or equivalent) are used, and it is always necessary to study the cytotoxicity of the matrix. It is essential to confirm that no traces of the organic solvent used are causing any cytotoxicity and that all materials used are indeed safe for eukaryotic cells.

Different assays can be performed to study cytotoxicity. Usually, the first analyses are performed *in vitro* using different eukaryotic cells related to the skin, mainly fibroblasts or keratinocytes. To study the viability of cells and draw conclusions about biocompatibility, different techniques may be used. Metabolic activity tests such as the neutral red, resazurin, lactate dehydrogenase assay, and

the MTS are colorimetric tests that allow cytotoxicity quantification by taking spectrophotometric measurements (Goonoo et al., 2014). In the case of the MTS assay, metabolically active cells use their mitochondrial dehydrogenase enzymes to transform tetrazolium salts into soluble formazan, whose absorbance can be measured at 490 nm (Malich et al., 1997). Besides, the cell-matrix interaction can be studied using confocal fluorescence microscopy (CFM). This dye-based technique enables the visualization of molecules, including those in out-of-focus planes, allowing for high-resolution images (Elliot, 2020).

2.4.5. Commercially available electrospun matrices

There are many examples in the literature where there has been a significant improvement in wound healing with electrospun products in pre-clinical models, both *in vitro* and *in vivo* (Gao et al., 2022; Khalid et al., 2020; Liu et al., 2022). However, not many of these products reach clinical trials. Some examples are the ones produced by Neotherix® technology (Omer et al., 2021) and Pathon and Tecophilic TM products (Azimi et al., 2020).

An essential aspect of the scaling-up process involves enhancing productivity. The main strategies to achieve this are based on increasing the jet numbers, achievable through the utilization of multiple needles or transitioning from the traditional electrospinning process to needleless electrospinning (Omer et al., 2021; Vass et al., 2020). However, even if the technical aspects can be managed proficiently, breaking into the pharmaceutical market remains a difficult milestone.

There are many specific requirements that need to be fulfilled (ISO 10993 standards and GMP conditions) and there are not many devices applicable to pharmaceutical industries available. Among these requirements, it is essential to get rid of any toxic residues that have been used during the process (mainly organic solvents used for polymer solubilization) (Luraghi et al., 2021) and to be sure that the final product is properly sterilized (Azimi et al., 2020). For example, the company Bioinicia (Valencia, Spain) has a GMP-standard electrospinning facility validated for biomedical and pharmaceutical products (currently testing in clinical trials the Rivelin patch) (Dziemidowicz et al., 2021). Other industrial-scale equipment that can be used in the pharmaceutical industry is PE2550 from INOVENSO (Istanbul, Turkey) and Electrospinning (Tong Li Tech)/NaBond (Hong Kong) (Omer et al., 2021). Besides, there is a demand for highly skilled workers, which restricts access to the technical aspects (Azimi et al., 2020).

Most of the commercial products developed using electrospinning are filters and masks though there are many patented products for biomedical applications (Muthukrishnan, 2022). **Table 4** enlists the currently available nanofiber matrices used in wound healing.

Table 4. Commercially available electrospun matrices used in wound healing applications. Based on Nadaf et al. (Nadaf et al., 2022), Omer et al. (Omer et al., 2021), with the company websites cited in the last column.

Product name	Company name	Description	Website
Nanotrix® (SNC Best™)	Stellenbosch Nanofiber Company (SNC)	Primary wound dressing for 2nd degree burns	https://www.sncfibers.com/product-development
SurgiCLOT®	St. Theresa Medical Inc.	Dextran patch containing fibrinogen and thrombin designed for bone bleeding	https://stteresamedical.com/technology/surgiclot
NanoCare®	Nanofiber Solutions	Wound healing dressing for veterinary applications	https://nanofibersolutions.com/product/nanocare/
Phoenix Wound Matrix RenovoDerm ®	RenovoDerm® & Nanofiber Solutions	Wound dressing for acute, chronic and burn wounds	https://www.renovoderm.tech/
SpinCare™	NanoMedic	Portable electrospinning device that creates a dressing directly over the wound	https://nanomedic.com/spincare/#spincare_fop

The number of commercially available electrospun products has been increasing in recent years. It is understandable that those intended for pharmaceutical applications are currently fewer, as they must satisfy numerous regulatory requirements to ensure the safety and efficacy of the final product. However, this market is growing quite rapidly, and further developments in the pharmaceutical industry are only a matter of time.

3. LITERATURE SUMMARY

Non-healing wounds are a major health concern, causing high patient mortality and morbidity. The skin regeneration follows different pathways and stages that can be disturbed due to a microbial infection (mainly caused by bacteria), causing an impediment to the healing process and resulting in chronic non-healing wounds. Therefore, many wound healing approaches are based on formulations that act against biofilm formation and bacterial growth. However, conventional drugs are facing a lowered efficacy due to AMR.

A. baumannii, P. aeruginosa, K. pneumoniae, S. aureus, and *E. coli* are multi-resistant bacterial pathogens that are commonly found in wounds, hindering their healing. In order to overcome AMR, new molecules and new topical drug delivery systems need to be investigated as alternative wound treatments.

In this dissertation, different antimicrobial agents are analysed against named multiresistant wound pathogens. To begin with, CAM, a conventional antibacterial drug whose use was reduced due to the toxicity concerns, has recently been reconsidered as a potential alternative due to the ongoing susceptibility of bacteria to this antibiotic. Moreover, novel AMPs (namely pleurocidin, D-pleurocidin-KR and temporin B L1FK) have been examined as relatively new drugs that maintain bacterial susceptibility. AMPs are known to be strong candidates for combating the development and spread of AMR owing to their broad and unspecific mechanism of action, as well as their rapid degradation upon contact with the environment. Besides, these molecules are also involved in other mechanisms that interact and promote the wound healing process. AMPs are found in the immune system regulating inflammatory and angiogenesis processes as well as cell migration and proliferation. For these reasons, it has been hypothesised that these molecules are a good strategy to fight AMR while enhancing wound healing.

Further to AMR, another important wound treatment concern is the formulation and/or drug delivery system used. The presence of wound exudate complicates the administration of conventional topical drugs that may be removed from the spot resulting in an ineffective treatment. Additionally, systemic formulations are used, however they may result in toxicity issues. In this study, we developed novel topical wound dressing formulations – electrospun matrices – formed using a nanotechnology approach that can be used to overcome these concerns.

Electrospinning is a versatile technique used for the fabrication of fibers in micro- to nanoscale. A high voltage electric field is applied in the metallic needle of a syringe loaded with an electrospinnable polymer causing the ejection of this solution onto a grounded collector. The accumulation of these polymeric nanofibers on top of each other results in the development of a non-woven matrix. The obtained fibrous dressings are very good candidates for the treatment of wounds. Their biocompatibility, high surface area to volume ratio, flexibility, strength, and porosity allow them to resemble the natural ECM, allowing sufficient gas-exchange and absorbability needed to maintain an appropriate moisture balance,

enhancing haemostasis and promoting wound healing. Besides, this technique is highly adjustable and may be affected by many different variables such as solution properties, electrospinning parameters (flow rate, voltage, and distance between the tip and collector), and ambient parameters. The electrospinning process allows the incorporation of active substances in the matrix. This can be done following different techniques, but here drug blending (mixing polymer and drug into a suitable polymer) and coaxial electrospinning (using a coaxial needle to form a core-shell structure) are utilized.

Although this technique is highly adjustable and many different types of matrices have been created before, it is not well known yet how to produce matrices with porous fibers. Here, different parameters were examined in order to develop this kind of matrices and analyse their effects on their mechanical properties, drug release, cellular attachment, and antibacterial activity.

As mentioned before, CAM and pleurocidin were the selected molecules to be included in electrospun matrices. Although the antibacterial activity of these drugs has been previously studied, these investigations have mainly been done using these molecules in solution and there are not many studies regarding the incorporation of AMPs into electrospun matrices. Thus, during this dissertation the incorporation of selected pleurocidin within matrices was investigated, including the assessment of the stability and functionality of this AMP inside the matrices. Moreover, the antibacterial activity of matrices and molecules in solution was compared in order to understand how this drug delivery system affects the behaviour of the molecule.

Common biocides are used and recommended by wound associations for the cleaning of wounds, however, their effects on the activity of other concomitant treatment are often neglected. Here, phenotypical effects caused by pleurocidin and different biocides used in wound healing (chlorhexidine digluconate, benzalkonium chloride, silver nitrate, silver sulfadiazine, octenidine dichloride, and PVP-iodine) were studied in combination in order to understand their antimicrobial properties when used together considering their potential use in clinics.

Although commercially available electrospun products have seen an increase in recent years, the reality is that there are still not many available on the market. This may be due to the high demands and requirements for pharmaceutical products and the fact that there are not many electrospinning facilities validated. This dissertation provides relevant information regarding the development and properties of porous fibers created using electrospinning as well as essential knowledge about AMP incorporation within electrospun matrices and the relation between these molecules and frequently used biocides. This information can help the electrospinning business bloom, where more products are expected to reach clinical application in the upcoming years.

4. AIMS OF STUDY

The general aims of this dissertation were to prepare and characterize novel electrospun matrices loaded with antimicrobial molecules for wound healing applications. Additionally, the study aimed to investigate the potential of combining an AMP with common biocides in solution to combat wound pathogens. In order to achieve these goals, the workload was divided into specific aims, which were to:

1. Develop porous fibers. To screen and select different solvent systems and electrospinning parameters for process optimization and tunability of porous fibers (I, II).
2. Develop CAM loaded matrices (I, II) and pleurocidin loaded matrices (III). CAM and pleurocidin were selected as antimicrobial molecules useful for wound infection treatment. In both cases, the electrospinning parameters needed to be studied and controlled for process optimization.
3. Characterise the morphology and drug content analysis of electrospun matrices (I, II, III).
4. Characterise the matrices using solid state analysis (I), mechanical properties assays (II), wettability (I) and drug release assays (I, III).
5. Evaluate the safety and biocompatibility of CAM loaded matrices (II).
6. Assess the antimicrobial action of drug loaded matrices (II, III).
7. Understand the activity of pleurocidin and different biocides against various antimicrobial-resistant wound pathogens (III) and to investigate the phenotypic effects (synergism, antagonism, or indifference) developed between them (III) as a potential combination treatment for wound healing.

5. MATERIALS AND METHODS

A summary of materials and methods is presented below. More detailed description of the methods is given in publications I–III.

5.1. Materials

5.1.1. Active pharmaceutical ingredients

Antimicrobial agents chloramphenicol (CAM) (I, II) and pleurocidin (III) were selected to be incorporated into electrospun matrices. CAM was obtained from Sigma-Aldrich Inc. (Darmstadt, Germany) and peptides were purchased from Cambridge Research Biomedicals (Cleveland, UK) and Pepceuticals (Enderby, UK) as desalted grade and amidated at the C-terminus. All AMPs were further purified.

Different biocides were studied (III): chlorhexidine digluconate, benzalkonium chloride, silver nitrate (BioReagent, >99% (titration)), silver sulfadiazine, octenidine dihydrochloride (octenidine) and PVP-iodine. All these biocides were purchased from Sigma-Aldrich.

5.1.2. Polymers, solvents and buffers

Polycaprolactone (PCL; Mn 80,000) (I, II) and polyvinyl alcohol (PVA, KURARAY POVALTM 26-88 FA, low MW, partially saponified) (III) were used as carrier polymers. PCL was obtained from Sigma-Aldrich while PVA was obtained as a gift from Kuraray.

Different solvents were used in combination as solvent systems (I, II) for PCL and CAM electrospinning. These were: acetone (ACE), chloroform (CF), dichloromethane (DCM), dimethyl sulfoxide (DMSO), tetrahydrofuran (THF), acetic acid (AA), and formic acid (FA). Trifluoroacetic acid (TFA), acetonitrile, and AA were used for peptide purification. All solvents mentioned were purchased from Sigma-Aldrich. Distilled water was selected as solvent (III) for PVA and pleurocidin electrospinning.

PBS (pH 7.4) was used for different applications (I, II, III).

5.1.3. Bacteria, fibroblasts, and growth media

Baby hamster kidney cells (BHK-21) were used for cell studies (II). Fibroblasts were grown in Glasgow minimal essential medium (GMEM; PAN Biotech, GMBH Aidenbach, Germany) supplemented with 7.5% fetal bovine serum (FBS), 2% tryptose phosphate broth (TPB, Difco, USA), 4-(2-hydroxyethyl)-1-piperazineethanesulfonic acid (HEPES) 1 M, 100 µg/mL penicillin (Sigma-Aldrich) and 100 µg/mL streptomycin (Sigma-Aldrich). Dulbecco's modified Eagle's medium (DMEM; phenol red, and serum-free medium) purchased from Sigma-Aldrich was used to study cell attachment and growth (II).

Relevant wound infection pathogens were used in these studies for the testing of antimicrobial activity. *Escherichia coli* DSM 1103 (II) and *Pseudomonas aeruginosa* DSM 1117 (II), were obtained from the Leibniz Institute DSMZ-German Collection of Microorganisms and Cell Cultures.

Strains utilized in the antibacterial activity studies of the peptide and biocides (III) included *Acinetobacter baumannii* AYE, *A. baumannii* ATCC 17978, *Pseudomonas aeruginosa* PAO1 (reference laboratory strain, obtained from infected wound), *P. aeruginosa* NCTC 13437 (multi-drug resistant). These bacteria along with epidemic methicillin-resistant *Staphylococcus aureus* EMRSA-15 (NCTC 13616), *Klebsiella pneumoniae* M6, NCTC 13368, and *Escherichia coli* NCTC 12923 were selected as relevant multiresistant bacteria to study the potential antimicrobial activity of the electrospun AMP-loaded matrices and peptide in solution. Bacteria specified above as NCTC were obtained through the British National Collection of Type Cultures (NCTC).

5.2. Methods

5.2.1. High performance liquid chromatography purification (III)

The crude peptide purchased was purified (III) using reverse phase chromatography with a Waters SymmetryPrep C8, 7mm, 19 x 300 mm column. A gradient of H_2O/TFA 0.1% and acetonitrile/TFA 0.1% was used and it is specified in **Table 5**. The collected phase was then vacuum centrifuged to eliminate acetonitrile, lyophilised, resolubilised in 10% AA and lyophilised again, removing the TFA counterion.

Table 5. Gradient elution program for peptide HPLC purification. Key: TFA: trifluoroacetic acid.

Time	% Acetonitrile/TFA	% H_2O/TFA	Flow (mL/min)
0	5	95	6.5
90	60	40	6.5
95	90	10	6.5
110	90	10	6.5
115	5	95	6.5
129	5	95	6.5
130	5	95	6.5

5.2.2. Preparation and characterization of electrospinning solutions (I, II, III)

In order to test the effect of humidity on the electrospinning process, different solvent systems and polymer concentrations were used (I, II). These solutions were magnetically stirred overnight and only up to 1 hour before electrospinning, when the polymer was completely dissolved, the antibacterial drug CAM was included in the mixture when needed.

In the case of matrices prepared using PVA (III), its dissolution in distilled water was enhanced by heating up the flask to 80 ± 5°C for up to 1 hour (Palo et al., 2019). The mixture was magnetically stirred overnight at room temperature (RT), and the AMP was added and stirred 20 ± 5 min prior to electrospinning.

All electrospinning solutions successfully electrospun are summarised in **Table 6**.

To properly understand the differences in rheological behaviour between the solvent systems and the polymer concentrations used (I,II), the viscosity was measured using an Anton Paar Physica MCR 101 (Anton Paar GmbH, Ostfildern, Germany) rotary rheometer. The viscosity was measured in triplicates using a rotational shear test and controlling the shear rates between 100 s^{-1} to 0 s^{-1} at 25.0 ± 0.2 ºC. Besides, the viscosity of two weeks aged PCL 15% w/V (THF:DMSO; 90:10 V/V%) and PCL 15% w/V (AA:FA; 75:25 V/V%) solutions was measured in order to understand the possible viscosity changes during storage.

5.2.3. Preparation of electrospun matrices (I, II, III)

Diverse electrospun matrices were prepared using different materials, parameters, and electrospinning techniques. Some of these preparations have not been stated here as the active molecule incorporated was found to be degraded or trapped in the final electrospun matrix, being unable to achieve their ultimate aim. Fortunately, a number of matrices were successfully developed that allowed us to study our multiple aims, beginning with the focus on developing matrices with pores on fibers (I), and the development of antimicrobial matrices (II, III). All matrices (I, II, III) were prepared using an ESR200RD robotized electrospinning system (NanoNC, Seoul, Republic of Korea) at RT (24 ± 2°C) and a distance between the spinneret and collector plate of 15 cm.

As the developed electrospun matrices were prepared using different techniques and parameters, the methods used in these preparations have been divided into the following paragraphs.

For the preparation of PCL and PCL-CAM matrices (I, II), monoaxial electrospinning using a plastic syringe (12 mL, 15.89 mm inner diameter) supplemented with a blunt metal needle (23G) was selected, collecting the fibers onto a stationary flat plate or a roller collector covered with an aluminium foil rotating at 40 rpm. The solution rate was 1 mL/h. The relative humidity (RH) within the electrospinning chamber was varied using humidifier AEG LBF 7138 (EHT Haustechnik GmbH, Nürnberg, Germany) using 19, 30, and 65% RH (I) termed

as low, medium, and high humidity, respectively or only 19% and 65% RH (II). The applied voltage was varied between 11, 13, and 15 kV (I) or 11 and 15 kV (II).

PVA matrices with and without AMP (III) were electrospun using the coaxial electrospinning technique. For this purpose, a plastic syringe (12 mL), supplemented with a concentric needle (p/n100-10- COAXIAL-2218, Rame-Hart Instrument Co) with an inner needle size of 22G and an outer needle size of 18G, was loaded with 4 mL of polymeric solution with and without active ingredient. For electrospinning, the two syringes were filled with the same amount of polymer solution. The amount varied between formulations from 2.5 to 4.5 mL. Fibers were collected on a roller collector rotating at 25 rpm and covered with an aluminium foil. The solution flow rate was lower in this case, being 0.2 – 0.3 mL/h and the RH varied between 16 and 30% (ambient conditions). The voltage selected was 15 kV.

Electrospun fiber matrices were stored in airtight plastic zip-lock bags at ambient conditions until one day before further analyses, when the samples were stored for 24 h at 0% RH in a desiccator (I, II). In the case of PVA matrices (III), these were stored at RT and 0% RH inside a vacuum desiccator (above silica gel) from their production until further analysis.

5.2.4. Characterisation of electrospun matrices

5.2.4.1. Morphology (I, II, III)

A scanning electron microscope (Zeiss EVO 15 MA, Germany) was used to study the surface topography of every matrix, its morphology, and fiber diameter (I, II, III). The randomly selected samples were mounted on aluminium stubs and magnetron-sputter-coated with a 3 nm platinum layer in an argon atmosphere prior to microscopy. Images of the top layer were collected and analysed. The mean diameter (N=100) (I, II, III) and the surface layer pore diameter (N=30) (I) were measured using Image J v.1.53i. software and shown together with the standard deviation (SD).

Besides, the porosity of the fibers was determined (I) based on the density and geometry of the matrix. The porosity was calculated using Eq. 3:

$$Porosity = \left(1 - \frac{\rho f}{\rho m}\right) \cdot 100 \quad (Equation\ 3)$$

Where ρf is the apparent density of the fiber matrix and ρm is the bulk density of the corresponding materials, hence PCL 1.145 g/ cm^3 and CAM 1.547 g/cm^3 were used. The apparent density was calculated based on the weight and volume of the matrix. The latter was calculated by measuring the thickness of the fiber matrix using a Precision-Micrometer 533.501 (Scala Messzeuge, Dettingen, Germany) and using the surface area (1 cm^2).

Surface porosity and specific surface area (S_{BET}) were determined (I) using Accelerated Surface Area and Porosimetry System (ASAP) 2020 (Micromeritics, Norcross, GA, USA). Further details about these methods are described in **Publication I**.

5.2.4.2. Mechanical analysis (II)

The mechanical behaviour of the dry and wet fiber matrices was studied (II) using a Brookfield CT3 Texture Analyzer (Middleboro, MA, USA) equipped with a 10 kg load cell. The tensile test method was used for analysis in line with the ASTM D-638 and ISO10350:1993 mechanical testing guidelines. Roller Cam accessory grips (TA-RCA; width of 25 mm) were used to fix the sample. Measurements were developed under ambient conditions. For wet fiber matrices, these were immersed in a buffer solution for 3 min or 24 h and then analysed. The thickness was measured as described above (*5.2.4.1. Morphology*). Young's modulus (MPa, linear region) and tensile strength (zero slope) (II) were calculated from each corresponding stress-strain curve. TexturePro CT software (AMTEK Brookfield, Middleboro, MA, USA) was used for data collection and analysis. Further details on sample preparation and parameters can be found in **Publication II**.

5.2.4.3. Contact angle, swelling, and weight loss (II)

The sessile drop method (OCA 15EC, DataPhysics Instruments GmbH, Filderstadt, Germany) was used in order to understand the hydrophilic/hydrophobic nature of the electrospun matrices and their wettability (II). The contact angle formed by a 5 μL drop of PBS at RT was measured at 0 and 30 s time-points. The contact angle was analysed using SCA20 software (DataPhysics Instruments GmbH, Filderstadt, Germany).

For swelling index and weight loss measurements (early *in vitro* degradation), the fiber matrices (II) were cut, weighted, and immersed in PBS at 37 ºC for 24 h. After that, the samples were placed on plastic Falcon Cell strainer sieves (Fisher Scientific, Thermo Fischer, USA) placed on a 50 mL Falcon tube to remove the free surface solution and weighed. The swelling index and weight loss were calculated as reported previously (Nazemi et al., 2014).

5.2.4.4. Solid state analysis (I)

The XRD patterns of the pure starting materials and electrospun fiber matrices were obtained with the X-ray diffractometer (D8 Advance, Bruker AXS GmbH, Karlsruhe, Germany). The XRD experiments were carried out in a symmetrical reflection mode (Bragg–Brentano geometry) with CuKa radiation (1.54 Å). The scattered intensities were measured with the LynxEye one-dimensional detector including 165 channels. The angular range was from 5º to 40º 2θ and the step size of 0.0198º 2θ.

ATR-FTIR spectroscopy was performed on pure substances and electrospun fiber matrices using an IR Prestige-21 spectrophotometer (Shimadzu Corp., Kyoto, Japan) and Specac Golden Gate Single Reflection ATR crystal (Specac Ltd., Orpington, UK). The spectra were collected between 600 and 4,000 cm^{-1}, each spectrum was the average of 60 scans. Spectra were collected using Shimadzu IRsolutions 1.5 software (Shimadzu Corp., Kyoto, Japan), and all spectra were normalized with OriginLab 6.1 software (OriginLab Corporation, Northampton, USA).

Thermal analysis was performed using DSC (PerkinElmer DSC4000, Melville, New York, USA). The crystallinity was calculated as shown in the literature before (Kweon et al., 2003). The electrospun fiber samples were weighed and sealed in an aluminum pan with 2 pinholes in the lid. Solvent casted films of the same composition were used for comparison (preparation of solvent casted films explained in **Publication I, Supplemental Appendix A**). A nitrogen purge with a flow rate of 20 mL/min was used in a furnace. The DSC runs were performed at a heating rate of 10 ºC/min from 30 ºC to 180 ºC for all samples. All DSC curves were normalized to a sample weight. Indium was used as a reference material.

5.2.4.5. Drug content (I, III)

The CAM loading and its distribution within the fiber matrix was studied (I) using the Shimadzu Prominence LC20 HPLC system with a PDA detector at 275 nm (Shimadzu Europa GmbH, Duisburg, Germany), according to the official European Pharmacopeia method for a related substance: CAM sodium succinate. HPLC was equipped with a column Phenomenex Luna C18(2), 250 x 4.6 mm, 5 µm, and the mobile phase used was a 20 g/L solution of phosphoric acid R, methanol R, and water R (5:40:55 V/V/V). The flow rate was 1.0 mL/min, and the injection volume was 20 µL. The CAM-loaded PCL fiber matrices were cut into 1 cm^2 pieces, weighed, and dissolved in CF and methanol (75:25%V/V). Pieces were taken from both the centre and edges of the fiber matrix to see if differences occurred in drug distribution.

The pleurocidin content was measured (III) using larger pieces of matrix (4 cm^2) as the theoretical content was smaller and a larger matrix was needed in order to detect the drug. These pieces were dissolved in an organic solvent and studied using the same HPLC system, detector, and column at 220 nm. For mobile phase A 0.1% (V/V) TFA in water and mobile phase B 0.1% (V/V) TFA in acetonitrile was used. The flow rate was 1.0 mL/min and the injection volume was 20 µL. Peptide solution in water (using the theoretical peptide concentration in the fiber matrix) was used as a control.

5.2.4.6. Drug release (I, III)

The CAM release was measured *in vitro* (I) using 1 cm^2 samples. These matrices were weighed and immersed into 10 mL of PBS at 37 ºC in 50 mL plastic tubes

which were put into a dissolution apparatus vessel (Dissolution system 2100, Distek Inc., NJ, USA) containing water and maintained at 37 ºC. The tubes were rotated by paddles at 100 rpm. Aliquots of 2 mL were removed and replaced with the same amount of buffer at set time points. The aliquots were analysed using UV-spectrophotometer (Shimadzu UV-1800). The wavelength of maximum absorption (λ = 278 nm) was chosen for the drug release analysis.

The pleurocidin release was studied (III) using the same apparatus as with CAM loaded matrices. However, in this case, 4 cm^2 samples were used, which were introduced in 5 mL of PBS at 37 ºC. Aliquots of 200 µL were removed and replaced with the same amount of buffer at set time points. These aliquots were analysed at λ = 220 nm. A control peptide solution based on the theoretical concentration was used to study the peptide behaviour and stability in the test conditions and collected at equal timepoints.

5.2.4.7. Cytotoxicity testing (II)

The fibroblast attachment and biocompatibility in electrospun matrices of different porosity and fiber diameters were evaluated using the MTS assay (II). The matrices were placed into 24-well plates using cell crown inserts (CellCrown, Scaffdex Oy, Finland). Then, a BHK-21 cell suspension (consisting approximately of 10^4 cells) was seeded on the electrospun matrices and DMEM, phenol red, and serum were added. The number of cells was determined using trypan blue exclusion (Invitrogen, Thermo Fischer, USA). After 24 h of incubation, more medium was added and, after 48 h, the matrices were removed from the inserts, placed in PBS, and transferred to DMEM. The MTS reagent (K300-500, Biovision, USA) was then added and incubated at 37 ºC and 5% CO_2 for 45 min. After this time, the matrices were removed, and the absorbance of the obtained coloured media was measured using a plate reader (Invitrogen, Thermo Fischer, USA) at 490 nm. The eukaryotic cell attachment and growth were also investigated using microscopy techniques (II).

SEM was performed using the same microscope mentioned in *5.2.4.1. Morphology*. However, in this case, the matrices were rinsed twice with PBS and fixed with 4% formaldehyde for 30 min at RT. Afterwards, they were rinsed again and dehydrated with increasing concentrations of ethanol (30, 60, and 96%). When dry, the SEM samples were prepared as described above.

Confocal Fluorescence Microscopy (CFM) using a LSM710 (Carl Zeiss, Munich, Germany) and Zen software (Zeiss) were also used for a deeper visualization of fibroblast attachment onto the fibers. After 48 h of the cell attachment experiment, matrices were removed from the inserts and rinsed in PBS solution. Then, they were placed in FM 4-64 (Invitrogen, Thermo Fischer, USA) staining solution for 2 minutes before being placed onto a microscope slide. To evaluate cell penetration through the fiber matrix, 3D micrographs were constructed using the *z*-stack images from CFM using Zen software. The *z*-stack image consisted of 101 slices with a depth of 134.95 µm, and the cell infiltration was measured using 3D measurements.

5.2.5. Antibacterial testing (II, III)

5.2.5.1. Antibacterial activity of AMPs and biocides in solution (III)

Minimum inhibitory concentration

The antibacterial activity of AMPs and biocides was assessed using a modified two-fold broth microdilution assay with modal MICs generated from at least three biological replicate experiments. The method broadly followed the EUCAST methodology (EUCAST, 2024), but in this case, non-cationic-adjusted MHB and polypropylene plates were used, which is recommended for cationic AMPs (Wiegand et al., 2008). All peptide and biocides stock solutions, except for silver sulphadiazine, were dissolved in Milli-Q water. Silver sulphadiazine was dissolved in DMSO:MHB (1:100) for solubility enhancement. These stocks were diluted in a two-fold dilution in media down on a 96-well plate (Greiner Bio-One GmbH, Frickenhausen, Germany) to a final volume of 100 µL. The same volume of bacterial suspension was then added, at a starting concentration of 10^5 CFU/mL, from a diluted overnight culture. Plates were incubated for 20 h at 37 ºC in static conditions. The OD_{600} was determined using a Clariostar plate reader (BMG Labtech). The MIC was defined as the lowest concentration where OD_{600} was below a value of 0.1 after subtracting the background absorbance and there was no visible growth.

Synergy checkerboard assay

Phenotypic effects (synergy, antagonism, additive, and indifferent) between pleurocidin and biocides in solution were assessed using standard microdilution checkerboard assay, whose schematics are shown in **Figure 6**.

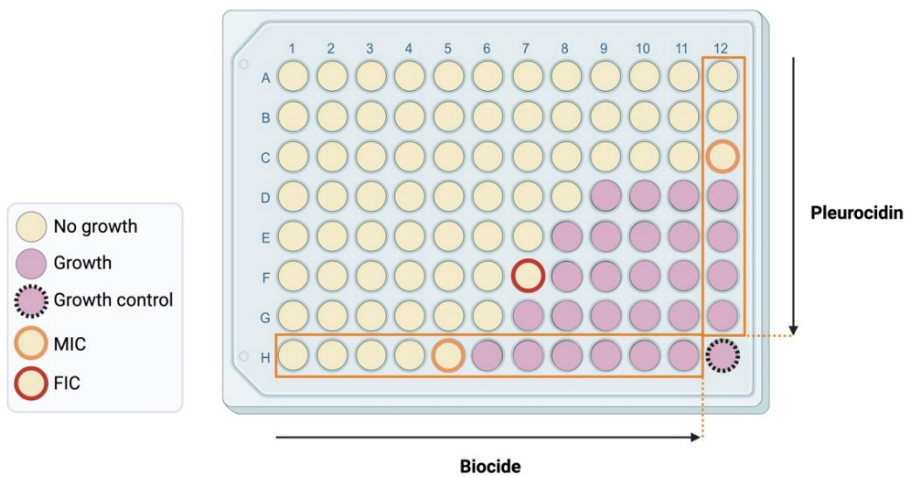

Figure 6. Checkerboard method for antimicrobial synergy testing. Created with BioRender.com.

The two-fold dilution series of pleurocidin and one biocide were prepared in MHB in each 96-well polypropylene microtiter plate to a final volume of 100 µL. The biocide was first diluted across the columns leaving the last one free from biocide (peptide MIC column). Then, the pleurocidin was diluted down the plate, leaving the last row free from pleurocidin (biocide MIC row). Afterwards, 100 µL of bacterial suspension, at a starting concentration of 10^5 CFU/mL, from a diluted overnight culture were added into each well. Preparing these two-fold dilutions in the same plate results in the second compound added (pleurocidin) decreasing its concentration by half with each dilution. However, the first compound (biocide) is not always reduced by half with each dilution. The biocide was first diluted across columns and then, during the pleurocidin dilution process, it got reduced again across rows. In the first row, where pleurocidin solution was added, the biocide was diluted by half. However, when pleurocidin was diluted through the following rows, the starting solution contained in row A consisted of pleurocidin but also biocide. This biocide is transferred to the following row, increasing its final concentration, and so this occurs across the plate. This deviation from a two-fold dilution series has been considered, and real concentrations for biocides calculated and incorporated into the analysis (**Publication III, Figure 5**). The growth or absence of growth was established using the same definition as the MIC. The FIC was calculated with the formula previously described in **Equation 2**.

FIC was calculated using three independent experiments and presented together with an arithmetic mean. FIC ≤ to 0.5 were considered strongly synergistic, and consistent with a recent interpretation of FIC, which stressed the importance of measuring the MIC in the same microarray plate, values of 0.5 to <1 were considered to indicate weak synergism (Fratini et al., 2017). Indifferent effect is defined when 1 < FIC < 2 and antagonism behaviour for FIC values ≥ 2 (EUCAST, 2000).

5.2.5.2. Antibacterial activity of drug loaded matrices (II, III)

Disk diffusion

Pleurocidin antibacterial activity within electrospun matrices was investigated using a disk diffusion assay. An overnight culture was diluted in MHB to an OD_{600} 0.01 and 200 µL of the bacterial suspension were spread around a MH agar plate. The matrices were cut into 0.6 cm diameter disks and controls were prepared using sterile filter paper, charging them with the calculated amount of peptide depending on the matrix weight. Pristine matrices and sterile filter paper (same size) were used as negative controls. When the MH agar plate and charged filter papers were dry, all disks were placed onto the agar plate. Agar plates were incubated at 37 ºC overnight. Then, the inhibition zone was measured.

Antibacterial activity assay

The antibacterial activity of pleurocidin loaded matrices was analysed using MIC-like assay (III). Pieces of 0.6 cm diameter of the electrospun matrices were

directly inserted into the wells of a 96-well polypropylene plate previously filled with MHB. The theoretical concentration of pleurocidin in each well was calculated based on each independent matrix weight and this information was used for the preparation of positive controls. Bacteria at a starting concentration of 10^5 CFU/mL, from a diluted overnight culture, were then added. Plates were incubated for 20 h at 37 ºC in static conditions. Matrices and controls were carefully removed from each well before using the plate reader (same Clariostar system that was used for MIC determination of biocides and pleurocidin in solution). Bacterial growth was visualised against a black surface.

Antibiofilm assay

The biofilm formation protocol used with CAM loaded matrices (II) was based on the work of Brackman et al. (Brackman et al., 2011), proved in our previous study (Preem et al., 2017). Overnight liquid cultures of *E. coli* and *P. aeruginosa* were grown from DMSO stocks in LB. The culture was diluted to 5 x 10^7 CFU/mL using DMEM supplemented with 10% FBS and 1 mL was placed onto 1 cm^2 matrices in 24 well-plates. These were incubated at 37 ºC for 24, 48, and 72 h. After that, the samples were rinsed twice with PBS and placed into 1 mL of fresh PBS in an Eppendorf tube. In order to disrupt the biofilm, alternating 30 s cycles of vortexing (Vortex-Genie 2, Scientific Industries) and sonication (Bandelin Sonorex digital 10 P, operating at 20% of maximum power) were performed. Each cycle was repeated 6 times, as this was proven to provide the best compromise between biofilm disruption and bacterial viability. The CFUs were determined by making 10-times dilutions of the suspension, plating 5 µL drops on LB agar plates, and incubating overnight at 37 ºC. Planktonic bacteria were as well plated as controls.

5.2.6. Statistical analysis

Results were expressed as an arithmetic mean (at least n=3) ± SD, unless mentioned otherwise.

Statistical significance between fiber diameter distributions (I, II, III) of different formulations was calculated by applying one-way ANOVA and post hoc *t*-test (two-sample assuming unequal variances) with MS Excel 365 software ($p<0.05$). In the case of multiple comparisons (II), Holm's method was used for adjusting *p*-values.

The drug release data (I) were fitted into mathematical models using the DDSolver, and add-in program for MS Excel. The Akaike Informative Criterion (AIC) and R^2 value were used to evaluate the applicability of the models.

A non-linear regression model (four-parameter logistic curve) was fitted using absorbance values (OD_{600}) of drug solution controls for bacterial strains (III). Data analysis was performed using GraphPad Prism 9 and Microsoft Excel v.16.67.

6. RESULTS AND DISCUSSION

6.1. Development of antimicrobial electrospun matrices

6.1.1. Composition and characterisation of electrospinning solutions (I, III)

In order to develop nano- or microfibrous matrices by electrospinning technique for wound healing applications there are a number of factors that need to be considered.

The selection of the polymer is an essential part, as it will be the base of the scaffold. For the purpose of wound healing, only safe and biocompatible polymers can be used, which is the case of both polymers selected: PCL and PVA. These polymers are biodegradable and well-studied molecules with good electrospinnability (Ali Zadeh et al., 2014; Vogt and Boccaccini, 2021). The polymer concentration directly modifies the viscosity of the solution and highly affects the electrospinning process (Luraghi et al., 2021). Therefore, different concentrations were tested and used for method optimization which are summarized in **Table 6**.

The solvent or solvents used to dissolve polymers and drugs also influence the process and the final physicochemical characteristics of the electrospun matrices. All solvent systems selected were known to be suitable for electrospinning based on their solubility, boiling point, and dielectric constants (Woodruff and Hutmacher, 2010). The organic solvents selected for the development of PCL matrices were carefully selected and evaluated for their ability to form porous fibers. The solvent systems selected are summarized in **Table 6**.

Two drugs (CAM and pleurocidin) were loaded in selected solutions, as stated in **Table 6**. As previously mentioned, these molecules possess antimicrobial properties although their chemical structures, properties, and clinical use widely differ.

The stability and potential degradation of these drugs in the chosen solvents were tested prior to electrospinning, confirming suitability.

Table 6. Polymers, solvents and drugs used for electrospinning. Key: AA: acetic acid; ACE: acetone; CAM: chloramphenicol; CF: chloroform; DCM: dichloromethane; DMSO: dimethyl sulfoxide; FA: formic acid; PCL: polycaprolactone; PVA: polyvinyl alcohol; THF: tetrahydrofuran. Drug concentration units are w/w based on the dry weight of the solid material.

Polymer	Polymer concentration %w/V	Solvent or solvent system	Solvent ratio % V/V	Drug	Drug concentration
PCL	12.5	THF:DMSO	90:10	-	-
	15	THF:DMSO	90:10	-	-
	15	THF:DMSO	90:10	CAM	4 % w/w
	12.5	CF:DMSO	90:10	-	-
	15	CF:DMSO	90:10	-	-
	12.5	ACE:DCM	50:50	-	-
	15	ACE:DCM	50:50	-	-
	15	AA:FA	75:25	-	-
	15	AA:FA	75:25	CAM	4 % w/w
PVA	Shell: 15 Core: 16	H_2O	NA	-	-
	Shell: 15 Core: 16	H_2O	NA	Pleurocidin (core)	0.7 % w/w

In order to characterise electrospinning solutions and predict their behaviour for electrospinning, the viscosity of solutions was measured (II). Selected solutions were the ones used for PCL 15% w/V without CAM, which enables to compare the effect of different solvent systems in terms of final solution viscosity. Different shear thinning properties and different viscosities were observed for each sample (**Publication I, Figure 1**). However, the same general pseudoplastic behaviour was found in all samples, wherein an increase in shear rate resulted in a decrease in viscosity.

The solution prepared with AA:FA as a solvent system was the one with the lowest viscosity, while others had similar viscosity values. These differences in viscosity are supported by the literature (Dobrzański et al., 2014) and can be explained due to the fact that different solvents can modify the polymer structure. They can narrow its molecular weight distribution through electrostatic interactions and/or degrade the polymer, resulting in a decrease in both its molecular weight and the viscosity of the solution (Chhabra and Richardson, 2011).

From these analysed samples, AA:FA and THF:DMSO solvent systems were selected for further evaluation as the ones with the lowest and highest viscosity values. In this case, these solutions were kept for two weeks in closed vials surrounded by parafilm and then, their viscosity was measured. This additional storage test gave information regarding the stability and change in their rheology behaviour, essential to design electrospinning experiments within applicable time ranges. After two weeks of storage, PCL 15% w/V AA:FA solution showed lower viscosity values which may be explained because AA is involved in the acidic hydrolysis of PCL, speeding up its degradation (Ekram et al., 2017). On the other hand, PCL 15% w/V THF:DMSO solution increased its viscosity after that time. We believe that this is due to the high evaporation rate of these solvents even when the vial was tightly closed. As observed, none of these solutions maintained their properties after storage, thus the electrospinning process was always conducted using fresh solutions.

6.1.2. Design of the electrospinning set-up (I, III)

PCL fibers were obtained using monoaxial electrospinning and simple drug blending where applicable. However, in the case of pleurocidin loaded PVA fibers, coaxial electrospinning was selected as a way to protect the active molecule, known to be easily degradable (Lee and Lee, 2008), and achieve higher drug concentrations within electrospun matrices.

The influence of various electrospinning parameters was investigated (I) and thus, the polymer concentration, voltage, and humidity were varied in order to investigate their effects on the final electrospun product, with a special interest in the formation of porous fibers.

In all cases, the RT (24 ± 2°C), the distance between the spinneret and the collector plate (15 cm) and the plastic syringe (12 mL) were kept constant. However, the flow rate was varied for process optimization.

In the case of PVA matrices, the main goal was to develop antibacterial matrices with high and stable AMP content and thus, the electrospinning parameters were optimised for this purpose. This setup required the use of a concentric needle that enabled to conduct coaxial electrospinning.

Successful and reproducible electrospinning was obtained with all formulations, although some selected parameters did not allow specific samples to create well-formed fibers due to the presence of beads, needle clogging, or solution dripping from the syringe.

6.1.3. Morphology of electrospun matrices and fiber porosity (I, II, III)

Using THF:DMSO solvent system and PCL 12.5% w/V, fibers with beads were produced, while PCL 15% w/V produced nice electrospinning and more uniform fibers (**Figure 7 A**), thus the latter polymer concentration was selected for further studies.

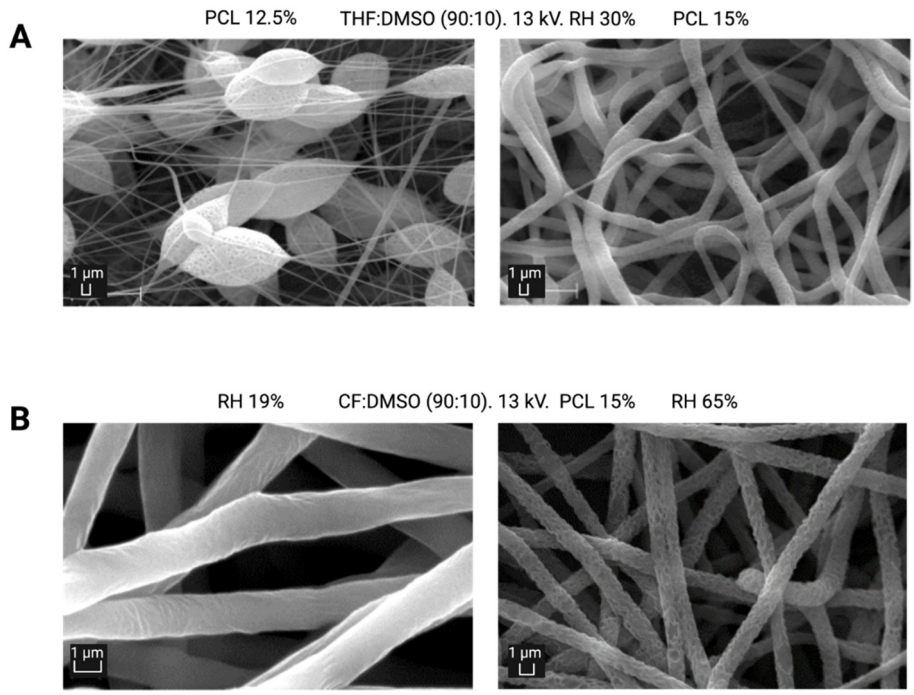

Figure 7. The effect of polymer concentration and RH on the morphology of electrospun fibers. **A.** Bead formation when using PCL 12.5% vs. fiber formation when using PCL 15% on fiber matrices prepared with THF:DMSO (90:10), at 13 kV and RH 30%. **B.** Smooth fibers when electrospinning was conducted at RH 19% vs. porous fibers when conducted at RH 65% on matrices prepared with CF:DMSO (90:10), at 13 kV and PCL 15%. Key: CF: chloroform; DMSO: dimethyl sulfoxide; PCL: polycaprolactone; THF: tetrahydrofuran; RH: relative humidity.

As expected, solutions prepared with higher PCL concentrations and thus, higher viscosity, generally produced fibers with larger fiber diameter. THF:DMSO, CF:DMSO and ACE:DCM solvent systems generated microfibers (mean fiber diameter approximately 1.5 ± 0.7 μm) while AA:FA solutions resulted in smaller fibers, creating nanofibers (0.25 ± 0.11 μm). No clear correlations were obtained between the fiber diameter and applied voltage (**Publication I, Figure 3, and Appendix Figure 2**).

However, the humidity clearly affects the morphology of the fibers (**Figure 7 B**). Using high RH conditions, porous microfibers were obtained with PCL and different binary solvent systems (THF:DMSO and CF:DMSO). However, this porous fiber morphology was not achieved under lower RH conditions (**Publication I, Figure 2**). The formation of pores on the surface of single fibers obtained by electrospinning is therefore greatly enhanced at higher RH levels, considering humidity as the main parameter affecting the pore formation when using the mentioned solvent systems and hydrophobic polymer. While increasing the voltage appeared to enhance surface porosity in single fibers, this effect was not uniformly observed across all tested solvent systems (**Publication I, Figure 3**).

The largest pores on fibers and highest fiber diameters were observed in PCL fibers when using the THF:DMSO solvent system and under high RH conditions. In contrast, fewer pores were obtained when using the ACE:DCM solvent system and no pores were observed at all when electrospinning PCL in AA:FA, even under high RH conditions (**Publication I, Figure 2**). These variations in pore size are attributed to the different evaporation rates of the solvents employed.

For further characterization and preparation of CAM-loaded fibers, various solvent systems and ambient conditions were selected. The THF:DMSO solvent system and high RH were chosen to produce "porous PCL microfibers". The AA:FA solvent system was selected to serve as a nanofiber matrix with no pores on single fibers, referred to as "non-porous PCL nanofibers". Additionally, the THF:DMSO solvent system and low RH were employed to produce microfibers with no pores on single fibers, serving as controls and termed "non-porous PCL microfibers".

SEM images were analysed to estimate the pore size on single fibers and achieve an initial understanding of the interconnectivity and an estimation of the cross-sectional pore area. Although a deeper pore size distribution analysis could have been conducted as reported previously using confocal laser scanning microscopy, segmentation of SEM micrographs, or other artificial visualization systems (Choong et al., 2015; Guo et al., 2018; Hotaling et al., 2015), these studies were beyond the scope of this work. The mean pore diameter for porous PCL microfibers without CAM was 0.28 ± 0.08 μm, whereas the incorporation of CAM within the fibers showed a decrease in their mean pore diameter down to 0.22 ± 0.08 μm, although no statistically significant differences were detected between these samples. However, smaller and fewer pores were visually observed on CAM loaded porous fibers.

The incorporation of CAM influenced both the pore formation and diameter on electrospun fibers. Being in line with the previous studies (Arbade et al., 2018), the addition of CAM in PCL fibers increased the fiber diameter in all formulations (**Publication I, Table 2**). However, the incorporation of drugs into electrospun matrices does not always lead to an increase in fiber diameter. In the case of PVA matrices, the addition of pleurocidin into the process led to significantly smaller fiber diameters (from 0.60 ± 0.17 μm in pristine fibers to 0.54 ± 0.09 μm in pleurocidin-loaded fibers) (**Publication III, Figure 1**).

To evaluate the difference in the porosity of the fiber matrices, the porosity was calculated as explained in the methods section. The porosity from all electrospun matrices tested ranged from 71.60 ± 0 % in CAM loaded porous microfiber matrices to 78.60 ± 2 % in pristine porous microfiber matrices, which matches with the range discussed in the literature for PCL electrospun matrices (Cortez Tornello et al., 2014). No large differences between all PCL electrospun matrices prepared were revealed in terms of porosity percentage. However, large differences were found on the surface pore diameters of the matrices between the samples. As expected, microfiber matrices (both porous and non-porous PCL THF:DMSO matrices) exhibited larger pores between the fibers compared to the nanofiber matrices (non-porous PCL AA:FA matrices). The pore diameter of microfiber matrices ranged from 13.24 ± 4.78 μm to 21.87 ± 7.30 μm, whereas the pores in nanofiber matrices ranged from 2.88 ± 1.22 μm to 3.65 ± 1.55 μm (**Publication I, Figure 2 and Table 2**). Larger pores on the surface of the matrix are known to be formed when single fibers have larger diameters (Pham et al., 2006).

BET analyses were used to study the specific surface area of the electrospun fibers. PCL THF:DMSO porous fibers had significantly smaller specific surface area values compared to the PCL THF:DMSO non-porous microfibers and PCL AA:FA non-porous nanofibers (1.70 ± 0.02 m^2/g, 5.12 ± 0.68 m^2/g and 8.23 ± 0.11 m^2/g, respectively).

As PCL AA:FA fibers exhibited the largest surface area, N_2 adsorption isotherms were also conducted (**Publication I, Figure 5**). This method characterized the sample in a larger relative pressure (P/P_0) range in comparison with the isotherms measured using krypton. It was observed that for values $P/P_0 < 0.2$, the isotherm resembles the type I isotherm, giving some indication about the microporosity. On the other hand, the end of the curve and entire profile resembles more a non-porous II isotherm.

All things considered, these results showed that non-porous PCL nanofiber matrices had larger specific surface area despite the presence of single fiber surface porosity of the PCL microfibers, thus surpassing the effect of pores, a theory that has been proven before (Huang et al., 2003).

6.1.4. Mechanical properties of electrospun matrices (II)

Porous microfibers (obtained using the THF:DMSO solvent system at high RH), nonporous microfibers (obtained using the same solvent system but at low RH) and nonporous nanofibers (obtained using the AA:FA solvent system at low RH) were selected for further mechanical properties characterisation. All these systems were electrospun with and without CAM (**Table 6**).

Nanofiber matrices were stiffer and more plastic compared to porous microfiber matrices (**Figure 8 A, C**). Nonporous microfiber matrices were the most resistant in stress-strain curves, showing a long elongation before breaking (**Figure 8 B**). Besides, nonporous microfiber matrices were also the samples with the highest tensile strength and Young's modulus, a difference that was statistically relevant when compared to nanofibers and porous microfibers, indicating that the presence of porosity (even when fibers are formed using the same polymer and solvent system) affects the plastic deformation behaviour (**Figure 9 A, B**).

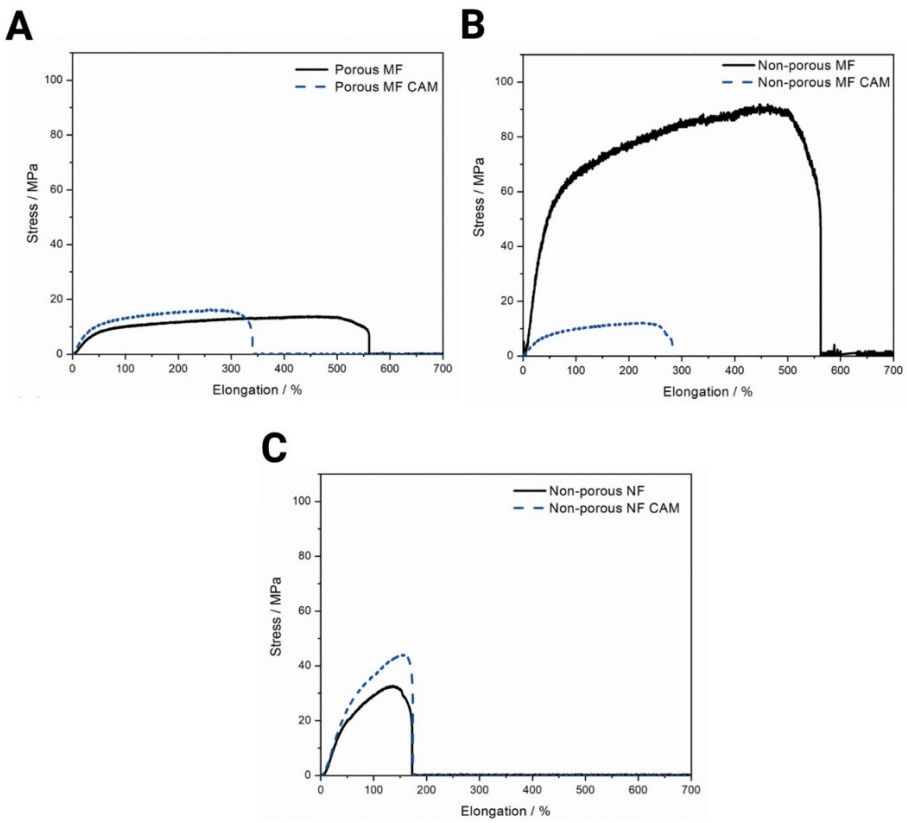

Figure 8. Representative stress-strain curves of **A.** porous microfiber matrices, **B.** nonporous microfiber matrices, and **C.** non-porous nanofiber matrices. Key: CAM: chloramphenicol; MF: microfibers; NF: nanofibers.

The fact that the presence of pores decreases the tensile strength of fibers is supported by the literature (D'Amato et al., 2018). This is studied by calculating the free volume changes through the *ortho*-positronium ($_o$-P) atom lifetime values, which gives information on the correlation between the macrostructural and microstructural porosities of fibers (Sebe et al., 2017, 2013). The size of the free volume of pores influences the mechanical properties as well as the drug release (Scheler, 2014; Zhang et al., 2017).

Nonetheless, the presence of pores on single fibers increased the elasticity of the microfiber matrices, which is shown in the highest elongation at break values (**Figure 9 C**). Besides, we have confirmed what was previously reported regarding the increase in the elongation at break for larger fibers (Tan et al., 2005). Clearly, the fiber diameter is a critical parameter on the development of matrices with different mechanical properties. It has been previously stated that PCL fibers with a diameter smaller than 500 nm had great tensile strength resistance (Baji et al., 2010).

When comparing nonporous nanofibers with porous microfibers, there appears to be a tendency for nanofibers to exhibit higher Young's modulus and tensile strength (**Figure 9 A, B**). Indeed, previous studies have reported higher tensile strength in fiber matrices with smaller diameters (Chew et al., 2006; Tan et al., 2005).

PCL fiber matrices have been widely investigated before and their mechanical properties have been declared to be affected not only by fiber diameter but also by the matrix structure and the solvent system used for electrospinning (Croisier et al., 2012). The solvent used in the electrospinning process (as it has been seen before for PCL matrices (Pok et al., 2010)) determines the polymer structure, such as its crystallinity, influencing the mechanical behaviour of matrices. Besides, the evaporation of the solvent within the fibers causes a relaxation process that significantly influences these properties (Arinstein and Zussman, 2011). For instance, nanofiber matrices (prepared with AA:FA solvent system) showed a less elastic behaviour compared to the others, which can be influenced by the solvent selection, as it has been previously described that the use of AA as an electrospinning solvent caused the formation of brittle nanofibers (Kanani and Bahrami, 2011).

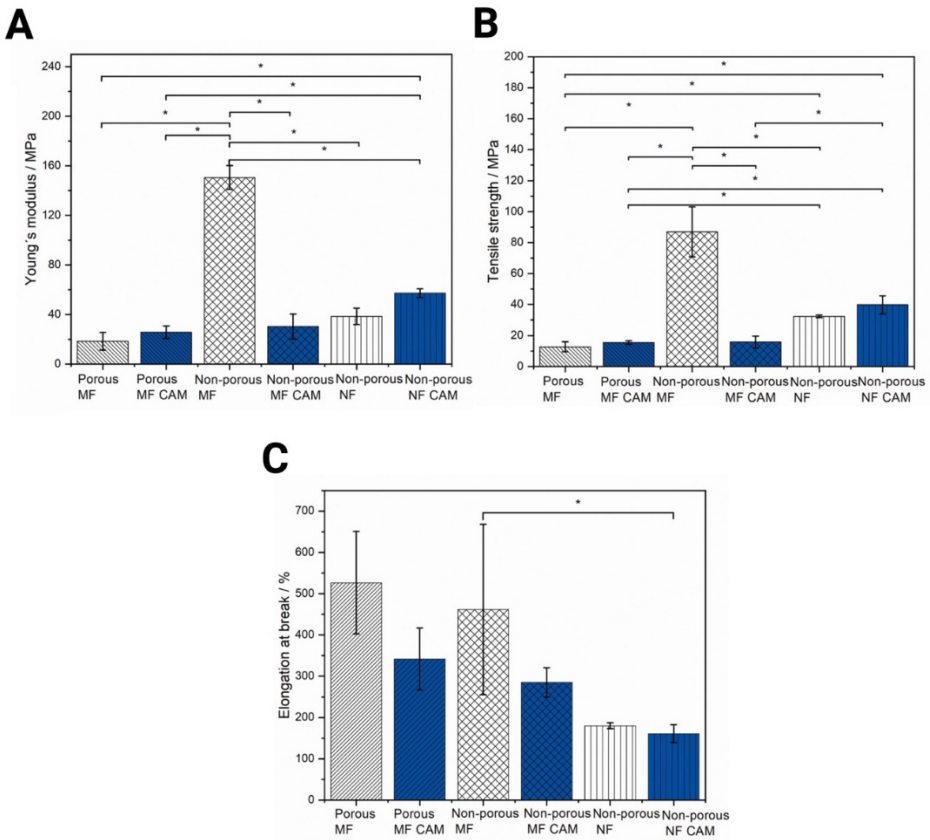

Figure 9. Mechanical properties of porous and non-porous PCL microfiber and nanofiber matrices with and without CAM. **A.** Young's modulus. **B.** Tensile strength. **C.** Elongation at break. Data are presented as mean ± SD (n=3). Key: * Statistical significance, $p < 0.05$. CAM: chloramphenicol; MF: microfibers; NF: nanofibers.

The addition of CAM into the fibers seemed to affect the mechanical properties of the matrices, although the analyses showed no statistically significant differences. The presence of CAM decreased the elongation at break in all samples, although it slightly increased tensile strength and Young's modulus values in the case of porous microfibers and nonporous nanofibers (**Figure 9**). There is no clear correlation in the effect on the mechanical properties of electrospun matrices when a drug is incorporated compared to pristine matrices, the effect depending on the selected drug (Chew et al., 2006; Nelson and Guyer, 2011). For example, it has been shown that linezolid improves the mechanical properties in PCL matrices (Tammaro et al., 2015). The outcome produced highly depends on the interactions formed between drugs and polymers, as it has been proven for polyester fibers (Chou and Woodrow, 2017), interactions that should be studied using solid-state analyses.

As these electrospun matrices are prepared with the final goal of being applied as wound dressings, more biorelevant testing was performed. Since the presence of wound exudate may influence the mechanical properties of the prepared matrices, here, buffer solution was used as a model liquid environment in which the electrospun matrices were immersed for further characterisation. There were no significant changes observed in the mechanical properties of pristine PCL matrices, compared to their respective dry matrices, after immersing the samples in buffer solution for 3 min and 24 h (**Publication II, Figure 3 A-C**). Neither were there changes in the elongation at break values for any of the samples (**Publication II, Figure 3 D**), nor significant differences in tensile strength and Young's modulus values between CAM loaded fibers and their corresponding wet conditions (**Publication II, Figure 3 C**). There were minor differences, not statistically significant, in the tensile strength of nonporous CAM-loaded fibers and porous microfibers with CAM, slightly decreasing this value when wet (**Publication II, Figure 3 A, C**), which can be explained as a consequence of drug release.

For wound healing purposes, these matrices should mimic the skin and its mechanical properties. The tensile strength of the healthy skin is approximately 20 MPa (Shevchenko et al., 2010), it has a Young's modulus value that can vary from 0.008 MPa (Pailler-Mattei et al., 2008) up to 70 MPa (Shevchenko et al., 2010) and an elongation at break range from 35 to 115% (Chen et al., 2017). Based on the results obtained, the mechanical properties of all electrospun matrices prepared comply with these ranges, successfully mimicking the skin. These properties enable the dressing to function as a tissue scaffold, where the stiffness dictates the cell-fiber matrix interactions (Jiang et al., 2018), needed to be sufficient to resist cells pulling themselves in any direction (Kennedy et al., 2017). Moreover, these electrospun matrices, used as dressings, need to be easily removable without destroying the freshly grown tissue in order to enhance and not deter the wound healing process.

6.1.5. Contact angle, swelling and weight loss (II)

Although it was shown that mechanical properties stay consistent after wetting the matrices, other attributes need to be investigated when matrices are in contact with a liquid environment as it is well known that it may increase the matrix degradation and release of the incorporated drug (Cui et al., 2008; Zupančič et al., 2018).

The nonporous pristine fiber matrices, both nano- and microfibers, showed a higher swelling index compared to porous microfiber matrices, although the difference was not statistically significant. However, there was a significant increase in the swelling index in the porous microfibers when CAM was present (**Figure 10 A**). The weight loss detected was very low in all cases (**Figure 10 B**). However, higher swelling index and weight loss were found in all CAM-loaded samples compared to pristine ones (**Figure 10 A, B**).

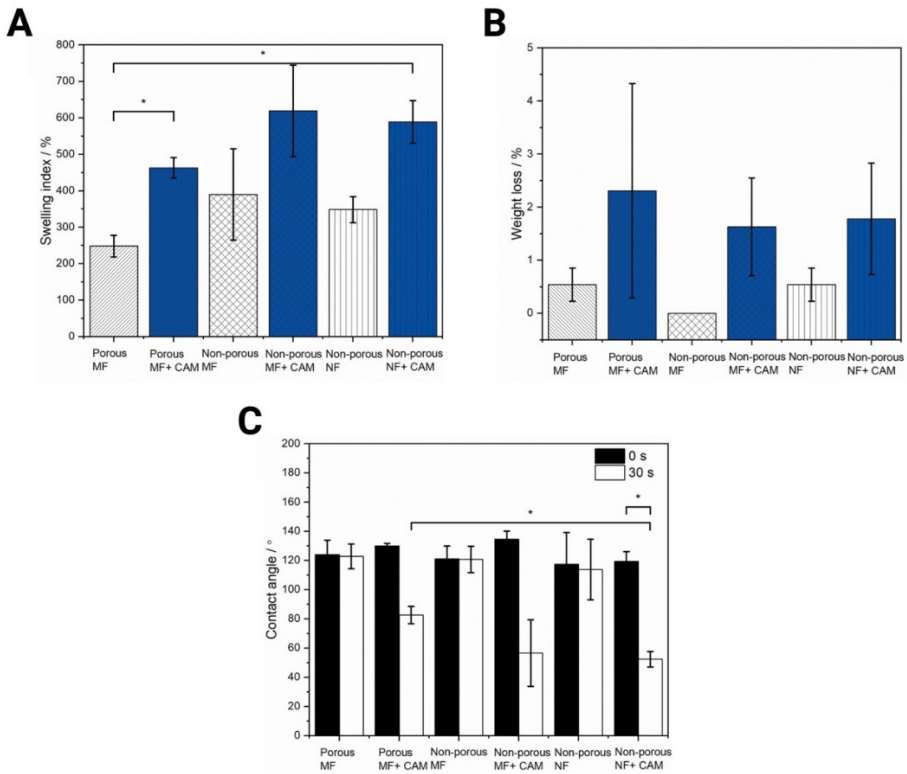

Figure 10. **A.** Swelling, **B.** weight loss, and **C.** wettability of electrospun fiber matrices when in contact with a buffer solution for different time periods. Data are presented as mean ± SD (n=3). Key: * Statistical significance, $p < 0.05$. CAM: chloramphenicol; MF: microfibers; NF: nanofibers.

The contact angle between matrices and a buffer droplet was measured in order to estimate the hydrophobicity of materials and change in time (**Figure 10 C**). After only 30 s in contact with the buffer, a difference in contact angle between the samples was observed, showing a contact angle decrease for all CAM-loaded matrices. The presence of CAM in the fibers provided a more hydrophilic behaviour to the matrices, as this molecule dissolves and enables the penetration of buffer into the scaffold. The correlation between hydrophilicity and contact angle reduction is stated in the European Pharmacopoeia (Ph. Eur, 2024). It is also noted that to enhance the wetting properties of these materials, and thus, reduce the contact angle, the surface roughness can be increased (Chau et al., 2009). However, no significant differences in contact angle were observed in our roughest mats (porous ones) compared to the others.

PCL is a hydrophobic polymer, however, the presence of CAM transmits some hydrophilicity into the matrices, which improves the drug release from the matrices (Chou et al., 2015; Preem et al., 2017; Yohe et al., 2012). As already

mentioned, all matrices containing CAM presented a higher swelling index. This change was followed by a modification in the morphology of the matrices such as an increase in fiber diameters (**Figure 10 A and Publication II, Appendix Figure S2**).

6.1.6. Solid state analysis (I)

The interaction between the drug and polymer highly influences the properties of electrospun matrices, affecting their mechanical properties, drug release and thus, their final antibacterial activity (Chou and Woodrow, 2017). The molecular structure of fiber matrices was investigated using different characterisation methods. The results showed no major changes between the spectra of all PCL electrospun matrices, suggesting that the polymer did not suffer considerable modifications although matrices were prepared using diverse solvent systems.

Using ATR-FTIR (**Figure 11 A**), PCL characteristic peaks were observed in all samples at 1,161 cm^{-1}, 1,238 cm^{-1}, and 1,720 cm^{-1}. Previously reported results were in a similar range (Kim et al., 2013). Spectral peaks found at 650 cm^{-1}, 813 cm^{-1}, 1,514 cm^{-1} and 1,681 cm^{-1} are attributable to CAM in an amorphous form, suggesting a transformation from its crystalline form to amorphous during the electrospinning process. This was confirmed by the absence of the peak at 1560 cm^{-1}, assigned only to the crystalline form of CAM (Preem et al., 2017). **Table 7** summarizes the assignments corresponding to these spectral peaks. CAM used in a similar concentration for the preparation of PCL fibers was previously detected in FTIR and XRD analyses in an earlier work (Preem et al., 2017), confirming the detection limits. Here, only in the case of nanofiber matrices (prepared using AA:FA solvent system), the characteristic CAM peak at 1,681 cm^{-1} was observed in the spectrum. Other peaks referring to CAM were also more defined in the spectra of nanofiber matrices compared to microfiber matrices (prepared using THF:DMSO solvent system), where only the peak at 1,514 cm^{-1} was clearly outlined. These differences between solvent systems in detecting the presence of CAM within matrices could probably be related to the intramolecular interactions or CAM location within the fibers (i.e. surface vs. core of the fibers) (Preem et al., 2017).

Table 7. Selected characteristic infrared bands. Key: CAM: chloramphenicol; PCL: poly-caprolactone; asym. stretch: asymmetric stretching; sym. stretch: symmetric stretching.

Molecule	Assignments	Wavenumber (cm^{-1})	Reference
PCL	C=O stretch	1720	(Elzein et al., 2004; Yang et al., 2014)
	COC asym. stretch	1238	(Elzein et al., 2004; Yang et al., 2014)
	COC sym. stretch	1161	(Elzein et al., 2004; Wang et al., 2013)
CAM	C=O stretch	1681	(Sajan et al., 2008)
	Ring stretch + N-H in-plane bend	1560	(Sajan et al., 2008)
	NO_2 asym. stretch	1514	(Sajan et al., 2008)
	C-Cl asym. stretch	813	(Sajan et al., 2008)
	Ring deformation	650	(Si et al., 2009)

XRD determination confirmed the presence of CAM in amorphous form within fiber matrices (**Figure 11 B**), as no reflections attributable to the crystalline form were observed in the diffractograms. PCL electrospun fibers containing amorphous CAM were previously reported (Preem et al., 2017). Conversely, PCL conserved its semicrystallinity, although there were alterations in the PCL reflections between samples. These may be explained by the properties of the sample surface and/or the effect of the different solvent systems on PCL. The decrease in the intensity ratio of two main peaks of PCL (I_{110}/I_{200}) confirmed the retardation of crystallization (Lee et al., 2003). However, the exact crystallinity could not be calculated due to the huge differences in the surface morphology between the samples.

Ultimately, DSC analyses were conducted. This technique confirmed the presence of CAM in its amorphous state, as no melting endotherm was observed on the thermogram (**Figure 11 C**). Moreover, in this case, it was possible to calculate the crystallinity degree of PCL fiber matrices through the melting endo-therm of PCL. Based on these results, it was observed that the solvent system used in electrospinning highly influenced the crystallinity degree of PCL. The highest crystallinity values were obtained when using pristine THF:DMSO matrices (68.09%) and the lowest when including CAM in the solution with the same solvent system (62.62%). Less PCL crystallinity was found in electrospun matrices compared to their respective control films (**Figure 11 C**). The highest T_m of PCL was shown when measuring pristine AA:FA matrices and the lowest T_m when including CAM in the same solution (same solvent system).

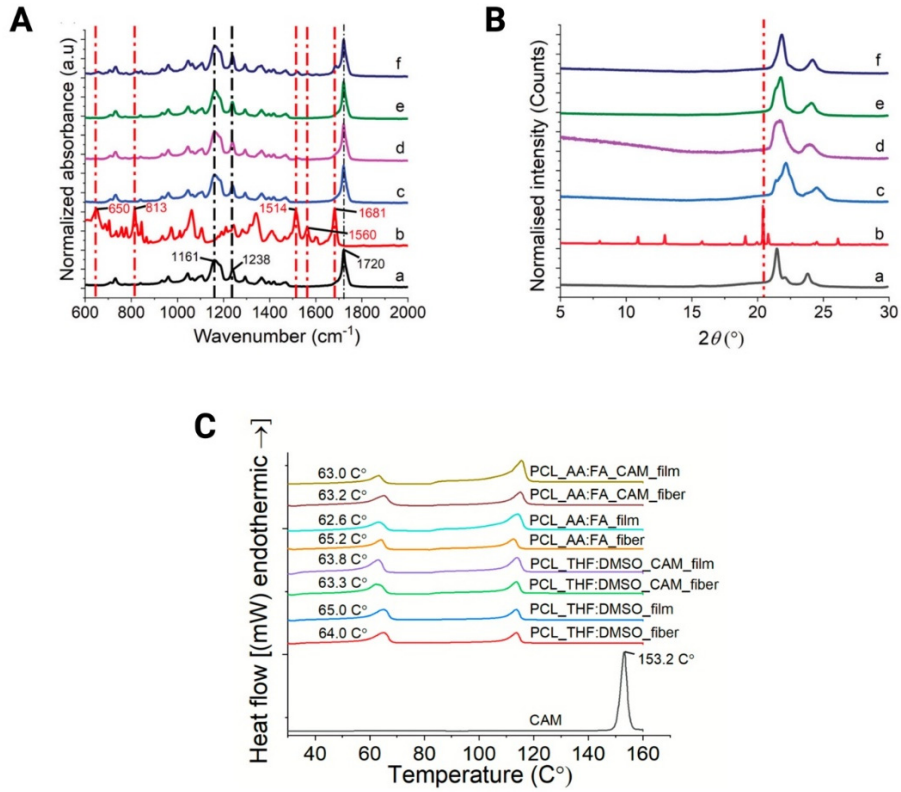

Figure 11. **A.** Attenuated total reflection infrared (ATR-FTIR) spectra, **B.** X-ray diffractometry (XRD) diffractograms and **C.** Differential scanning calorimetry (DSC) thermograms of PCL, CAM and electrospun fibers. Black and red dotted lines indicate the presence of characteristic PCL and CAM peaks/reflection. Key: a: PCL; b: CAM; c: porous microfibers; d: porous microfibers with CAM; e: non-porous nanofibers; f: non-porous nanofibers with CAM; AA: acetic acid; CAM: chloramphenicol; DMSO: dimethyl sulfoxide; FA: formic acid; PCL: polycaprolactone; THF: tetrahydrofuran.

In conclusion, CAM was found in an amorphous form within all electrospun matrices. Besides, the PCL crystallinity degree was influenced depending on the solvent system used for electrospinning. It seems that the electrospinning process has enabled the transformation of both drug and polymer into a more amorphous/less crystalline state.

6.1.7. Drug content and release (I, III)

The theoretical concentration of CAM used to prepare PCL matrices was 4% w/w based on the dry weight of the solid material. However, a drug content assay was conducted to confirm that no degradation occurred during electrospinning. The results obtained support the successful incorporation of CAM within all matrices, with more than 80% of the drug being incorporated in the worst-case scenario

(non-porous microfibers) and up to 94% in the best case (non-porous nanofibers) (**Publication I, Appendix Table A2**).

In the case of PVA matrices, the theoretical pleurocidin concentration was 0.7% w/w in solid state. This is almost three times higher than previously reported (Wang et al., 2015) and it was selected as it was hypothesised to be sufficient to kill some of the common wound pathogens. Here, HPLC measurements showed an efficient drug incorporation, as measured pleurocidin within the fiber matrix was 0.8% w/w. This small deviation from the theoretical concentration is most likely related to the analysis method. However, it confirms the peptide stability during the electrospinning process. Most probably, the use of PVA, which is a well-known hydrophilic, biocompatible, and water-soluble polymer (Aslam et al., 2018), along with water (eliminating the need for harsh solvents) in the preparation of the electrospinning solution, promoted the high stability of the drug and its incorporation into the fiber matrices. Besides, coaxial electrospinning was used, a technique that is well known for its capability to encapsulate and protect drugs (Yarin, 2011; Yu et al., 2011). Furthermore, knowing that pleurocidin is an AMP molecule that degrades relatively easily both in powder and aqueous solution at RT (within 24 h), the stability of the peptide within our PVA fibers was assessed. Consequently, after 6 months of storage at RT and 0% RH, 0.5% ± 0.04% w/w of pleurocidin was measured within the matrix, indicating that the matrices maintain sufficient peptide to remain active.

Nevertheless, a successful drug incorporation does not necessarily mean a good release, which is most needed when these dressings are conceived to fight wound pathogens. All electrospun PCL fiber matrices showed an initial burst release followed by a slower release independently of their morphology (**Figure 12**). However, the grade of burst release and the cumulative amount of released drug highly diverged. The highest amount of CAM released from the matrix was achieved from PCL nanofibers, where an initial burst release of 66.9 ± 4% occurred which followed a slower release that hit 72.6 ± 7.7% after 96 h. Without a doubt, the high surface area to volume ratio of nanofibers provided a faster release, overweighing the presence of porosity of microfiber matrices (which obtained a final release of 59.2 ± 3.2%). On the contrary, non-porous microfiber matrices released only 20% of the drug. Probably, only the drug placed on the matrix surface was released and the rest was entrapped within the matrix. It is the greatest difference in drug release reported (to the best of our knowledge) between matrices that have the exact same composition (drug-polymer-solvent) and electrospinning parameters but differ for the humidity used, and thus porosity obtained. Such large differences in the drug release have been obtained before but in that case, besides humidity, the polymer composition was also modified (Yuan et al., 2018). Many studies have been undertaken to investigate the effect of pore size and porosity of electrospun fiber matrices on drug release (Naseri et al., 2015; Soliman et al., 2011). However, there is a scarce number of reports analysing the effect of single fiber porosity on drug release behaviour (Ren et al., 2018; Yaru et al., 2018). Here, porous microfibers showed a significantly faster release compared to the non-porous microfibers. This may be explained by the

fact that porosity enhances penetration of the medium into these hydrophobic matrices, which is of high relevance considering that the drug release from PCL electrospun fiber matrices has been described to occur through a diffusion process (McInnes et al., 2018).

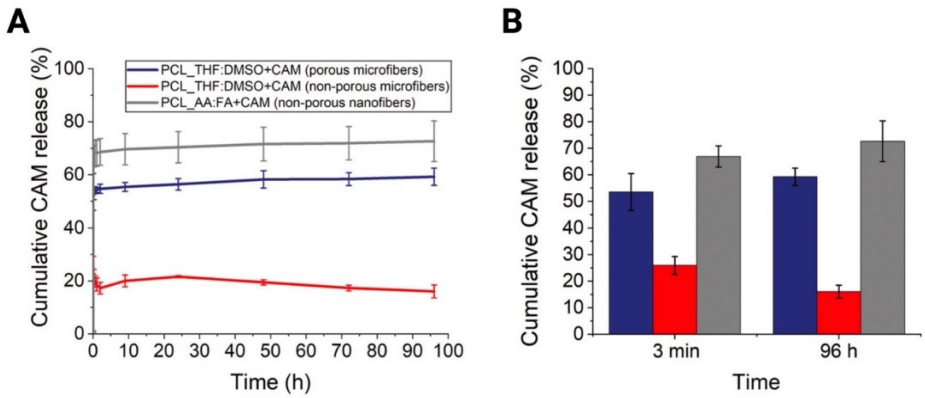

Figure 12. Cumulative drug release **A.** profiles and **B.** percentages of PCL electrospun matrices in phosphate buffered saline at 37 ºC. Data are presented as mean ± SD (n = 3). Key: AA: acetic acid; CAM: chloramphenicol; DMSO: dimethyl sulfoxide; FA: formic acid; PCL: polycaprolactone; THF: tetrahydrofuran.

Besides the remarkably greater surface area to volume ratio of nanofiber matrices, their larger drug release may be influenced by the solvent system used to prepare these matrices (AA:FA) in comparison with the one used to prepare microfiber matrices (THF:DMSO). As it has been observed via ATR-FTIR, the detection and molecular interaction between PCL and CAM inside the matrices is distinct depending on this factor. Solvents may modify the polymer properties causing changes in its molecular weight, viscosity of the electrospinning solution, and electrospinnability (D'Amato et al., 2017). Moreover, each solvent has an evaporation rate and thus, the amount of residual solvent found in the terminal product may differ, influencing the matrix formation. Consequently, all these changes in chemical parameters and morphology of the matrices may lead to drug release variations. For instance, our group has previously incorporated CAM into PCL matrices using CF:methanol (75:25% V/V) as a solvent system (Preem et al., 2017), and in this case a prolonged drug release was shown. From there, we defined a diffusion-based mechanism (Preem et al., 2017).

A possible chemical interaction between PCL and AA:FA solvent system may occur in this acidic and more hydrophilic environment (compared to THF:DMSO and CF:methanol), resulting in the modification of PCL surface properties and leading to the selective localization of CAM on the fiber surface. Moreover, the interaction of PCL and CAM could be achieved through weak interactions that enable a faster release (Širc et al., 2012). The introduction of a charge in the PCL backbone caused by an acidic environment could increase PCL hydrophilicity

(Pok et al., 2010), leading to a faster release. CF and THF are high dissolution solvents for PCL that enhance the creation of PCL aggregates, while other weaker solvents lead to the formation of a filamentous structure (Pok et al., 2010). Similarly to what occurs with the effect of hydrophobicity/hydrophilicity ratio in molecular interactions (i.e. stronger CAM attachments with hydrophobic moieties), the PCL structure formed within electrospun fibers, as well as the morphology of fibers themselves are common criteria that determine the drug release behaviour (Pok et al., 2010).

The CAM release from our porous PCL microfibers and non-porous PCL nanofibers followed a diffusion model, showing a good correlation with the Korsmeyer-Peppas equation, as previously described for CAM release from PCL matrices (Preem et al., 2017). The AIC for porous PCL microfibers was 18.87 and R^2 0.99, while for non-porous PCL nanofibers, the AIC was 48.15 and R^2 0.96. However, it was not possible to fit the drug release kinetics of non-porous microfibers with any tested equations. Here the Korsmeyer-Peppas equation gave an AIC of 59.30 and R^2 0.82. Therefore, in this case, diffusion may not be the main drug release mechanism, which may be more linked to the desorption of the embedded CAM from the fiber surface or nanopores (not detected) (Srikar et al., 2009).

In the case of PVA matrices, drug release was studied, although, no clear conclusions could be obtained. The maximum amount released was 40%, however, the results showed high variation (**Figure 13**). This variable drug release behaviour may be explained by the physicochemical characteristics of cationic AMP pleurocidin which may affect the results. For instance, laboratory materials (e.g. polystyrene) are known to largely affect electrostatic interactions and therefore adsorption of AMPs onto the testing container (Wiegand et al., 2008). Moreover, self-aggregation (Clark et al., 2021) may result in precipitate and make it difficult to conduct the measurements with this experimental setup. In addition, PVA is a biodegradable hydrophilic polymer, and its presence may also lead to the formation of complexes with AMPs, potentially altering their adhesiveness on surfaces. Therefore, the traditional drug release assay does not allow to make reliable assumptions about pleurocidin release from these coaxially prepared PVA matrices and further investigation is needed to understand this behaviour. As a comparison, it was previously reported that approximately 40% of pleurocidin is released after 15 min from monoaxial PVA fibers containing 0.25% w/w of the AMP (Wang et al., 2015). However, this result cannot be extrapolated here as the amount of pleurocidin and the electrospinning technique used for the preparation of matrices differed.

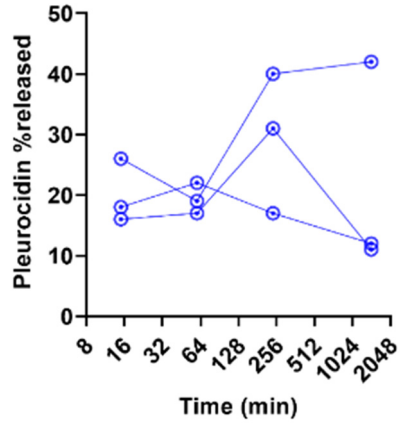

Figure 13. The release profiles of AMP pleurocidin from electrospun PVA fiber matrix (n=3). Pleurocidin concentration in solution measured over 24 h.

6.1.8. Cytotoxicity testing (II)

Wound dressings, as any other medical device, need to be safe and biocompatible. Moreover, it is crucial to explore how the morphology of electrospun matrices impacts cell attachment and proliferation, as, in order to promote wound healing, skin cells need to grow in close contact with the dressing. Here, PCL matrices were investigated using fibroblasts and MTS assay. Porous microfiber matrices with CAM showed the highest absorbance for formazan dye, suggesting that there are more metabolically active cells attached to these matrices and thus, they have proliferated more easily in this condition compared to the others (**Publication II, Figure 5 A**). Porosity enhances cell attachment and proliferation, as statistically higher MTS signal was found on pristine porous microfiber matrices compared to the non-porous ones. A trend that was maintained, though not as pronounced (not statistically significant) between CAM loaded fibers (**Publication II, Figure 5 A**).

SEM images and CFM were used to observe and construct 3D view micrographs to investigate the fibroblast-matrices interactions and distribution along the matrices. In all cases, the cells were evenly distributed on the surface layer of the matrix (**Figure 14**). Confirming the MTS results, the highest number of cells and the deeper cell infiltration (40 µm) was found on porous microfiber matrices loaded with CAM (**Figure 14 E**), followed by non-porous microfiber matrices (**Figure 14 A**) and non-porous nanofiber matrices (**Figure 14 B**), where cells where only found on the matrix surface. The matrix and single fiber morphology clearly affect the ability of cells to permeate the matrix (Loh and Choong, 2013; Sharifi et al., 2016). The matrix pore size is critical in the cellular infiltration behaviour, affecting the ability to spread within the matrix, and even the

dimension of the cells may affect the results (Farooque et al., 2014). It has been observed that fibroblasts are able to deform their cytoskeleton up to 10% of the nucleus size in order to migrate through small pores (Wolf et al., 2013). Nonetheless, the infiltration process is smoother when cells encounter bigger pores. This is the case of microfiber matrices compared to nanofibers, leading to improved cell attachment and deeper penetration. Moreover, the surface porosity of single fibers also contributes to a better cell proliferation, as it has been seen for our porous microfibers compared to the non-porous ones (**Figure 14 A, E**). This may be related to the more hydrophilic nature of these matrices (previously proved through wettability and contact angle measurements), where aqueous medium easily accesses the inner parts of the matrix, presumably enhancing cell penetration.

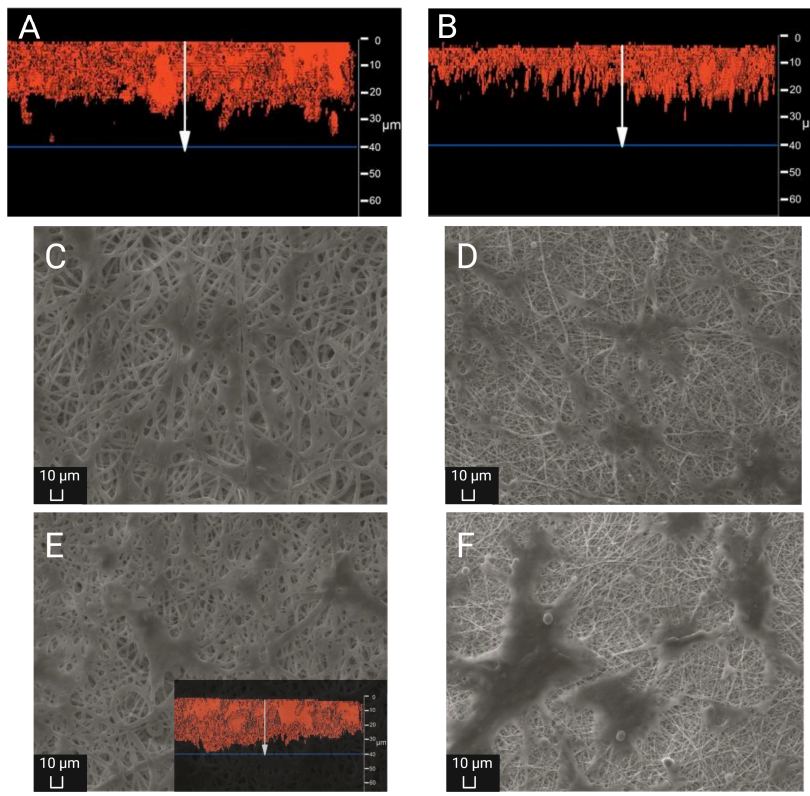

Figure 14. SEM images (**A, B**) and CFM 3D micrographs (**C-F**) showing fibroblast attachment and infiltration into PCL electrospun matrices. **A.** Non-porous microfiber matrices. **B.** Nanofiber matrices. **C.** Porous microfiber pristine matrices. **D**. Nanofiber pristine matrices. **E.** CAM loaded porous microfiber matrices. **F.** CAM loaded nanofiber matrices. Key: CAM: chloramphenicol; CFM: confocal fluorescence microscopy; SEM: scanning electron microscopy.

CAM has proven to be biocompatible and safe to BHK-21 cells, as no significant differences were found between the cell attachment of pristine and CAM loaded fibers (**Figure 14 C-F)**. This conclusion was previously stated for PCL and similar concentrations of CAM (Jalili-Firoozinezhad et al., 2017; Mulhall et al., 1983).

6.2. Antibacterial testing (II, III)

6.2.1. Antibacterial activity of AMPs and biocides (III)

Antibacterial activity of AMPs

Conversely to CAM, which is a model antibacterial drug frequently used in clinics whose MIC and AMR have been widely investigated, AMPs are still quite novel molecules that require further investigation. Here, three different AMPs (pleurocidin, D-pleurocidin-KR, and temporin B L1FK) were selected and tested to explore their antibacterial activity against selected wound pathogens. This previous characterisation provided essential information to select an appropriate AMP for the incorporation of this drug into an electrospun matrix.

Pleurocidin and its analogue showed a stronger potency compared to temporin B L1FK, whereas, as expected, the modified peptide D-pleurocidin-KR was more effective than its parent peptide (**Table 8**). A close comparison of the pleurocidin peptides was performed by Manzo et al. (Manzo et al., 2020), where D-pleurocidin-KR was first created to enhance pleurocidin antimicrobial activity and reduce cytotoxicity, which was successfully proven both *in vitro* and in a murine model. Their metabolomic studies showed that the mechanism of action of D-pleurocidin-KR differs from its parent peptide, attributed to its greater conformational flexibility and the contribution from membrane damage.

All these peptides inhibit the growth of *A. baumannii* at lower concentrations than they do for *P. aeruginosa.* This may be explained by the resistance mechanisms of *P. aeruginosa*, which have been profoundly studied (Haghi et al., 2018; Pang et al., 2019; Qin et al., 2022). Its intrinsic resistance is caused by efflux pumps, modified outer membrane permeability, bacterial encapsulation formed by extracellular polysaccharides, and enzymes that inactivate antimicrobial drugs.

Biocides

Biocides are extensively employed in the prophylaxis and management of wound infections. Notably, recent guidelines for managing burn infections advocate the use of topical biocides, such as silver sulphadiazine, specifically for second- and third-degree burns (Yoshino et al., 2020). Typically, biocides, often in the form of solutions or creams, are utilized. Additionally, antimicrobial wound patches, containing biocides like silver, are frequently employed in the treatment of infected wounds (Haidari et al., 2020; May et al., 2022). However, in instances where innovative wound dressings incorporating AMPs, such as pleurocidin, are utilized, these are likely to be employed concomitantly with conventional wound

care modalities, including the irrigation of the wound with biocide solutions (European Wound Management Association (EWMA), 2006). Consequently, our investigation sought to assess the impact of biocides on the antibacterial activity and efficacy of pleurocidin. For this purpose, an initial antibacterial assessment of commonly used biocides was developed, in order to determine the sensitivity of selected multiresistant wound pathogens.

Here, silver nitrate, silver sulphadiazine, octenidine, PVP-iodine, chlorhexidine and benzalkonium chloride were selected as frequently applied biocides used in wound management. Multiresistant bacterial strains, *P. aeruginosa* PAO1 and NCTC 13437 and *A. baumannii* AYE and ATCC 17978 were used to determine the efficacy of these biocides. For this purpose, MIC assays were conducted, and the results are shown in **Table 8**. All biocides inhibit the growth of tested bacterial strains at lower MIC than the concentration that is commonly used in clinics for wound care applications.

As it happened with AMPs, *A. baumannii* exhibits higher sensitivity to biocides, with growth inhibition occurring at lower concentrations than observed for *P. aeruginosa.* This may be related to the ability of this pathogen to prevent the entrance of antimicrobials into its cytoplasmic membrane, which has been previously described for QAC (Gilbert and Moore, 2005). *P. aeruginosa* NCTC 13437 showed the highest level of resistance to benzalkonium chloride, requiring a concentration 32 times greater than that effective against *A. baumannii* strains.

The most potent biocide was octenidine, where just 4 μg/mL was needed to inhibit the growth of all bacteria tested, followed by chlorhexidine. Both silver biocides showed a similar MIC, in line with their similar mechanism of action which was previously discussed. PVP-iodine is known to be highly effective for wound infection prevention and treatment, being able to eradicate all ESKAPE pathogens and biofilms even in the presence of blood (Barreto et al., 2020). Nevertheless, the results shown here, highlight that its potency compared to other biocides tested is quite low. However, its multiple mechanisms of action that provide it with an excellent lack of antimicrobial resistance and its ability to promote wound healing while exhibiting low cytotoxicity, permits its use in a higher dose compared to the alternative treatments (Barreto et al., 2020).

Table 8. Reference minimum inhibitory concentration (MIC) of AMPs and various biocides against different bacterial strains. At least three independent experiments were performed in triplicate. Results are shown as a range where there were fluctuations. For comparison, properties of common biocide formulations are provided.

Bacterial Strain	**AMP Concentration (µg/mL)**			**Biocide Concentration (µg/mL)**					
	Pleurocidin	D-Pleurocidin-KR	Temporin B L1FK	Chlorhexidine Digluconate	Benzalkonium Chloride	Silver Nitrate	Silver Sulphadiazine	Octenidine Dichloride	Povidone Iodine
A. baumannii AYE	2	2-4	4-8	4-8	8	8	8-32	4	2500
A. baumannii ATCC 17978	2	4	8-16	4	8	8	16-32	4	2500
P. aeruginosa NCTC 13437	32	4	128	4-8	256	4-16	32	4	2500
P. aeruginosa PAO1	16	8	128	4-16	64	8-16	32	4	5000
EMRSA-15	16	-	-	-	-	-	-	-	-
K. pneumoniae M6	4	-	-	-	-	-	-	-	-
K. pneumoniae NCTC 13368	2-4	-	-	-	-	-	-	-	-
E. coli NCTC 12923	1	-	-	-	-	-	-	-	-
Concentration in use (µg/mL)	-	-	-	5000-40000 (0.5-4% solution)	13000 (0.13% solution)	5000 (0.5 % solution)	10 (1% cream)	500-1000 (0.05-0.1% solution)	100000 (10% solution)
References	-	-	-	(Williamson et al., 2017)	(Pereira and Tagkopoulos, 2019)	(Moyer et al., 1965)	(White and Cooper, 2005)	(J. Y. Maillard et al., 2021)	(Williamson et al., 2017)

6.2.2. Antibacterial activity of drug loaded matrices (II, III)

6.2.2.1. CAM loaded matrices (II)

PCL matrices loaded with CAM were tested against *E. coli* and *P. aeruginosa*. When CAM-loaded matrices were tested against planktonic *E. coli*, an effective killing was observed after 72 h (**Figure 15 A**), which nicely correlates to the drug release behaviour previously defined for these matrices (**Figure 12**). No differences in the activity were observed between the types of CAM loaded matrices (**Figure 15 A**). However, various outcomes were observed when these matrices were investigated on biofilm formation. Most importantly, the presence of CAM inside the fibers significantly diminished the formation of biofilm in all cases (**Figure 15 B**). Moreover, differences in CFU were found after 48 h depending on the sample, highlighting the high growth of biofilm on pristine matrices.

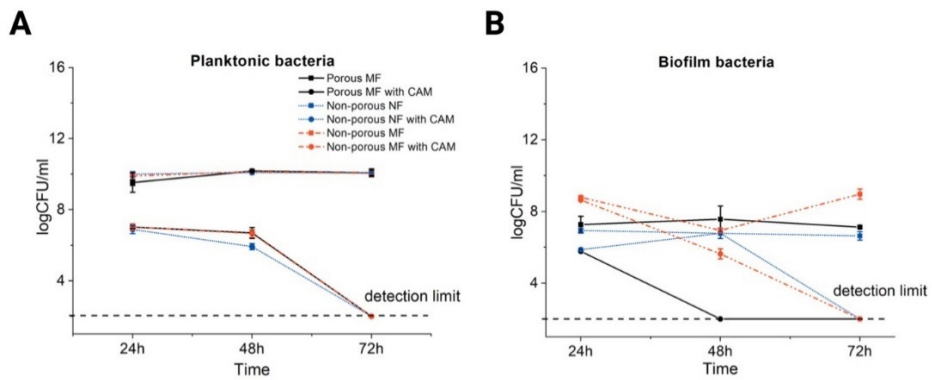

Figure 15. **A.** Antibacterial activity of PCL electrospun matrices with and without CAM on *E. coli* and **B.** biofilm formation and antibiofilm activity. Data are presented as mean ± SD (n=3). Detection limit refers to the CFU that can be counted by the plate method (200 CFU/mL). Key: AA: acetic acid; CAM: chloramphenicol; MF: microfibers; NF: nanofibers; PCL: polycaprolactone.

After 24 h, non-porous microfiber matrices showed more biofilm formation than porous microfiber matrices, while these matrices obtained similar CFUs as nanofiber matrices. However, after 48 h, there was a huge difference in the activity of CAM loaded porous microfibers and CAM loaded nanofibers, whereas the latter maintained the formation of biofilm, porous microfibers showed a great antibiofilm decrease, lowering the CFUs to the detection limit (**Figure 15 B**). Besides, non-porous microfibers remarkably decreased the formation of biofilm, although it was not until after 72 h that they reached the lower detection limit. In all CAM loaded matrices, it was not possible to detect CFU after 72 h.

Based on these results, we can conclude that microfiber matrices tend to inhibit biofilm formation to a greater degree than nanofiber matrices. The effect

on bacterial proliferation of diverse fiber sizes has been previously investigated and it has been revealed that, usually, bacteria attach and grow more favourably when fibers are similar in size to bacterial cells (Abrigo et al., 2015). Thus, microfiber matrices should have been a better framework for bacterial attachment, however, this was not our case. Other studies have reported supporting evidence of the bacterial attachment on smaller (nano-scale) matrices (De Cesare et al., 2019; Hu et al., 2019), corresponding in one case, to PCL matrices electrospun using CF:ethanol as solvent system. The considerable attachment to nanofibers may be explained due to the different organic molecules that bacteria excrete in the biofilm formation process, that allows the adhesion of cells onto the fibers (De Cesare et al., 2019). Besides, other matrix parameters such as wettability, surface charge, and specific chemistry of the fibers influence cell attachment and proliferation (Abrigo et al., 2015).

Conversely, the surface morphology of the matrices may negatively affect bacterial attachment, reducing the contact area between cells and fibers (Cheng et al., 2019; Hsu et al., 2013). For instance, nanoscale surface pores may create energetic interactions that avoid cell attachment and thus, biofilm formation (Anselme et al., 2010; Feng et al., 2014). In our study, the presence of surface pores barely affected biofilm formation, as it can be seen for pristine matrices (**Figure 15 B**).

Unquestionably, the drug release behaviour of CAM loaded matrices and the presence of this drug within the matrix influence biofilm formation on the matrices. Porous microfibers, which have proven to be more hydrophilic, are the ones with better antibiofilm properties. Conversely, nanofiber matrices are the ones with faster and most efficient drug release (**Figure 12**), thus the remaining drug within the matrices is lower, which could explain the biofilm growth. On the other hand, other samples with lower drug release provided better antibiofilm properties.

The antibacterial activity of these matrices was also tested against *P. aeruginosa*. However, none of them showed growth inhibition against this pathogen (**Publication II, Appendix Figure S 5**), which is known to be resistant to CAM (Li et al., 1994; Morita et al., 2014).

6.2.2.2. Pleurocidin loaded matrices (III)

Based on the MICs results, both pleurocidin and D-pleurocidin-KR were first selected for incorporation into electrospun matrices. However, the first attempts resulted in peptide degradation and poor release behaviour, thus no antibacterial activity was observed. The higher cost of D-pleurocidin-KR production led to the selection of pleurocidin as the antimicrobial molecule to be incorporated in further analyses.

Pleurocidin loaded matrices were tested against eight pathogenic bacterial strains found in wound infections (*P. aeruginosa* PAO1 and NCTC 13437, EMRSA-15, *K. pneumoniae* M6 and NCTC 13368, *A. baumannii* AYE and ATCC 17978, and *E. coli* NCTC 12923).

An initial characterisation of the antimicrobial activity of these matrices was investigated using a disk diffusion assay. However, this method was unsuccessful as the peptide was not able to diffuse along the matrix nor controls prepared with sterile filter paper (where the corresponding amount of peptide, depending on the matrix weight, was incorporated) (**Figure 16**). In order to study the peptide diffusion along the agar plate, sterile filter papers were charged with a higher amount of pleurocidin (32 and 64 µg). In this case, some peptide diffused through the agar and a small inhibition zone was observed (**Figure 16**). However, the peptide incorporated into electrospun matrices was not sufficient to observe any diffusion. This can be explained by the interactions between the cationic moieties of AMP with the negatively charged sulphate and sugar components of the agaropectin in agar (Lehrer et al., 1991).

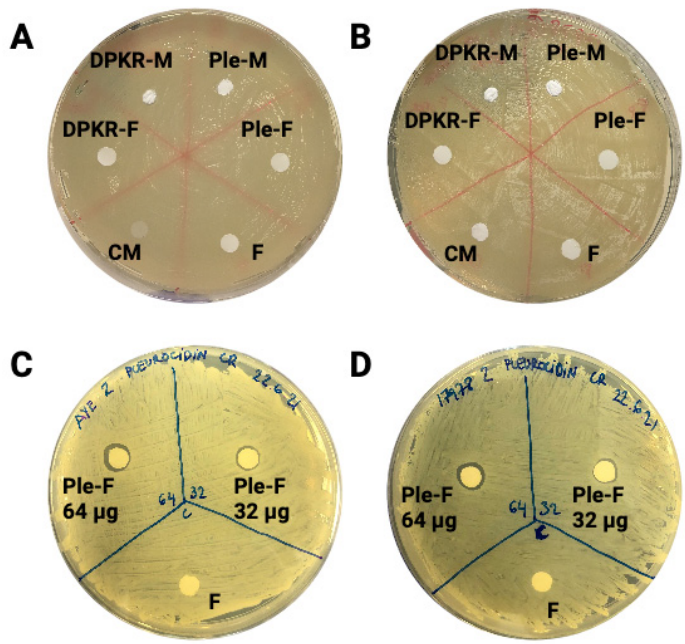

Figure 16. Disk diffusion assay using AMPs loaded electrospun matrices and controls. **A, B.** D-pleurocidin-KR and pleurocidin loaded matrices and their controls against *A. baumannii* AYE and *A. baumannii* ATCC 17978, respectively. **C, D.** Sterile filter papers charged with 32 and 64 µg of pleurocidin against *A. baumannii* AYE and *A. baumannii* ATCC 17978, respectively. Key: CM: control matrix; DPKR-M: D-pleurocidin-KR loaded matrix; DPKR-F: D-pleurocidin-KR charged filter paper; F: filter paper; Ple-M: pleurocidin loaded matrix; Ple-F: pleurocidin charged filter paper.

Therefore, an assay was developed in order to study the antibacterial activity of pleurocidin loaded matrices, where they were immersed into a liquid environment in a 96-microtiter plate (more details in the Methods section). All matrices were able to completely inhibit the growth of all strains except for *P. aeruginosa* NCTC 13437, where a total inhibition was only found on matrices with the highest weight (and hence a higher amount of AMP) (**Figure 17**). These results were in line with the pleurocidin MIC already tested for these bacteria, whose drug concentration response curves (obtained using a non-linear regression model) are shown in **Figure 17**.

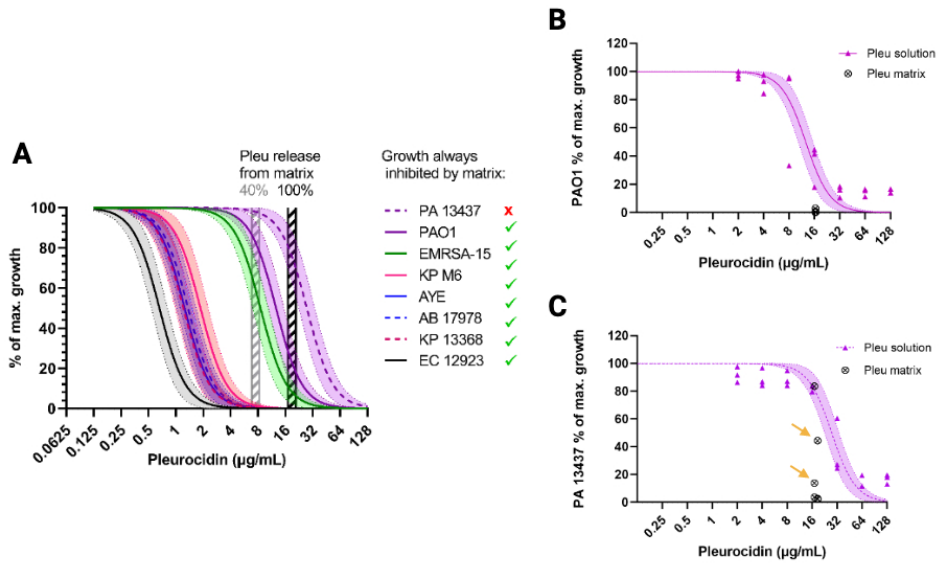

Figure 17. The efficacy of **A.** pleurocidin solution and pleurocidin loaded PVA matrices against selected bacterial strains. Pleurocidin concentration range released from the matrix (40% and 100% shown) and available in the well was calculated from an average 0.6 cm diameter piece of pleurocidin loaded PVA matrix, based on the theoretical content. **B.** pleurocidin containing PVA matrices against *P. aeruginosa* PAO1. **C.** pleurocidin containing PVA matrices against *P. aeruginosa* NCTC 13437. Yellow arrows indicate the matrices that are unable to successfully inhibit bacterial growth. Drug concentration response curves were obtained using a non-linear regression model (four-parameter logistic curve) using the percentage of maximal growth based on absorbance values (OD600) from the control pleurocidin solution. Key: AYE: *A. baumannii* AYE; AB 17978: *A. baumannii* ATCC 17978; EC 12923: *E. coli* NCTC 12923; EMRSA-15: *S. aureus* EMRSA-15; KP 13328: *K. pneumoniae* NCTC 13368; KP M6: *K. pneumoniae* M6; PAO1: *P. aeruginosa* PAO1; PA 13437: *P. aeruginosa* NCTC 13437; Pleu: pleurocidin.

As explained above, it was not possible to directly measure and estimate the pleurocidin release behaviour from the matrices. However, it is needed to calculate how much peptide could be available based on the theoretical concentration of the matrices in order to compare their activity with the peptide used in solution. For this purpose, we calculated that assuming 100% release from the matrices and variations in weight of the 0.6 cm diameter matrices used for these assays, the concentration range of pleurocidin that could be found in the well was 16.5 – 20.5 µg/mL. Besides, using as a reference the previously reported result already mentioned of 40% release (Wang et al., 2015), also pleurocidin concentrations after a 40% release were calculated from our matrices, resulting in a pleurocidin range of 6.6 – 8.2 µg/mL.

The calculated pleurocidin released, when assuming 40% release, would not be sufficient to inhibit EMRSA-15 and both *P. aeruginosa* strains based on the MICs of these strains. Consequently, the range of isolates from the panel used here whose inhibition was hindered by the coaxially electrospun matrices suggests that the functional pleurocidin released from the matrices is close to its maximum content.

In order to get a better understanding of the effect of weight variations of matrices on the growth inhibition of *P. aeruginosa* strains, further analyses were developed. As expected, pleurocidin produced a dose-dependent killing, confirming the peptide release and functionality after electrospinning into the matrix. The growth of *P. aeruginosa* NCTC 13437 was completely inhibited only when using a pleurocidin matrix weighing 500 µg, however full inhibition of *P. aeruginosa* PAO1 was reached with a 400-µg matrix (**Publication III, Figure 3**).

The half-maximal inhibitory concentrations (IC_{50}) of pleurocidin differ depending on whether the peptide was placed in solution or within electrospun matrices (assuming maximal release). For both *P. aeruginosa* strains, the inhibition achieved with loaded matrices significantly surpasses what is achieved by freshly made pleurocidin solution. This effect has been previously suggested by Wang et al. (Wang et al., 2015), and it was also confirmed here. Undoubtedly, although we were unable to determine the exact drug amount of pleurocidin released from these matrices, to be effective against bacteria, pleurocidin must have been released from the matrices. However, pleurocidin is an easily degradable peptide (within 24 h in aqueous solution) and its stability may be hindered in contact with the bacterial environment. Most probably, the protection that electrospun fibers, especially coaxially electrospun fibers, confer to the AMP highly influences its stability against this environment facilitating the availability and functionality of the peptide. Moreover, bacterial attachment to fiber matrices (as previously studied with PCL matrices) may be enhanced, facilitating the interaction between these cells and the AMP.

6.2.3. Interactions between pleurocidin and different biocides (III)

The use of concomitant treatments is habitually used in wound management, mainly involving the application of a biocide and the administration of a systemic antibiotic (Percival et al., 2014). However, the combination of drugs needs to be investigated, as the resulting outcome may not be wished, causing health issues of major significance that may even lead to death. Therefore, the combination of pleurocidin with each biocide was tested here to reveal the advantageous effects or potential risks of these molecules used together against *P. aeruginosa* and *A. baumannii* strains.

Fortunately, weak synergism was found in most of the cases (**Publication III, Figure 4**). *A. baumannii* strains showed very similar FICs against all combinations tested, however, there were relevant differences between *P. aeruginosa* strains. It has been previously reported that different combinations of antibiotics and biocides lead to very different outcomes against *P. aeruginosa* (Pietsch et al., 2021). This was confirmed here, where the effects produced by different combinations of diverse biocides and pleurocidin showed very different results in the case of *P. aeruginosa*, especially *P. aeruginosa* PAO1 (**Figure 12**). In the case of this pathogen, pleurocidin in combination with both silver biocides and PVP-iodine behave synergistically at almost all drug concentrations, while the combination of pleurocidin and octenidine showed indifferent effects. Conversely, pleurocidin in combination with benzalkonium chloride and chlorhexidine showed an antagonistic effect. Moreover, a more staggering revelation was observed when the same drug combination gave opposite results when applied to different *P. aeruginosa* strains. *P. aeruginosa* NCTC 13437 was effectively killed by a modest synergy obtained between pleurocidin and benzalkonium chloride, conversely, the behaviour between these two molecules showed a strong antagonist effect against *P. aeruginosa* PAO1 (**Publication III, Figure 4 C and 4 D**). This inter-strain variation has been previously described for this bacterium when using gentamicin and chlorhexidine (Barnham and Kerby, 1980) and also when combining silver nanoparticles and meropenem (Markowska et al., 2014; Pietsch et al., 2021).

A deeper microdilution checkerboard analysis was conducted to understand this behaviour at different concentrations of these molecules (**Publication III, Figure 5**). When two antimicrobial molecules are used in combination, the goal is to reduce the concentrations needed to kill pathogens, thereby enhancing the activity of both. This was the case for most pleurocidin and benzalkonium chloride combinations against tested bacteria. However, this did not occur for *P. aeruginosa* PAO1 (**Figure 18**). This phenotypical behaviour was also observed at a lower level for chlorhexidine and pleurocidin combinations against both *P. aeruginosa* strains (**Publication III, Appendix Figure S2**). No other combinations tested showed this antagonistic phenomenon.

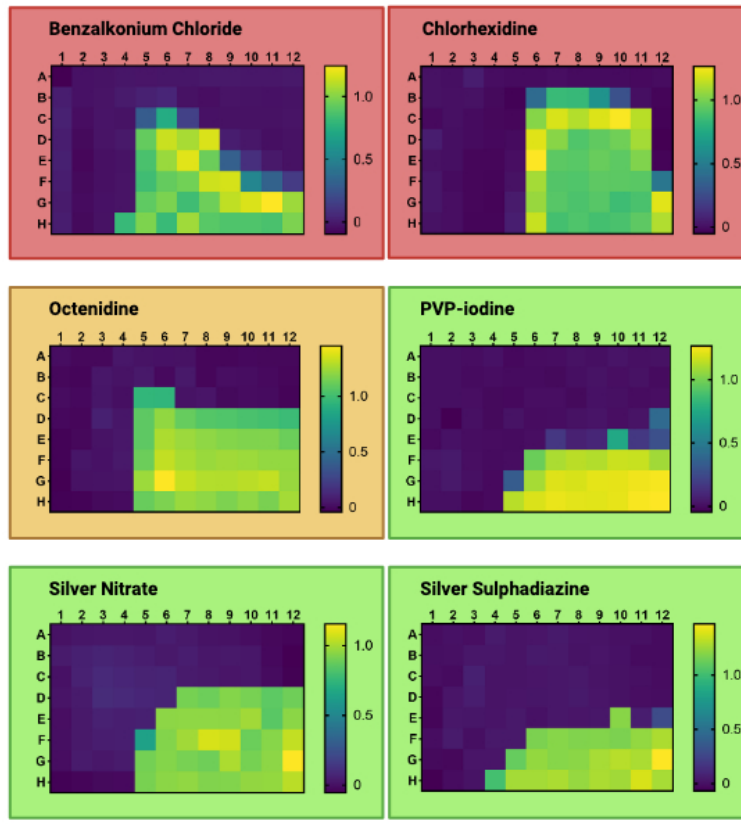

Figure 18. Microdilution checkerboard analysis revealing the co-activity of pleurocidin and different biocides against *P. aeruginosa* PAO1. The extent of bacterial inhibition after 24 h is shown as a heat plot, full bacterial growth (measured at OD600) is represented by the lightest colour. One representative experiment of three biological replicates is shown. Coloured squares around heat plots represent antagonism (red), indifferent behaviour (orange), or synergy (green) based on the FIC values for each case.

Silver nitrate and silver sulphadiazine showed similar synergistic effects when used together with pleurocidin, which is in line with the theory that molecules with similar mechanisms of action show similar interaction effects (Pietsch et al., 2021).

In conclusion, based on our results, pleurocidin can be used in combination with silver nitrate, silver sulphadiazine, octenidine, and PVP-iodine for the treatment of infections caused by tested pathogenic bacterial strains, as these molecules have shown weak synergism or an additive effect. However, the risk produced by the concomitant administration of pleurocidin and benzalkonium chloride and pleurocidin and chlorhexidine must be considered. Further analysis of a broader panel of *P. aeruginosa* strains is vital for understanding the interactions and limitations of this drug administration.

7. CONCLUSIONS

This dissertation has successfully addressed challenges and achieved all the aims proposed. The preparation and assessment of different electrospun matrices have been accomplished, demonstrating their efficacy as antibacterial drug delivery systems with potential applications as wound dressings. Specific conclusions are outlined below:

- The formation of pristine and CAM-loaded porous microfibers was achieved only when PCL was selected as polymer and THF:DMSO was used as the solvent system while using high RH (65%). This underscores the critical role of humidity and solvent system selection in achieving this outcome. These findings provide valuable insights into the limited information available on the preparation of porous drug-loaded fibers.
- Electrospinning parameters for process optimization were successfully selected and CAM was incorporated into PCL electrospun matrices using THF:DMSO and AA:FA solvent systems, managing the formation of micro- and nanofibers, respectively. Additionally, pleurocidin was incorporated into PVA matrices using coaxial electrospinning.
- The morphology of fiber matrices was influenced by various factors including polymer concentration, the solvent system used, drug incorporation, and other parameters affecting electrospinning, such as environmental conditions (e.g. humidity). The impact of these parameters on matrix morphology has been previously described in the literature and confirmed in this dissertation. However, specific considerations regarding the choice of solvent systems, drugs, and polymers provide useful information for the future development of these electrospun matrices and others with similar characteristics.
- Based on the results obtained, both dry and wet PCL electrospun matrices successfully mimic the mechanical properties of skin and show promise for use as wound dressings. However, it is crucial to note that the porosity of the fibers, fiber diameter, and choice of solvent system highly influence the mechanical properties of the matrices. Therefore, careful consideration of these factors is essential for the development of electrospun matrices intended for this application.
- The presence of wound exudate requires the study of matrices in contact with a liquid environment. The contact angle, swelling index and weight loss of fiber matrices are in close correlation with their hydrophilicity/hydrophobicity ratio. Thus, incorporating hydrophilic CAM within hydrophobic PCL resulted in increased swelling index and weight loss, along with a decreased contact angle compared to pristine matrices.
- The electrospinning process and selected solvent systems influenced the solid state of CAM and PCL. CAM was found in an amorphous form within all electrospun PCL matrices. These solid state analyses provide

valuable insights regarding chemical interactions that influence other matrix characteristics, including drug release behaviour.

- The utilization of harsh solvents and high voltage during electrospinning can occasionally lead to drug degradation, resulting in matrices containing less drug than theoretically planned, which directly affects their activity. For this reason, drug content within matrices must be measured. Here, an efficient drug incorporation was achieved in all developed electrospun matrices. PCL matrices assimilated 80% of CAM, while all pleurocidin was successfully incorporated within PVA matrices. This high pleurocidin content confirms the exceptional stability of the peptide during the coaxial electrospinning process, thereby improving the previously obtained results.
- The drug release from electrospun matrices was significantly affected by their hydrophilicity. In the case of PCL hydrophobic matrices, the presence of porous fibers facilitated medium penetration and drug diffusion, leading to enhanced release. Conversely, non-porous microfibers released only 20% of the incorporated CAM. The great surface area of nanofiber matrices and the use of the AA:FA solvent system further improved drug release from these matrices.
- CAM loaded matrices are safe and biocompatible, enhancing cell attachment and growth and thus, promoting wound healing. The best results were obtained for matrices with larger pores and the ones with porous fibers, which exhibited the highest hydrophilicity. This highlights the presence of pores as a favorable property for wound dressings.
- All antimicrobial drugs and biocides tested successfully inhibit the growth of selected wound pathogens, with the exception of CAM loaded matrices that were unable to kill *P. aeruginosa*. This pathogen showed the most resistant behaviour against all tested molecules. The resistant nature of this pathogen is well documented, and these results confirm it. Further research must pay especial attention to this pathogen when assessing antimicrobial efficacy.
- All PCL matrices loaded with CAM effectively inhibited the planktonic growth of *E. coli*. The antibiofilm effect of CAM loaded matrices highly depended on their drug release behaviour, which in turn was influenced by their morphology and hydrophilicity. Consequently, porous microfibers exhibited the most pronounced antibiofilm effect.
- Average 0.6 cm diameter pieces of pleurocidin loaded matrices were able to inhibit the growth of all bacteria tested except for *P. aeruginosa* NCTC 13437. Only when heavier pieces of matrices were used (500 μg), its inhibition was achieved. This highlights the relation between drug amount and antimicrobial activity.
- The inhibition achieved with pleurocidin loaded matrices significantly surpasses what is achieved by freshly prepared pleurocidin solution. This can be attributed to the protection that coaxially electrospun fibers confer to the peptide and the interaction formed between pathogens and matrices.

This electrospinning method proves to be a promising strategy for future antimicrobial applications, particularly when fragile drugs are used.

- Pleurocidin can be used in combination with silver nitrate, silver sulphadiazine, octenidine, and PVP-iodine, where indifferent or synergistic behaviour was found against all bacteria tested. However, caution is warranted when considering the concomitant use of pleurocidin with benzalkonium chloride and chlorhexidine, as antagonistic behaviour has been observed in such combinations.

In summary, the preparation of electrospun matrices involves numerous parameters that require careful consideration. This dissertation provides valuable insights into the development of electrospun fibers using both monoaxial and coaxial techniques; shedding light on factors influencing pore formation on the fiber surface and the correlation between matrix morphology, mechanical properties, and drug release. Future research on these antimicrobial matrices should include additional *ex vivo* and/or *in vivo* experiments to confirm their efficacy under more biorelevant conditions, with the ultimate goal of clinical application.

8. REFERENCES

Abdulmalik, S., Gallo, J., Nip, J., Katebifar, S., Arul, M., Lebaschi, A., Munch, L.N., Bartly, J.M., Choudhary, S., Kalajzic, I., Banasavadi-Siddegowdae, Y.K., Nukavarapu, S.P., Kumbar, S.G., 2023. Nanofiber matrix formulations for the delivery of Exendin-4 for tendon regeneration: In vitro and in vivo assessment. Bioact. Mater. 25, 42–60. https://doi.org/10.1016/j.bioactmat.2023.01.013

Abrigo, M., Kingshott, P., McArthur, S.L., 2015. Bacterial response to different surface chemistries fabricated by plasma polymerization on electrospun nanofibers. Biointerphases 10. https://doi.org/10.1116/1.4927218

Abushaheen, M.A., Muzaheed, Fatani, A.J., Alosaimi, M., Mansy, W., George, M., Acharya, S., Rathod, S., Divakar, D.D., Jhugroo, C., Vellappally, S., Khan, A.A., Shaik, J., Jhugroo, P., 2020. Antimicrobial resistance, mechanisms and its clinical significance. Disease-a-Month 66. https://doi.org/10.1016/j.disamonth.2020.100971

Agarwal, S., Burgard, M., Greiner, A., Joachim, W., 2016. Electrospinning : A Practical Guide to Nanofibers. Berlin/Boston: De Gruyter, Inc.

Agarwal, S., Wendorff, J.H., Greiner, A., 2008. Use of electrospinning technique for biomedical applications. Polymer (Guildf). 49, 5603–5621. https://doi.org/10.1016/J.POLYMER.2008.09.014

Ali Zadeh, M.M., Keyanpour-Rad, M., Ebadzadeh, T., 2014. Effect of viscosity of polyvinyl alcohol solution on morphology of the electrospun mullite nanofibres. Ceram. Int. 40, 5461–5466. https://doi.org/10.1016/J.CERAMINT.2013.10.132

Andrews, J.M., 2001. Determination of minimum inhibitory concentrations. J. Antimicrob. Chemother. 48 Suppl 1, 5–16. https://doi.org/10.1093/JAC/48.SUPPL_1.5

Anghel, E.L., DeFazio, M. V., Barker, J.C., Janis, J.E., Attinger, C.E., 2016. Current concepts in debridement: Science and strategies. Plast. Reconstr. Surg. 138, 82S-93S. https://doi.org/10.1097/PRS.0000000000002651

Anselme, K., Davidson, P., Popa, A.M., Giazzon, M., Liley, M., Ploux, L., 2010. The interaction of cells and bacteria with surfaces structured at the nanometre scale. Acta Biomater. 6, 3824–3846. https://doi.org/10.1016/J.ACTBIO.2010.04.001

Arbade, G.K., Jathar, S., Tripathi, V., Patro, T.U., 2018. Antibacterial, sustained drug release and biocompatibility studies of electrospun poly (ε- caprolactone)/ chloramphenicol blend nanofiber scaffolds. Biomed. Phys. Eng. Express 4. https://doi.org/10.1088/2057-1976/aac1a4

Arinstein, A., Zussman, E., 2011. Electrospun Polymer Nanofibers : Mechanical and Thermodynamic Perspectives. J. Polym. Sci. Part B Polym. Phys. 49, 691–707. https://doi.org/10.1002/polb.22247

Arras, S.D.M., Fraser, J.A., 2016. Chemical inhibitors of non-homologous end joining increase targeted construct integration in cryptococcus neoformans. PLoS One 11, 1–14. https://doi.org/10.1371/journal.pone.0163049

Aslam, M., Kalyar, M.A., Raza, Z.A., 2018. Polyvinyl alcohol: A review of research status and use of polyvinyl alcohol based nanocomposites. Polym. Eng. Sci. 58, 2119–2132. https://doi.org/10.1002/pen.24855

Azimi, B., Maleki, H., Zavagna, L., de la Ossa, J.G., Linari, S., Lazzeri, A., Danti, S., 2020. Bio-based electrospun fibers for wound healing. J. Funct. Biomater. 11. https://doi.org/10.3390/JFB11030067

Baji, A., Mai, Y.-W., Wong, S.-C., Abtahi, M., Chen, P., 2010. Electrospinning of polymer nanofibers: Effects on oriented morphology, structures and tensile properties.

Compos. Sci. Technol. 70, 703–718. https://doi.org/10.1016/J.COMPSCITECH.2010.01.010
Barnham, M., Kerby, J., 1980. Antibacterial activity of combinations of chlorhexidine with neomycin and gentamicin. J. Hosp. Infect. 1, 77–81. https://doi.org/10.1016/0195-6701(80)90034-1
Barreto, R., Barrois, B., Lambert, J., Malhotra-Kumar, S., Santos-Fernandes, V., Monstrey, S., 2020. Addressing the challenges in antisepsis: focus on povidone iodine. Int. J. Antimicrob. Agents 56, 106064. https://doi.org/10.1016/j.ijantimicag.2020.106064
Berenbaum, M.C., 1978. A method for testing for synergy with any number of agents. J. Infect. Dis. 137, 122–130. https://doi.org/10.1093/infdis/137.2.122
Bigliardi, P.L., Alsagoff, S.A.L., El-Kafrawi, H.Y., Pyon, J.K., Wa, C.T.C., Villa, M.A., 2017. Povidone iodine in wound healing: A review of current concepts and practices. Int. J. Surg. 44, 260–268. https://doi.org/10.1016/j.ijsu.2017.06.073
Bock, L.J., Ferguson, P.M., Clarke, M., Pumpitakkul, V., Wand, M.E., Fady, P.E., Allison, L., Fleck, R.A., Shepherd, M.J., Mason, A.J., Sutton, J.M., 2021. *Pseudomonas aeruginosa* adapts to octenidine via a combination of efflux and membrane remodelling. Commun. Biol. 4, 1058. https://doi.org/10.1038/s42003-021-02566-4
Brackman, G., Cos, P., Maes, L., Nelis, H.J., Coenye, T., 2011. Quorum sensing inhibitors increase the susceptibility of bacterial biofilms to antibiotics in vitro and in vivo. Antimicrob. Agents Chemother. 55, 2655–2661. https://doi.org/10.1128/AAC.00045-11
Brook, I., 1992. Aerobic and anaerobic bacteriology of intracranial abscesses. Pediatr. Neurol. 8, 210–214. https://doi.org/10.1016/0887-8994(92)90070-F
Bunaciu, A.A., Udriştioiu, E. gabriela, Aboul-Enein, H.Y., 2015. X-Ray Diffraction: Instrumentation and Applications. Crit. Rev. Anal. Chem. 45, 289–299. https://doi.org/10.1080/10408347.2014.949616
Cadogan, J., Baldwin, D., Carpenter, S., Davey, J., Harris, H., Purser, K., Wicks, G., 2011. Identification, diagnosis and treatment of wound infection. Nurs. Stand. 26, 44–48. https://doi.org/10.7748/ns.26.11.44.s49
Cai, M., He, H., Zhang, X., Yan, X., Li, J., Chen, F., Yuan, D., Ning, X., 2019. Efficient synthesis of PVDF/PI side-by-side bicomponent nanofiber membrane with enhanced mechanical strength and good thermal stability. Nanomaterials 9, 39. https://doi.org/10.3390/nano9010039
Carmona-Cruz, S., Orozco-Covarrubias, L., Sáez-de-Ocariz, M., 2022. The Human Skin Microbiome in Selected Cutaneous Diseases. Front. Cell. Infect. Microbiol. 12, 834135. https://doi.org/10.3389/FCIMB.2022.834135/BIBTEX
Casper, C.L., Stephens, J.S., Tassi, N.G., Chase, D.B., Rabolt, J.F., 2004. Controlling Surface Morphology of Electrospun Polystyrene Fibers : Effect of Humidity and Molecular Weight in the Electrospinning Process. Macromolecules 37, 573–578. https://doi.org/10.1021/ma0351975
Cerca, N., Pier, G.B., Vilanova, M., Oliveira, R., Azeredo, J., 2005. Quantitative analysis of adhesion and biofilm formation on hydrophilic and hydrophobic surfaces of clinical isolates of Staphylococcus epidermidis. Res. Microbiol. 156, 506–514. https://doi.org/10.1016/J.RESMIC.2005.01.007
Chau, T.T., Bruckard, W.J., Koh, P.T.L., Nguyen, A. V., 2009. A review of factors that affect contact angle and implications for flotation practice. Adv. Colloid Interface Sci. 150, 106–115. https://doi.org/10.1016/j.cis.2009.07.003

Chen, S., Liu, B., Carlson, M.A., Gombart, A.F., Reilly, D.A., Xie, J., 2017. Recent advances in electrospun nanofibers for wound healing. Nanomedicine 12, 1335–1352. https://doi.org/10.2217/NNM-2017-0017

Cheng, Y., Feng, G., Moraru, C.I., 2019. Micro-and nanotopography sensitive bacterial attachment mechanisms: A review. Front. Microbiol. 10, 410243. https://doi.org/10.3389/FMICB.2019.00191/BIBTEX

Chew, S.Y., Hufnagel, T.C., Lim, C.T., Leong, K.W., 2006. Mechanical properties of single electrospun drug-encapsulated nanofibres. Nanotechnology 17, 3880. https://doi.org/10.1088/0957-4484/17/15/045

Chhabra, R.P., Richardson, J.F., 2011. Non-Newtoninan Flow and Applied Rheology: Engineering Applications., 2nd ed. Butterworth-Heinemann.

Choong, L.T., Yi, P., Rutledge, G.C., 2015. Three-dimensional imaging of electrospun fiber mats using confocal laser scanning microscopy and digital image analysis. J. Mater. Sci. 50, 3014–3030. https://doi.org/10.1007/s10853-015-8834-2

Chou, S.-F., Woodrow, K.A., 2017. Relationships between mechanical properties and drug release from electrospun fibers of PCL and PLGA blends. J. Mech. Behav. Biomed. Mater. 65, 724–733. https://doi.org/10.1016/J.JMBBM.2016.09.004

Chou, S.F., Carson, D., Woodrow, K.A., 2015. Current strategies for sustaining drug release from electrospun nanofibers. J. Control. Release 220, 584–591. https://doi.org/10.1016/j.jconrel.2015.09.008

Chou, T.C., Talalay, P., 1984. Quantitative analysis of dose-effect relationships: the combined effects of multiple drugs or enzyme inhibitors. Adv. Enzyme Regul. 22, 27–55. https://doi.org/10.1016/0065-2571(84)90007-4

Clark, S., Jowitt, T.A., Harris, L.K., Knight, C.G., Dobson, C.B., 2021. The lexicon of antimicrobial peptides: a complete set of arginine and tryptophan sequences. Commun. Biol. 4, 1–14. https://doi.org/10.1038/s42003-021-02137-7

Clitherow, K.H., Murdoch, C., Spain, S.G., Handler, A.M., Colley, H.E., Stie, M.B., Mørck Nielsen, H., Janfelt, C., Hatton, P. V., Jacobsen, J., 2019. Mucoadhesive electrospun patch delivery of lidocaine to the oral mucosa and investigation of spatial distribution in a tissue Using MALDI-Mass Spectrometry Imaging. Mol. Pharm. 16, 3948–3956. https://doi.org/10.1021/ACS.MOLPHARMACEUT.9B00535/ASSET/IMAGES/LARGE/MP9B00535_0008.JPEG

Cole, A.M., Weis, P., Diamond, G., 1997. Isolation and characterization of pleurocidin, an antimicrobial peptide in the skin secretions of winter flounder. J. Biol. Chem. 272, 12008–12013. https://doi.org/10.1074/jbc.272.18.12008

Cortez Tornello, P.R., Caracciolo, P.C., Cuadrado, T.R., Abraham, G.A., 2014. Structural characterization of electrospun micro/nanofibrous scaffolds by liquid extrusion porosimetry: A comparison with other techniques. Mater. Sci. Eng. C 41, 335–342. https://doi.org/10.1016/j.polymer.2016.02.046

Crofts, T.S., Sontha, P., King, A.O., Wang, B., Biddy, B.A., Zanolli, N., Gaumnitz, J., Dantas, G., 2019. Discovery and characterization of a nitroreductase capable of conferring bacterial resistance to chloramphenicol. Cell Chem Biol 26, 559–570. https://doi.org/10.1016/j.chembiol.2019.01.007.Discovery

Croisier, F., Duwez, A.-S., Jérôme, C., Léonard, A.F., van der Werf, K.O., Dijkstra, P.J., Bennink, M.L., 2012. Mechanical testing of electrospun PCL fibers. Acta Biomater. 8, 218–224. https://doi.org/10.1016/J.ACTBIO.2011.08.015

Cui, W., Li, X., Zhou, S., Weng, J., 2008. Degradation patterns and surface wettability of electrospun fibrous mats. Polym. Degrad. Stab. 93, 731–738. https://doi.org/10.1016/J.POLYMDEGRADSTAB.2007.12.002

D'Amato, A.R., Bramson, M.T.K., Corr, D.T., Puhl, D.L., Gilbert, R.J., Johnson, J., 2018. Solvent Retention in Electrospun Fibers Affects Scaffold Mechanical Properties. Electrospinning 2, 15–28. https://doi.org/10.1515/ESP-2018-0002

D'Amato, A.R., Puhl, D.L., Ziemba, A.M., Johnson, C.D.L., Doedee, J., Bao, J., Gilbert, R.J., 2019. Exploring the effects of electrospun fiber surface nanotopography on neurite outgrowth and branching in neuron cultures. PLoS One 14, 1–18. https://doi.org/10.1371/journal.pone.0211731

D'Amato, A.R., Schaub, N.J., Cardenas, J.M., Fiumara, A.S., Troiano, P.M., Fischetti, A., Gilbert, R.J., 2017. Removal of retained electrospinning solvent prolongs drug release from electrospun PLLA fibers. Polymer (Guildf). 123, 121–127. https://doi.org/10.1016/J.POLYMER.2017.07.008

De Cesare, F., Di Mattia, E., Zussman, E., Macagnano, A., 2019. A study on the dependence of bacteria adhesion on the polymer nanofibre diameter. Environ. Sci. Nano 6, 778–797. https://doi.org/10.1039/C8EN01237G

De Souza, G.S., De Jesus Sonego, L., Santos Mundim, A.C., De Miranda Moraes, J., Sales-Campos, H., Lorenzón, E.N., 2022. Antimicrobial-wound healing peptides: Dual-function molecules for the treatment of skin injuries. Peptides 148, 170707. https://doi.org/10.1016/j.peptides.2021.170707

Di Blasio, S., Clarke, M., Hind, C.K., Asai, M., Laurence, L., Benvenuti, A., Hassan, M., Semenya, D., Man, D.K.-W., Horrocks, V., Manzo, G., Van Der Lith, S., Lam, C., Gentile, E., Annette, C., Bosse, J., Li, Y., Panaretou, B., Langford, P.R., Robertson, B.D., Lam, J.K.W., Sutton, J.M., McArthur, M., Mason, A.J., 2022. Bolaamphiphile Analogues of 12-bis-THA Cl 2 Are Potent Antimicrobial Therapeutics with Distinct Mechanisms of Action against Bacterial, Mycobacterial, and Fungal Pathogens . mSphere 8, 1–20. https://doi.org/10.1128/msphere.00508-22

Dobrzański, L.A., Hudecki, A., Chladek, G., Król, W., Mertas, A., 2014. Surface properties and antimicrobial activity of composite nanofibers of polycaprolactone with silver precipitations. Arch. Mater. Sci. Eng. 70, 53–60.

Doern, C.D., 2014. When does 2 plus 2 equal 5? A review of antimicrobial synergy testing. J. Clin. Microbiol. 52, 4124–4128. https://doi.org/10.1128/JCM.01121-14

Dowd, S.E., Wolcott, R.D., Kennedy, J., Jones, C., Cox, S.B., 2011. Molecular diagnostics and personalised medicine in wound care: Assessment of outcomes. J. Wound Care 20, 232–239. https://doi.org/10.12968/jowc.2011.20.5.232

Drago, L., 2019. Chloramphenicol resurrected: A journey from antibiotic resistance in eye infections to biofilm and ocular microbiota. Microorganisms 7, 278. https://doi.org/10.3390/microorganisms7090278

Dziemidowicz, K., Sang, Q., Wu, J., Zhang, Z., Zhou, F., Lagaron, J.M., Mo, X., Parker, G.J.M., Yu, D.G., Zhu, L.M., Williams, G.R., 2021. Electrospinning for healthcare: recent advancements. J. Mater. Chem. B 9, 939–951. https://doi.org/10.1039/d0tb02124e

Ekram, B., Abdel-Hady, B.M., El-Kady, A.M., Amr, S.M., Waley, A.I., Guirguis, O.W., 2017. Optimum parameters for the production of nano-scale electrospun polycaprolactone to be used as a biomedical material. Adv. Nat. Sci. Nanosci. Nanotechnol. 8, 045018. https://doi.org/10.1088/2043-6254/aa92b4

Elliot, A.D., 2020. Confocal Microscopy: Principles and Modern Practices. Curr Protoc Cytom 92, e68. https://doi.org/10.1002/cpcy.68.

Elsherbiny, D.A., Abdelgawad, A.M., Shaheen, T.I., Abdelwahed, N.A.M., Jockenhoevel, S., Ghazanfari, S., 2023. Thermoresponsive nanofibers loaded with antimicrobial α-aminophosphonate-o/w emulsion supported by cellulose nanocrystals for smart

wound care patches. Int. J. Biol. Macromol. 233, 123655. https://doi.org/10.1016/j.ijbiomac.2023.123655
Elzein, T., Nasser-Eddine, M., Delaite, C., Bistac, S., Dumas, P., 2004. FTIR study of polycaprolactone chain organization at interfaces. J. Colloid Interface Sci. 273, 381–387. https://doi.org/10.1016/J.JCIS.2004.02.001
Eriksson, E., Liu, P.Y., Schultz, G.S., Martins-Green, M.M., Tanaka, R., Weir, D., Gould, L.J., Armstrong, D.G., Gibbons, G.W., Wolcott, R., Olutoye, O.O., Kirsner, R.S., Gurtner, G.C., 2022. Chronic wounds: Treatment consensus. Wound Repair Regen. 30, 156–171. https://doi.org/10.1111/wrr.12994
EUCAST, 2024. EUCAST reading guide for broth microdilution [WWW Document]. URL https://www.eucast.org/ast_of_bacteria/mic_determination (accessed 3.8.24).
EUCAST, 2000. Terminology relating to methods for the determination of susceptibility of bacteria to antimicrobial agents. Clin. Microbiol. Infect. Dis. 6, 503–508. https://doi.org/10.1046/j.1469-0691.2000.00149.x
European Wound Management Association (EWMA), 2006. Position Document: Management of wound infection.
Farooque, T.M., Camp, C.H., Tison, C.K., Kumar, G., Parekh, S.H., Simon, C.G., 2014. Measuring stem cell dimensionality in tissue scaffolds. Biomaterials 35, 2558–2567. https://doi.org/10.1016/J.BIOMATERIALS.2013.12.092
Feng, G., Cheng, Y., Wang, S.Y., Hsu, L.C., Feliz, Y., Borca-Tasciuc, D.A., Worobo, R.W., Moraru, C.I., 2014. Alumina surfaces with nanoscale topography reduce attachment and biofilm formation by *Escherichia coli* and *Listeria* spp. Biofouling 30, 1253–1268. https://doi.org/10.1080/08927014.2014.976561
Fox, C.L., Modak, S.M., 1974. Mechanism of silver sulfadiazine action on burn wound infections. Antimicrob. Agents Chemother. 5, 582–588. https://doi.org/10.1128/AAC.5.6.582
Fratini, F., Mancini, S., Turchi, B., Friscia, E., Pistelli, L., Giusti, G., Cerri, D., 2017. A novel interpretation of the Fractional Inhibitory Concentration Index: The case Origanum vulgare L. and Leptospermum scoparium J. R. et G. Forst essential oils against Staphylococcus aureus strains. Microbiol. Res. 195, 11–17. https://doi.org/10.1016/j.micres.2016.11.005
Gao, S., Chen, T., Wang, Z., Ji, P., Xu, L., Cui, W., Wang, Y., 2022. Immuno-activated mesenchymal stem cell living electrospun nanofibers for promoting diabetic wound repair. J. Nanobiotechnology 20, 1–20. https://doi.org/10.1186/s12951-022-01503-9
Gera, S., Kankuri, E., Kogermann, K., 2021. Antimicrobial peptides – Unleashing their therapeutic potential using nanotechnology. Pharmacol. Ther. 107990. https://doi.org/10.1016/j.pharmthera.2021.107990
Ghasemvand, F., Kabiri, M., Hassan-Zadeh, V., Simchi, A., 2023. Chitosan, polyethylene oxide/polycaprolactone electrospun core/shell nanofibrous mat containing rosuvastatin as a novel drug delivery system for enhancing human mesenchymal stem cell osteogenesis. Front. Mol. Biosci. 10, 1–13. https://doi.org/10.3389/fmolb.2023.1220357
Gilbert, P., Moore, L.E., 2005. Cationic antiseptics: Diversity of action under a common epithet. J. Appl. Microbiol. 99, 703–715. https://doi.org/10.1111/j.1365-2672.2005.02664.x
Goel, N., Fatima, S.W., Kumar, S., Sinha, R., Khare, S.K., 2021. Antimicrobial resistance in biofilms: Exploring marine actinobacteria as a potential source of antibiotics and biofilm inhibitors. Biotechnol. Reports 30, e00613. https://doi.org/10.1016/j.btre.2021.e00613

Goonoo, N., Bhaw-Luximon, A., Jhurry, D., 2014. In vitro and in vivo cytocompatibility of electrospun nanofiber scaffolds for tissue engineering applications. RSC Adv. 4, 31618–31642. https://doi.org/10.1039/c4ra05218h

Gopal, R., Kaur, S., Ma, Z., Chan, C., Ramakrishna, S., Matsuura, T., 2006. Electrospun nanofibrous filtration membrane. J. Memb. Sci. 281, 581–586. https://doi.org/10.1016/J.MEMSCI.2006.04.026

Gould, K., 2016. Antibiotics: From prehistory to the present day. J. Antimicrob. Chemother. 71, 572–575. https://doi.org/10.1093/jac/dkv484

Grassi, L., Maisetta, G., Maccari, G., Esin, S., Batoni, G., 2017. Analogs of the frog-skin antimicrobial peptide temporin 1Tb exhibit a wider spectrum of activity and a stronger antibiofilm potential as compared to the parental peptide. Front. Chem. 5, 1–13. https://doi.org/10.3389/fchem.2017.00024

Guo, J.W., Lin, Z.Y., Chang, C.J., Lu, C.H., Chen, J.K., 2018. Protein valves prepared by click reaction grafting of poly(N-isopropylacrylamide) to electrospun poly(vinyl chloride) fibrous membranes. Appl. Surf. Sci. 439, 313–322. https://doi.org/10.1016/j.apsusc.2017.12.215

Habif, T.P., 2015. Clinical Dermatology E-Book. Elsevier Health Sciences.

Haghi, F., Zeighami, H., Monazami, A., Toutouchi, F., Nazaralian, S., Naderi, G., 2018. Diversity of virulence genes in multidrug resistant *Pseudomonas aeruginosa* isolated from burn wound infections. Microb. Pathog. 115, 251–256. https://doi.org/10.1016/j.micpath.2017.12.052

Haidari, H., Garg, S., Vasilev, K., Kopecki, Z., Cowin, A., 2020. Silver-based wound dressings: current issues and future developments for treating bacterial infections. Wound Pract. Res. 28, 173–180. https://doi.org/10.33235/wpr.28.4.173-180

Haider, A., Haider, S., Kang, I.K., 2018. A comprehensive review summarizing the effect of electrospinning parameters and potential applications of nanofibers in biomedical and biotechnology. Arab. J. Chem. 11, 1165–1188. https://doi.org/10.1016/j.arabjc.2015.11.015

Hall, M.J., Middleton, R.F., Westmacott, D., 1983. The fractional inhibitory concentration (FIC) index as a measure of synergy. J. Antimicrob. Chemother. 11, 427–433. https://doi.org/10.1093/jac/11.5.427

Haridas, A.K., Sharma, C.S., Sritharan, V., Rao, T.N., 2014. Fabrication and surface functionalization of electrospun polystyrene submicron fibers with controllable surface roughness. RSC Adv. 4, 12188–12197. https://doi.org/10.1039/c3ra44170a

Heal, C.F., Buettner, P.G., Cruickshank, R., Graham, D., Browning, S., Pendergast, J., Drobetz, H., Gluer, R., Lisec, C., 2009. Does single application of topical chloramphenicol to high risk sutured wounds reduce incidence of wound infection after minor surgery? Prospective randomised placebo controlled double blind trial. BMJ 338, 211–214. https://doi.org/10.1136/bmj.a2812

Hotaling, N.A., Bharti, K., Kriel, H., Simon, C.G., 2015. DiameterJ: A validated open source nanofiber diameter measurement tool. Biomaterials 61, 327–338. https://doi.org/10.1016/j.biomaterials.2015.05.015

Hsu, L.C., Fang, J., Borca-Tasciuc, D.A., Worobo, R.W., Moraru, C.I., 2013. Effect of micro- and nanoscale topography on the adhesion of bacterial cells to solid surfaces. Appl. Environ. Microbiol. 79, 2703–2712. https://doi.org/10.1128/AEM.03436-12/ASSET/32E69D34-9431-43E6-91FE-35F4F656DED8/ASSETS/GRAPHIC/ZAM9991043110008.JPEG

Hu, M.X., Li, J.N., Guo, Q., Zhu, Y.Q., Niu, H.M., 2019. Probiotics Biofilm-Integrated Electrospun Nanofiber Membranes: A New Starter Culture for Fermented Milk

Production. J. Agric. Food Chem. 67, 3198–3208. https://doi.org/10.1021/ACS.JAFC.8B05024/SUPPL_FILE/JF8B05024_SI_001.PDF
Hu, X., Liu, S., Zhou, G., Huang, Y., Xie, Z., Jing, X., 2014. Electrospinning of polymeric nanofibers for drug delivery applications. J. Control. Release 185, 12–21. https://doi.org/10.1016/j.jconrel.2014.04.018
Huang, C., Thomas, N.L., 2018. Fabricating porous poly(lactic acid) fibres via electrospinning. Eur. Polym. J. 99, 464–476. https://doi.org/10.1016/j.eurpolymj.2017.12.025
Huang, Z.M., Zhang, Y.Z., Kotaki, M., Ramakrishna, S., 2003. A review on polymer nanofibers by electrospinning and their applications in nanocomposites. Compos. Sci. Technol. 63, 2223–2253. https://doi.org/10.1016/S0266-3538(03)00178-7
Hübner, N.O., Siebert, J., Kramer, A., 2010. Octenidine dihydrochloride, a modern antiseptic for skin, mucous membranes and wounds. Skin Pharmacol. Physiol. 23, 244–258. https://doi.org/10.1159/000314699
Jalili-Firoozinezhad, S., Mohamadzadeh Moghadam, M.H., Ghanian, M.H., Ashtiani, M.K., Alimadadi, H., Baharvand, H., Martin, I., Scherberich, A., 2017. Polycaprolactone-templated reduced-graphene oxide liquid crystal nanofibers towards biomedical applications. RSC Adv. 7, 39628–39634. https://doi.org/10.1039/C7RA06178A
Jiang, S., Li, S.C., Huang, C., Chan, B.P., Du, Y., 2018. Physical Properties of Implanted Porous Bioscaffolds Regulate Skin Repair: Focusing on Mechanical and Structural Features. Adv. Healthc. Mater. 7, 1700894. https://doi.org/10.1002/ADHM.201700894
Johnson, J.B., Walsh, K.B., Naiker, M., Ameer, K., 2023. The Use of Infrared Spectroscopy for the Quantification of Bioactive Compounds in Food: A Review. Molecules 28, 3215. https://doi.org/10.3390/molecules28073215
Jones, D.R.H., Ashby, M.F., 2019. Engineering Materials 1: An Introduction to Properties, Applications and Design, Fifth. ed. Elsevier.
Kaiser, P., Wächter, J., Windbergs, M., 2021. Therapy of infected wounds: overcoming clinical challenges by advanced drug delivery systems. Drug Deliv. Transl. Res. 11, 1545. https://doi.org/10.1007/S13346-021-00932-7
Kanani, A.G., Bahrami, S.H., 2011. Effect of Changing Solvents on Poly (ε-Caprolactone) Nanofibrous Webs Morphology. J. Nanomater. 2011, 724153. https://doi.org/10.1155/2011/724153
Karge, H.G., Weitkamp, J., 2008. Adsorption and Diffusion, 1st ed. Springler Berlin / Heidelberg.
Kennedy, K.M., Bhaw-Luximon, A., Jhurry, D., 2017. Cell-matrix mechanical interaction in electrospun polymeric scaffolds for tissue engineering: Implications for scaffold design and performance. Acta Biomater. 50, 41–55. https://doi.org/10.1016/J.ACTBIO.2016.12.034
Khalid, A., Bai, D., Abraham, A.N., Jadhav, A., Linklater, D., Matusica, A., Nguyen, D., Murdoch, B.J., Zakhartchouk, N., Dekiwadia, C., Reineck, P., Simpson, D., Vidanapathirana, A.K., Houshyar, S., Bursill, C.A., Ivanova, E.P., Gibson, B.C., 2020. Electrospun Nanodiamond-Silk Fibroin Membranes: A Multifunctional Platform for Biosensing and Wound-Healing Applications. ACS Appl. Mater. Interfaces 12, 48408–48419. https://doi.org/10.1021/acsami.0c15612
Kim, G., Yoon, H., Park, Y., 2010. Drug release from various thicknesses of layered mats consisting of electrospun polycaprolactone and polyethylene oxide micro/nanofibers. Appl. Phys. A Mater. Sci. Process. 100, 1197–1204. https://doi.org/10.1007/s00339-010-5785-y

Kim, G.M., Le, K.H.T., Giannitelli, S.M., Lee, Y.J., Rainer, A., Trombetta, M., 2013. Electrospinning of PCL/PVP blends for tissue engineering scaffolds. J. Mater. Sci. Mater. Med. 24, 1425–1442. https://doi.org/10.1007/s10856-013-4893-6

Kweon, H., Yoo, M.K., Park, I.K., Kim, T.H., Lee, H.C., Lee, H.-S., Oh, J.-S., Akaike, T., Cho, C.-S., 2003. A novel degradable polycaprolactone networks for tissue engineering. Biomaterials 24, 801–808. https://doi.org/10.1016/S0142-9612(02)00370-8

Laidmäe, I., Nieminen, H., Salmi, A., Paulin, T., Rauhala, T., Falck, K., Yliruusi, J., Heinämäki, J., Haeggström, E., 2016. Device and method to produce nanofibers (EP3274491B1).

Lanno, G.-M., Kowalczyk, T., Blonski, S., Putrinš, M., Tenson, T., Korczyk, P., Kogermann, K., 2022. Fibers electrospinning including microfluidics method (PCT/EP/2022/076874).

Larkin, P., 2011. Infrared and Raman Spectroscopy: Principles and Spectral Interpretation, 1st ed. Elsevier.

Laye, P.G., Warrington, S.B., Methods, G.T., Heal, G.R., Price, D.M., Wilson, R., 2002. Principles of Thermal Analysis and Calorimetry. Royal Society of Chemistry.

Leaper, D.J., Schultz, G., Carville, K., Fletcher, J., Swanson, T., Drake, R., 2014. Extending the TIME concept: what have we learned in the past 10 years? Int. Wound J. 9, 1–19.

Lee, J., Lee, D.G., 2008. Structure-antimicrobial activity relationship between pleurocidin and its enantiomer. Exp. Mol. Med. 40, 370–376. https://doi.org/10.3858/emm.2008.40.4.370

Lee, K.H., Kim, H.Y., Khil, M.S., Ra, Y.M., Lee, D.R., 2003. Characterization of nanostructured poly(ε-caprolactone) nonwoven mats via electrospinning. Polymer (Guildf). 44, 1287–1294. https://doi.org/10.1016/S0032-3861(02)00820-0

Lehrer, R.I., Rosenman, M., Harwig, S.S.S.L., Jackson, R., Eisenhauer, P., 1991. Ultrasensitive assays for endogenous antimicrobial polypeptides. J. Immunol. Methods 137, 167–173. https://doi.org/10.1016/0022-1759(91)90021-7

Li, X.-Z., Livermore, D.M., Nikaidol, H., Poole, (K, Krebes, K., Mcnally, C., Neshat, S., 1994. Role of efflux pump(s) in intrinsic resistance of *Pseudomonas aeruginosa*: resistance to tetracycline, chloramphenicol, and norfloxacin. Antimicrob. Agents Chemother. 38, 1732. https://doi.org/10.1128/AAC.38.8.1732

Lindholm, C., Searle, R., 2016. Wound management for the 21st century : combining effectiveness and efficiency. Int. Wound J. 13, 5–15. https://doi.org/10.1111/iwj.12623

Liu, T., Zhang, Z., Liu, J., Dong, P., Tian, F., Li, F., Meng, X., 2022. Electrospun kaolin-loaded chitosan/PEO nanofibers for rapid hemostasis and accelerated wound healing. Int. J. Biol. Macromol. 217, 998–1011. https://doi.org/10.1016/j.ijbiomac.2022.07.186

Livingston, R.J., Butterworth, J.W., Belt, P., 2013. Reaction or infection: Topical chloramphenicol treatment. Ann. R. Coll. Surg. Engl. 95, 20–21. https://doi.org/10.1308/003588413X13511609955418

Loh, Q.L., Choong, C., 2013. Three-Dimensional Scaffolds for Tissue Engineering Applications: Role of Porosity and Pore Size. Tissue Eng. Part B Rev. 19, 485–502. https://doi.org/10.1089/TEN.TEB.2012.0437

Lorenz, K., Preem, L., Sagor, K., Putrinš, M., Tenson, T., Kogermann, K., 2023. Development of In Vitro and Ex Vivo Biofilm Models for the Assessment of Antibacterial Fibrous Electrospun Wound Dressings. Mol. Pharm. 20, 1230–1246. https://doi.org/10.1021/ACS.MOLPHARMACEUT.2C00902

Luong-Van, E., Grøndahl, L., Chua, K.N., Leong, K.W., Nurcombe, V., Cool, S.M., 2006. Controlled release of heparin from poly(ε-caprolactone) electrospun fibers. Biomaterials 27, 2042–2050. https://doi.org/10.1016/J.BIOMATERIALS.2005.10.028

Luraghi, A., Peri, F., Moroni, L., 2021. Electrospinning for drug delivery applications: A review. J. Control. Release 334, 463–484. https://doi.org/10.1016/j.jconrel.2021.03.033

Maillard, J.-Y., Kampf, G., Cooper, R., 2021. Antimicrobial stewardship of antiseptics that are pertinent to wounds: the need for a united approach. JAC-Antimicrobial Resist. 3, 1–20. https://doi.org/10.1093/jacamr/dlab027

Maillard, J.Y., Kampf, G., Cooper, R., 2021. Antimicrobial stewardship of antiseptics that are pertinent to wounds: The need for a united approach. JAC-Antimicrobial Resist. 3. https://doi.org/10.1093/jacamr/dlab027

Malanovic, N., Ön, A., Pabst, G., Zellner, A., Lohner, K., 2020. Octenidine: Novel insights into the detailed killing mechanism of Gram-negative bacteria at a cellular and molecular level. Int. J. Antimicrob. Agents 56, 106146. https://doi.org/10.1016/j.ijantimicag.2020.106146

Malich, G., Markovic, B., Winder, C., 1997. The sensitivity and specificity of the MTS tetrazolium assay for detecting the in vitro cytotoxicity of 20 chemicals using human cell lines. Toxicology 124, 179–192. https://doi.org/10.1016/S0300-483X(97)00151-0

Manzo, G., Hind, C.K., Ferguson, P.M., Amison, R.T., Hodgson-Casson, A.C., Ciazynska, K.A., Weller, B.J., Clarke, M., Lam, C., Man, R.C.H., Shaughnessy, B.G.O., Clifford, M., Bui, T.T., Drake, A.F., Atkinson, R.A., Lam, J.K.W., Pitchford, S.C., Page, C.P., Phoenix, D.A., Lorenz, C.D., Sutton, J.M., Mason, A.J., 2020. A pleurocidin analogue with greater conformational flexibility, enhanced antimicrobial potency and in vivo therapeutic efficacy. Commun. Biol. 3, 1–16. https://doi.org/10.1038/s42003-020-01420-3

Markowska, K., Grudniak, A.M., Krawczyk, K., Wróbel, I., Wolska, K.I., 2014. Modulation of antibiotic resistance and induction of a stress response in *Pseudomonas aeruginosa* by silver nanoparticles. J. Med. Microbiol. 63, 849–854. https://doi.org/10.1099/jmm.0.068833-0

Martinengo, L., Olsson, M., Bajpai, R., Soljak, M., Upton, Z., Schmidtchen, A., Car, J., Järbrink, K., 2019. Prevalence of chronic wounds in the general population: systematic review and meta-analysis of observational studies. Ann. Epidemiol. 29, 8–15. https://doi.org/10.1016/j.annepidem.2018.10.005

May, A., Kopecki, Z., Carney, B., Cowin, A., 2022. Antimicrobial silver dressings: a review of emerging issues for modern wound care. ANZ J. Surg. 92, 379–384. https://doi.org/10.1111/ans.17382

Mayslich, C., Grange, P.A., Dupin, N., 2021. *Cutibacterium acnes* as an opportunistic pathogen: an update of its virulence-associated factors. Microorganisms 9, 1–21. https://doi.org/https:// doi.org/10.3390/microorganisms 9020303

Mcdonnell, G., Russell, A.D., 1999. Antiseptics and disinfectants: Activity, action, and resistance. Clin. Microbiol. Rev. 12, 147–179. https://doi.org/10.1128/cmr.12.1.147

McInnes, S.J.P., Macdonald, T.J., Parkin, I.P., Nann, T., Voelcker, N.H., 2018. Electrospun composites of polycaprolactone and porous silicon nanoparticles for the tunable delivery of small therapeutic molecules. Nanomaterials 8, 205. https://doi.org/10.3390/nano8040205

Meade, E., Slattery, M.A., Garvey, M., 2021. Biocidal resistance in clinically relevant microbial species: A major public health risk. Pathogens 10, 1–14. https://doi.org/10.3390/pathogens10050598

Megelski, S., Stephens, J.S., Chase, D.B., Rabolt, J.F., 2002. Micro- and Nanostructured Surface Morphology on Electrospun Polymer Fibers. Macromolecules 35, 8456–8466. https://doi.org/10.1021/ma020444a

Mestas, J., Hughes, C.C.W., 2004. Of Mice and Not Men: Differences between Mouse and Human Immunology. J. Immunol. 172, 2731–2738.

Mianehro, A., 2022. Electrospun Bioscaffold Based on Cellulose Acetate and Dendrimer-modified Cellulose Nanocrystals for Controlled Drug Release. Carbohydr. Polym. Technol. Appl. 3, 100187. https://doi.org/10.1016/J.CARPTA.2022.100187

Miao, F., Li, Y., Tai, Z., Zhang, Y., Gao, Y., Hu, M., Zhu, Q., 2021. Antimicrobial Peptides: The Promising Therapeutics for Cutaneous Wound Healing. Macromol. Biosci. 21, 1–30. https://doi.org/10.1002/mabi.202100103

Michael, C.A., Dominey-Howes, D., Labbate, M., 2014. The antimicrobial resistance crisis: Causes, consequences, and management. Front. Public Heal. 2, 1–8. https://doi.org/10.3389/fpubh.2014.00145

Mizan, M.H., Gurave, P.M., Rastgar, M., Rahimpour, A., Srivastava, R.K., Sadrzadeh, M., 2023. "Biomass to Membrane": Sulfonated Kraft Lignin / PCL Superhydrophilic Electrospun Membrane for Gravity-Driven Oil-in- Water Emulsion Separation. ACS Appl. Mater. Interfaces. https://doi.org/10.1021/acsami.3c09964

Modak, S.M., Fox, C.L., 1973. Binding of silver sulfadiazine to the cellular components of *Pseudomonas aeruginosa*. Biochem. Pharmacol. 22, 2391–2404. https://doi.org/10.1016/0006-2952(73)90341-9

Modak, S.M., Sampath, L., Fox, C.L., 1988. Combined topical use of silver sulfadiazine and antibiotics as a possible solution to bacterial resistance in burn wounds. J. Burn Care Rehabil. 9, 359–363. https://doi.org/10.1097/00004630-198807000-00009

Morais, D.C., Fontes, M.L., Oliveira, A.B., Gabbai-Armelin, P.R., Ferrisse, T.M., De Oliveira, L.F.C., Brighenti, F.L., Barud, H.S., De Sousa, F.B., 2023. Combining Polymer and Cyclodextrin Strategy for Drug Release of Sulfadiazine from Electrospun Fibers. Pharmaceutics 15, 1890. https://doi.org/10.3390/PHARMACEUTICS15071890/S1

Morita, Y., Tomida, J., Kawamura, Y., 2014. Responses of *Pseudomonas aeruginosa* to antimicrobials. Front. Microbiol. 4, 422. https://doi.org/10.3389/FMICB.2013.00422

Moyer, C., Brentano, L., Gravens, D., Margraf, H., Monafo, W., 1965. Treatment of Large Human Burns With 0.5% Silver Nitrate Solution. Arch. Surg. 90, 812–867.

Mulhall, A., De Louvois, J., Hurley, R., 1983. Chloramphenicol toxicity in neonates: its incidence and prevention. BMJ (Clinical research ed.) 287, 1424–1427. https://doi.org/10.1136/BMJ.287.6403.1424

Murray, C.J., Ikuta, K.S., Sharara, F., Swetschinski, L., Robles Aguilar, G., Gray, A., Han, C., Bisignano, C., Rao, P., Wool, E., Johnson, S.C., Browne, A.J., Chipeta, M.G., Fell, F., Hackett, S., Haines-Woodhouse, G., Kashef Hamadani, B.H., Kumaran, E.A.P., McManigal, B., Agarwal, R., Akech, S., Albertson, S., Amuasi, J., Andrews, J., Aravkin, A., Ashley, E., Bailey, F., Baker, S., Basnyat, B., Bekker, A., Bender, R., Bethou, A., Bielicki, J., Boonkasidecha, S., Bukosia, J., Carvalheiro, C., Castañeda-Orjuela, C., Chansamouth, V., Chaurasia, S., Chiurchiù, S., Chowdhury, F., Cook, A.J., Cooper, B., Cressey, T.R., Criollo-Mora, E., Cunningham, M., Darboe, S., Day, N.P.J., De Luca, M., Dokova, K., Dramowski, A., Dunachie, S.J., Eckmanns, T., Eibach, D., Emami, A., Feasey, N., Fisher-Pearson, N., Forrest, K., Garrett, D., Gastmeier, P., Giref, A.Z., Greer, R.C., Gupta, V., Haller, S., Haselbeck, A., Hay, S.I., Holm, M., Hopkins, S., Iregbu, K.C., Jacobs, J., Jarovsky, D., Javanmardi, F., Khorana, M., Kissoon, N., Kobeissi, E., Kostyanev, T., Krapp, F., Krumkamp, R.,

Kumar, A., Kyu, H.H., Lim, C., Limmathurotsakul, D., Loftus, M.J., Lunn, M., Ma, J., Mturi, N., Munera-Huertas, T., Musicha, P., Mussi-Pinhata, M.M., Nakamura, T., Nanavati, R., Nangia, S., Newton, P., Ngoun, C., Novotney, A., Nwakanma, D., Obiero, C.W., Olivas-Martinez, A., Olliaro, P., Ooko, E., Ortiz-Brizuela, E., Peleg, A.Y., Perrone, C., Plakkal, N., Ponce-de-Leon, A., Raad, M., Ramdin, T., Riddell, A., Roberts, T., Robotham, J.V., Roca, A., Rudd, K.E., Russell, N., Schnall, J., Scott, J.A.G., Shivamallappa, M., Sifuentes-Osornio, J., Steenkeste, N., Stewardson, A.J., Stoeva, T., Tasak, N., Thaiprakong, A., Thwaites, G., Turner, C., Turner, P., van Doorn, H.R., Velaphi, S., Vongpradith, A., Vu, H., Walsh, T., Waner, S., Wangrangsimakul, T., Wozniak, T., Zheng, P., Sartorius, B., Lopez, A.D., Stergachis, A., Moore, C., Dolecek, C., Naghavi, M., 2022. Global burden of bacterial antimicrobial resistance in 2019: a systematic analysis. Lancet 399, 629–655. https://doi.org/10.1016/s0140-6736(21)02724-0

Muthukrishnan, L., 2022. An overview on electrospinning and its advancement toward hard and soft tissue engineering applications. Colloid Polym. Sci. 300, 875–901. https://doi.org/10.1007/s00396-022-04997-9

Nadaf, A., Gupta, A., Hasan, N., Fauziya, N., Ahmad, S., Kesharwani, P., Ahmad, F.J., 2022. Recent update on electrospinning and electrospun nanofibers: current trends and their applications. RSC Adv. 12, 23808–23828. https://doi.org/10.1039/d2ra02864f

Naseri, N., Mathew, A.P., Girandon, L., Fröhlich, M., Oksman, K., 2015. Porous electrospun nanocomposite mats based on chitosan–cellulose nanocrystals for wound dressing: effect of surface characteristics of nanocrystals. Cellulose 22, 521–534. https://doi.org/10.1007/S10570-014-0493-Y/FIGURES/8

Natarajan, L., New, J., Dasari, A., Yu, S., Manan, M.A., 2014. Surface morphology of electrospun PLA fibers: Mechanisms of pore formation. RSC Adv. 4, 44082–44088. https://doi.org/10.1039/c4ra06215a

Nazemi, K., Moztarzadeh, F., Jalali, N., Asgari, S., Mozafari, M., 2014. Synthesis and characterization of poly(lactic-co-glycolic) acid nanoparticles-loaded chitosan/bioactive glass scaffolds as a localized delivery system in the bone defects. Biomed Res. Int. 898930. https://doi.org/10.1155/2014/898930

Nelson, E.E., Guyer, A.E., 2011. The development of the ventral prefrontal cortex and social flexibility. Dev. Cogn. Neurosci. 1, 233–245. https://doi.org/10.1016/j.dcn.2011.01.002.The

Neugirg, B.R., Burgard, M., Greiner, A., Fery, A., 2016. Tensile versus AFM testing of electrospun PVA nanofibers: Bridging the gap from Microscale to nanoscale. J. Polym. Sci. Part B Polym. Phys. 54, 2418–2424. https://doi.org/10.1002/polb.24225

Odds, F.C., 2003. Synergy, antagonism, and what the chequerboard puts between them. J. Antimicrob. Chemother. 52, 1. https://doi.org/10.1093/jac/dkg301

Oh, Y., Kwon, D.S., Jo, E., Kang, Y., Sim, S., Kim, J., 2023. Formation of sub-100-nm suspended nanowires with various materials using thermally adjusted electrospun nanofibers as templates. Microsystems Nanoeng. 9, 15. https://doi.org/10.1038/s41378-022-00459-y

Omer, S., Forgách, L., Zelkó, R., Sebe, I., 2021. Scale-up of electrospinning: Market overview of products and devices for pharmaceutical and biomedical purposes. Pharmaceutics 13, 1–21. https://doi.org/10.3390/pharmaceutics13020286

Oztemur, J., Sezgin, H., Ozdemir, S., Tezcan-unlu, H., 2023. Investigation of biodegradability and cellular activity of PCL / PLA and PCL / PLLA electrospun webs for tissue engineering applications. Biopolymers e23564. https://doi.org/10.1002/bip.23564

Pai, C.L., Boyce, M.C., Rutledge, G.C., 2009. Morphology of porous and wrinkled fibers of polystyrene electrospun from dimethylformamide. Macromolecules 42, 2102–2114. https://doi.org/10.1021/ma802529h

Pailler-Mattei, C., Bec, S., Zahouani, H., 2008. In vivo measurements of the elastic mechanical properties of human skin by indentation tests. Med. Eng. Phys. 30, 599–606. https://doi.org/10.1016/J.MEDENGPHY.2007.06.011

Palo, M., Rönkönharju, S., Tiirik, K., Viidik, L., Sandler, N., Kogermann, K., 2019. Bi-layered polymer carriers with surface modification by electrospinning for potential wound care applications. Pharmaceutics 11, 678. https://doi.org/10.3390/pharmaceutics11120678

Pang, Z., Raudonis, R., Glick, B.R., Lin, T.J., Cheng, Z., 2019. Antibiotic resistance in *Pseudomonas aeruginosa*: mechanisms and alternative therapeutic strategies. Biotechnol. Adv. 37, 177–192. https://doi.org/10.1016/j.biotechadv.2018.11.013

Park, C.H., Chung, M.Y., Unnithan, A.R., Kim, C.S., 2015. Creation of a functional graded nanobiomembrane using a new electrospinning system for drug release control and an in vitro validation of drug release behavior of the coating membrane. Mater. Sci. Eng. C 50, 133–140. https://doi.org/10.1016/J.MSEC.2015.02.001

Patel, S., Akhtar, N., 2017. Antimicrobial peptides (AMPs): The quintessential 'offense and defense' molecules are more than antimicrobials. Biomed. Pharmacother. 95, 1276–1283. https://doi.org/10.1016/j.biopha.2017.09.042

Patrzykat, A., Friedrich, C.L., Zhang, L., Mendoza, V., Hancock, R.E.W., 2002. Sublethal concentrations of pleurocidin-derived antimicrobial peptides inhibit macromolecular synthesis in *Escherichia coli.* Antimicrob. Agents Chemother. 46, 605–614. https://doi.org/10.1128/AAC.46.3.605-614.2002

Paul, M., Carrara, E., Retamar, P., Tängdén, T., Bitterman, R., Bonomo, R.A., de Waele, J., Daikos, G.L., Akova, M., Harbarth, S., Pulcini, C., Garnacho-Montero, J., Seme, K., Tumbarello, M., Lindemann, P.C., Gandra, S., Yu, Y., Bassetti, M., Mouton, J.W., Tacconelli, E., Rodríguez-Baño, J., 2022. European Society of Clinical Microbiology and Infectious Diseases (ESCMID) guidelines for the treatment of infections caused by multidrug-resistant Gram-negative bacilli (endorsed by European society of intensive care medicine). Clin. Microbiol. Infect. 28, 521–547. https://doi.org/10.1016/j.cmi.2021.11.025

Pennycook, S.J., 2005. Encyclopedia of Condensed Matter Physics. Elsevier.

Percival, S.L., Lipsky, B., Mccarty, S.M., 2014. Biofilms and Wounds : An Overview of the Evidence. Adv. Wound Care 4, 373–381. https://doi.org/10.1089/wound.2014.0557

Pereira, B.M.P., Tagkopoulos, I., 2019. Benzalkonium chlorides: Uses, regulatory status, and microbial resistance. Appl. Environ. Microbiol. 85, 1–13. https://doi.org/10.1128/AEM.00377-19

Peter, M., Binulal, N.S., Soumya, S., Nair, S. V., Furuike, T., Tamura, H., Jayakumar, R., 2010. Nanocomposite scaffolds of bioactive glass ceramic nanoparticles disseminated chitosan matrix for tissue engineering applications. Carbohydr. Polym. 79, 284–289. https://doi.org/10.1016/j.carbpol.2009.08.001

Ph. Eur, 2024. European Pharmacopoeia. Wettability of porous solids including powders (2.9.45.) 429–432.

Pham, Q.P., Sharma, U., Mikos, A.G., 2006. Electrospun poly (E-caprolactone) microfiber and multilayer nanofiber/microfiber scaffolds: Characterization of scaffolds and measurement of cellular infiltration. Biomacromolecules 7, 2796–2805. https://doi.org/10.1021/bm060680j

Piaggesi, A., Läuchli, S., Bassett, 2018. Advanced therapies in wound management. J. Wound Care 27, Suppl 6.
Pietsch, F., Heidrich, G., Nordholt, N., Schreiber, F., 2021. Prevalent Synergy and Antagonism Among Antibiotics and Biocides in *Pseudomonas aeruginosa*. Front. Microbiol. 11, 1–6. https://doi.org/10.3389/fmicb.2020.615618
Pinheiro Bruni, G., dos Santos Acunha, T., de Oliveira, J.P., Martins Fonseca, L., Tavares da Silva, F., Martins Guimarães, V., da Rosa Zavareze, E., 2020. Electrospun protein fibers loaded with yerba mate extract for bioactive release in food packaging. J. Sci. Food Agric. 100, 3341–3350. https://doi.org/10.1002/JSFA.10366
Pok, S.W., Wallace, K.N., Madihally, S. V., 2010. In vitro characterization of polycaprolactone matrices generated in aqueous media. Acta Biomater. 6, 1061–1068. https://doi.org/10.1016/J.ACTBIO.2009.08.002
Preem, L., Mahmoudzadeh, M., Putrins, M., Meos, A., Laidma, I., Koivuniemi, A., Bunker, A., Tenson, T., Kogermann, K., 2017. Interactions between Chloramphenicol, Carrier Polymers, and Bacteria − Implications for Designing Electrospun Drug Delivery Systems Countering Wound Infection. Mol. Pharm. 14, 4417–4430. https://doi.org/10.1021/acs.molpharmaceut.7b00524
Prestinaci, F., Pezzotti, P., Pantosti, A., 2015. Antimicrobial resistance: A global multifaceted phenomenon. Pathog. Glob. Health 109, 309–318. https://doi.org/10.1179/2047773215Y.0000000030
Probst, S., Apelqvist, J., Bjarnsholt, T., Lipsky, B., Ousey, K., Peters, E., 2022. Antimicrobials and Non-healing Wounds: An Update. J. Wound Manag. 23(3Sup1), S1–S33. https://doi.org/10.35279/jowm2022.23.03.sup01
Puca, V., Marulli, R.Z., Grande, R., Vitale, I., Niro, A., Molinaro, G., Prezioso, S., Muraro, R., Di Giovanni, P., 2021. Microbial species isolated from infected wounds and antimicrobial resistance analysis: Data emerging from a three-years retrospective study. Antibiotics 10, 1162. https://doi.org/10.3390/antibiotics10101162
Qin, S., Xiao, W., Zhou, C., Pu, Q., Deng, X., Lan, L., Liang, H., Song, X., Wu, M., 2022. *Pseudomonas aeruginosa*: pathogenesis, virulence factors, antibiotic resistance, interaction with host, technology advances and emerging therapeutics. Signal Transduct. Target. Ther. 7, 1–27. https://doi.org/10.1038/s41392-022-01056-1
Rashid, T.U., Gorga, R.E., Krause, W.E., 2021. Mechanical Properties of Electrospun Fibers—A Critical Review. Adv. Eng. Mater. 23, 1–26. https://doi.org/10.1002/adem.202100153
Razouq, H., Berger, T., Hüsing, N., Diwald, O., 2023. Vapor phase-grown TiO2 and ZnO nanoparticles inside electrospun polymer fibers and their calcination-induced organization. Monatshefte fur Chemie 154, 849–856. https://doi.org/10.1007/s00706-023-03093-0
Refate, A., Mohamed, Y., Mohamed, M., Sobhy, M., Samhy, K., Khaled, O., Eidaroos, K., Batikh, H., El-Kashif, E., El-Khatib, S., Mehanny, S., 2023. Influence of electrospinning parameters on biopolymers nanofibers, with emphasis on cellulose & chitosan. Heliyon 9, e17051. https://doi.org/10.1016/j.heliyon.2023.e17051
Ren, X., Han, Y., Wang, J., Jiang, Y., Yi, Z., Xu, H., Ke, Q., 2018. An aligned porous electrospun fibrous membrane with controlled drug delivery – An efficient strategy to accelerate diabetic wound healing with improved angiogenesis. Acta Biomater. 70, 140–153. https://doi.org/10.1016/j.actbio.2018.02.010
Rice, L.B., 2008. Federal funding for the study of antimicrobial resistance in nosocomial pathogens: No ESKAPE. J. Infect. Dis. 197, 1079–1081. https://doi.org/10.1086/533452

Richards, R.M.E., Taylor, R.B., Xing, D.K.L., 1991. An evaluation of the antibacterial activities of combinations of sulfonamides, trimethoprim, dibromopropamidine, and silver nitrate compared with their uptakes by selected bacteria. J. Pharm. Sci. 80, 861–867. https://doi.org/10.1002/jps.2600800912

Rodrigues, M., Kosaric, N., Bonham, C.A., Gurtner, G.C., 2019. Wound healing: A cellular perspective. Physiol. Rev. 99, 665–706. https://doi.org/10.1152/physrev.00067.2017

Roell, K.R., Reif, D.M., Motsinger-Reif, A.A., 2017. An introduction to terminology and methodology of chemical synergy-perspectives from across disciplines. Front. Pharmacol. 8, 1–11. https://doi.org/10.3389/fphar.2017.00158

Rzycki, M., Drabik, D., Szostak-Paluch, K., Hanus-Lorenz, B., Kraszewski, S., 2021. Unraveling the mechanism of octenidine and chlorhexidine on membranes: Does electrostatics matter? Biophys. J. 120, 3392–3408. https://doi.org/10.1016/j.bpj.2021.06.027

Saiman, L., 2007. Clinical utility of synergy testing for multidrug-resistant *Pseudomonas aeruginosa* isolated from patients with cystic fibrosis: "the motion for." Paediatr. Respir. Rev. 8, 249–255. https://doi.org/10.1016/j.prrv.2007.04.006

Sajan, D., Sockalingum, G.D., Manfait, M., Hubert Joe, I., Jayakumar, V.S., 2008. NIR-FT Raman, FT-IR and surface-enhanced Raman scattering spectra, with theoretical simulations on chloramphenicol. J. Raman Spectrosc. 39, 1772–1783. https://doi.org/10.1002/JRS.2033

Sanchaniya, J.V., Lasenko, I., Kanukuntla, S.P., Mannodi, A., Viluma-Gudmona, A., Gobins, V., 2023. Preparation and Characterization of Non-Crimping Laminated Textile Composites Reinforced with Electrospun Nanofibers. Nanomaterials 13, 1949. https://doi.org/10.3390/nano13131949

Santajit, S., Indrawattana, N., 2016. Mechanisms of Antimicrobial Resistance in ESKAPE Pathogens. Biomed Res. Int. 2016, 2475067. https://doi.org/10.1155/2016/2475067

Scheler, S., 2014. The polymer free volume as a controlling factor for drug release from poly(lactide-co-glycolide) microspheres. J. Appl. Polym. Sci. 131, 39740. https://doi.org/10.1002/APP.39740

Schneider, L.A., Korber, A., Grabbe, S., Dissemond, J., 2007. Influence of pH on wound-healing: A new perspective for wound-therapy? Arch. Dermatol. Res. 298, 413–420. https://doi.org/10.1007/s00403-006-0713-x

Sebe, I., Ostorházi, E., Bodai, Z., Eke, Z., Szakács, J., Kovács, N.K., Zelkó, R., 2017. In vitro and in silico characterization of fibrous scaffolds comprising alternate colistin sulfate-loaded and heat-treated polyvinyl alcohol nanofibrous sheets. Int. J. Pharm. 523, 151–158. https://doi.org/10.1016/j.ijpharm.2017.03.044

Sebe, I., Szabó, B., Nagy, Z.K., Szabó, D., Zsidai, L., Kocsis, B., Zelkó, R., 2013. Polymer structure and antimicrobial activity of polyvinylpyrrolidone-based iodine nanofibers prepared with high-speed rotary spinning technique. Int. J. Pharm. 458, 99–103. https://doi.org/10.1016/J.IJPHARM.2013.10.011

Sharifi, F., Irani, S., Zandi, M., Soleimani, M., Atyabi, S.M., 2016. Comparative of fibroblast and osteoblast cells adhesion on surface modified nanofibrous substrates based on polycaprolactone. Prog. Biomater. 5, 213–222. https://doi.org/10.1007/S40204-016-0059-1/FIGURES/6

Sheet, S., Vinothkannan, M., Balasubramaniam, S., Subramaniyan, S.A., Acharya, S., Lee, Y.S., 2018. Highly Flexible Electrospun Hybrid (Polyurethane/Dextran/Pyocyanin) Membrane for Antibacterial Activity via Generation of Oxidative Stress.

ACS Omega 3, 14551–14561. https://doi.org/10.1021/ACSOMEGA.8B01607/SUPPL_FILE/AO8B01607_SI_001.PDF
Shen, A.Y., Haddad, E.J., Hunter-Smith, D.J., Rozen, W.M., 2018. Efficacy and adverse effects of topical chloramphenicol ointment use for surgical wounds: a systematic review. ANZ J. Surg. 88, 1243–1246. https://doi.org/10.1111/ans.14465
Shevchenko, R. V., James, S.L., James, S.E., 2010. A review of tissue-engineered skin bioconstructs available for skin reconstruction. J. R. Soc. Interface 7, 229–258. https://doi.org/10.1098/RSIF.2009.0403
Si, M.Z., Kang, Y.P., Zhang, Z.G., 2009. Surface-enhanced Raman scattering (SERS) spectra of chloramphenicol in Ag colloids prepared by microwave heating method. J. Raman Spectrosc. 40, 1319–1323. https://doi.org/10.1002/JRS.2286
Silver, S., Phung, L.T., Silver, G., 2006. Silver as biocides in burn and wound dressings and bacterial resistance to silver compounds. J. Ind. Microbiol. Biotechnol. 33, 627–634. https://doi.org/10.1007/S10295-006-0139-7
Sin Cheow, W., Wook Chang, M., Hadinoto, K., 2010. Antibacterial Efficacy of Inhalable Levofloxacin-Loaded Polymeric Nanoparticles Against E. coli Biofilm Cells: The Effect of Antibiotic Release Profile. Pharm. Res. 27, 1597–1609. https://doi.org/10.1007/s11095-010-0142-6
Širc, J., Hobzová, R., Kostina, N., Munzarová, M., Juklíčková, M., Lhotka, M., Kubinová, Š., Zajícová, A., Michálek, J., 2012. Morphological characterization of nanofibers: Methods and application in practice. J. Nanomater. 2012, 327369. https://doi.org/10.1155/2012/327369
Soliman, S., Sant, S., Nichol, J.W., Khabiry, M., Traversa, E., Khademhosseini, A., 2011. Controlling the porosity of fibrous scaffolds by modulating the fiber diameter and packing density. J. Biomed. Mater. Res. Part A 96A, 566–574. https://doi.org/10.1002/JBM.A.33010
Srikar, R., Megaridis, C.M., Yarin, A.L., Bazilevsky, A. V., 2009. Desorption-Limited Mechanism of Release From Polymer Nanofibers. Proc. ASME Int. Manuf. Sci. Eng. Conf. MSEC2008 2, 465–474. https://doi.org/10.1115/MSEC_ICMP2008-72054
Stachewicz, U., Bailey, R.J., Wang, W., Barber, A.H., 2012. Size dependent mechanical properties of electrospun polymer fibers from a composite structure. Polymer (Guildf). 53, 5132–5137. https://doi.org/10.1016/J.POLYMER.2012.08.064
Summerfield, A., Meurens, F., Ricklin, M.E., 2015. The immunology of the porcine skin and its value as a model for human skin. Mol. Immunol. 66, 14–21. https://doi.org/10.1016/J.MOLIMM.2014.10.023
Syed, M.H., Khan, M.R., Ahmad, M., Mohd, K., Dalour, M., Beg, H., Abdullah, N., 2023. A Review on Current Trends and Future Prospectives of Electrospun Biopolymeric Nanofibers for Biomedical Applications. Eur. Polym. J. 112352. https://doi.org/10.1016/j.eurpolymj.2023.112352
Tammaro, L., Saturnino, C., D'Aniello, S., Vigliotta, G., Vittoria, V., 2015. Polymorphic solidification of Linezolid confined in electrospun PCL fibers for controlled release in topical applications. Int. J. Pharm. 490, 32–38. https://doi.org/10.1016/J.IJPHARM.2015.04.070
Tan, E.P.S., Ng, S.Y., Lim, C.T., 2005. Tensile testing of a single ultrafine polymeric fiber. Biomaterials 26, 1453–1456. https://doi.org/10.1016/j.biomaterials.2004.05.021
Terreni, M., 2021. New antibiotics for multidrug-resistant bacterial strains: Latest research developments and future perspectives. Molecules 26, 2671. https://doi.org/10.3390/molecules26092671

Thakkar, S., Misra, M., 2017. Electrospun polymeric nanofibers: New horizons in drug delivery. Eur. J. Pharm. Sci. 107, 148–167. https://doi.org/10.1016/j.ejps.2017.07.001

Tottoli, E.M., Benedetti, L., Chiesa, E., Pisani, S., Bruni, G., Genta, I., Conti, B., Ceccarelli, G., Dorati, R., 2023. Electrospun Naringin-Loaded Fibers for Preventing Scar Formation during Wound Healing. Pharmaceutics 15, 747. https://doi.org/10.3390/pharmaceutics15030747

Van Vuuren, S.F., Suliman, S., Viljoen, A.M., 2009. The antimicrobial activity of four commercial essential oils in combination with conventional antimicrobials. Lett. Appl. Microbiol. 48, 440–446. https://doi.org/10.1111/j.1472-765X.2008.02548.x

Van Zyl, R.L., Seatlholo, S.T., Van Vuuren, S.F., Viljoen, A., 2010. Pharmacological interactions of essential oil constituents on the viability of micro-organisms. Nat. Prod. Commun. 5, 1381–1386. https://doi.org/10.1177/1934578x1000500909

Vass, P., Szabó, E., Domokos, A., Hirsch, E., Galata, D., Farkas, B., Démuth, B., Andersen, S.K., Vigh, T., Verreck, G., Marosi, G., Nagy, Z.K., 2020. Scale-up of electrospinning technology: Applications in the pharmaceutical industry. Wiley Interdiscip. Rev. Nanomedicine Nanobiotechnology 12, 1–24. https://doi.org/10.1002/wnan.1611

Vogt, L., Boccaccini, A.R., 2021. Random and aligned electrospun poly(ε-caprolactone) (PCL)/poly(1,8-octanediol-co-citrate) (POC) fiber mats for cardiac tissue engineering using benign solvents. Eur. Polym. J. 160, 110772. https://doi.org/10.1016/J.EURPOLYMJ.2021.110772

Vos, T., Allen, C., Arora, M., Barber, R.M., Brown, A., Carter, A., Casey, D.C., Charlson, F.J., Chen, A.Z., Coggeshall, M., Cornaby, L., Dandona, L., Dicker, D.J., Dilegge, T., Erskine, H.E., Ferrari, A.J., Fitzmaurice, C., Fleming, T., Forouzanfar, M.H., Fullman, N., Goldberg, E.M., Graetz, N., Haagsma, J.A., Hay, S.I., Johnson, C.O., Kassebaum, N.J., Kawashima, T., Kemmer, L., Khalil, I.A., Kyu, H.H., Leung, J., Lim, S.S., Lopez, A.D., Marczak, L., Mokdad, A.H., Naghavi, M., Nguyen, G., Nsoesie, E., Olsen, H., Pigott, D.M., Pinho, C., Rankin, Z., Reinig, N., Sandar, L., Smith, A., Stanaway, J., Steiner, C., Teeple, S., Thomas, B.A., Troeger, C., Wagner, J.A., Wang, H., Wanga, V., Whiteford, H.A., Zoeckler, L., Alexander, L.T., Anderson, G.M., Bell, B., Bienhoff, K., Biryukov, S., Blore, J., Brown, J., Coates, M.M., Daoud, F., Estep, K., Foreman, K., Fox, J., Friedman, J., Frostad, J., Godwin, W.W., Hancock, J., Huynh, C., Iannarone, M., Kim, P., Kutz, M., Masiye, F., Millear, A., Mirarefin, M., Mooney, M.D., Moradi-Lakeh, M., Mullany, E., Mumford, J.E., Ng, M., Rao, P., Reitsma, M.B., Reynolds, A., Roth, G.A., Shackelford, K.A., Sivonda, A., Sligar, A., Sorensen, R.J.D., Sur, P., Vollset, S.E., Woodbrook, R., Zhou, M., Murray, C.J.L., Ellenbogen, R.G., Kotsakis, G.A., Mock, C.N., Anderson, B.O., Futran, N.D., Jensen, P.N., Watkins, D.A., Bhutta, Z.A., Nisar, M.I., Akseer, N., Abajobir, A.A., Knibbs, L.D., Lalloo, R., Scott, J.G., Alam, N.K.M., Gouda, H.N., Guo, Y., McGrath, J.J., Jeemon, P., Dandona, R., Kumar, G.A., Gething, P.W., Bisanzio, D., Deribew, A., Ali, R., Bennett, D.A., Rahimi, K., Kinfu, Y., Duan, L., Li, Y., Liu, S., Jin, Y., Wang, L., Ye, P., Liang, X., Azzopardi, P., Gibney, K.B., Meretoja, A., Alam, K., Borschmann, R., Colquhoun, S.M., Patton, G.C., Weintraub, R.G., Szoeke, C.E.I., Ademi, Z., Taylor, H.R., Lozano, R., Campos-Nonato, I.R., Campuzano, J.C., Gomez-Dantes, H., Heredia-Pi, I.B., Mejia-Rodriguez, F., Montañez Hernandez, J.C., Rios Blancas, M.J., Servan-Mori, E.E., Mensah, G.A., Salomon, J.A., Thorne-Lyman, A.L., Ajala, O.N., Bärnighausen, T., Ding, E.L., Farvid, M.S., Wagner, G.R., Osman, M., Shrime, M.G., Fitchett, J.R.A., Abate, K.H., Gebrehiwot, T.T., Gebremedhin, A.T., Abbafati, C., Abbas, K.M., Abd-Allah, F.,

Abraham, B., Abubakar, I., Banerjee, A., Benzian, H., Abu-Raddad, L.J., Abu-Rmeileh, N.M., Ackerman, I.N., Buchbinder, R., Gabbe, B., Thrift, A.G., Adebiyi, A.O., Akinyemi, R.O., Fürst, T., Adou, A.K., Afanvi, K.A., Agardh, E.E., Badawi, A., Popova, S., Agarwal, A., Ahmad Kiadaliri, A., Norrving, B., Ahmadieh, H., Yaseri, M., Jahanmehr, N., Al-Aly, Z., Driscoll, T.R., Kemp, A.H., Leigh, J., Mekonnen, A.B., Aldhahri, S.F., Altirkawi, K.A., Alegretti, M.A., Alemu, Z.A., Alhabib, S., Alkerwi, A., Alla, F., Guillemin, F., Allebeck, P., Rabiee, R.H.S., Carrero, J.J., Fereshtehnejad, S.M., Weiderpass, E., Havmoeller, R., Al-Raddadi, R., Alsharif, U., Alvis-Guzman, N., Amare, A.T., Melaku, Y.A., Ciobanu, L.G., Amberbir, A., Amini, H., Karema, C.K., Ammar, W., Harb, H.L., Amrock, S.M., Andersen, H.H., Antonio, C.A.T., Aregay, A.F., Betsu, B.D., Hailu, G.B., Yebyo, H.G., Ärnlöv, J., Larsson, A., Artaman, A., Asayesh, H., Assadi, R., Atique, S., Avokpaho, E.F.G.A., Avokpaho, E.F.G.A., Awasthi, A., Ayala Quintanilla, B.P., Bacha, U., Balakrishnan, K., Barac, A., Barker-Collo, S.L., Mohammed, S., Barregard, L., Petzold, M., Barrero, L.H., Basu, A., Bazargan-Hejazi, S., Beghi, E., Sheth, K.N., Bell, M.L., Huang, J.J., Santos, I.S., Bensenor, I.M., Lotufo, P.A., Berhane, A., Wolfe, C.D., Bernabé, E., Hay, R.J., Roba, H.S., Beyene, A.S., Bhala, N., Fürst, T., Piel, F.B., Steiner, T.J., Bhatt, S., Greaves, F., Majeed, A., Soljak, M., Biadgilign, S., Bikbov, B., Bjertness, E., Htet, A.S., Boufous, S., Degenhardt, L., Resnikoff, S., Calabria, B., Mitchell, P.B., Brainin, M., Brazinova, A., Majdan, M., Lo, W.D., Shen, J., Breitborde, N.J.K., Buckle, G.C., Butt, Z.A., Lal, A., Carabin, H., Cárdenas, R., Carpenter, D.O., Castañeda-Orjuela, C.A., Castillo Rivas, J., Catalá-López, F., Catalá-López, F., Chang, J., Chiang, P.P., Chibueze, C.E., Chisumpa, V.H., Choi, J.J., Chowdhury, R., Christensen, H., Christopher, D.J., Cirillo, M., Cooper, C., Cortinovis Biotech, M.D., Giussani Biol, G., Perico, D.N., Remuzzi, G., Crump, J.A., Derrett, S., Poulton, R.G., Damtew, S.A., Deribe, K., Hailu, A.D., Giref, A.Z., Haile, D., Jibat, T., Taye, B., Dargan, P.I., das Neves, J., Massano, J., Santos, J. V., Davey, G., Davis, A.C., Newton, J.N., Steel, N., De Leo, D., Del Gobbo, L.C., Dellavalle, R.P., Des Jarlais, D.C., Dharmaratne, S.D., Dhillon, P.K., Ganguly, P., Zodpey, S., Diaz-Torné, C., Dubey, M., Rahman, M.H.U., Ram, U., Singh, A., Verma, R.K., Yadav, A.K., Duncan, B.B., Kieling, C., Schmidt, M.I., Ebrahimi, H., Pishgar, F., Farzadfar, F., Kasaeian, A., Parsaeian, M., Heydarpour, P., Malekzadeh, R., Roshandel, G., Sepanlou, S.G., Rahimi-Movaghar, V., Elyazar, I., Endres, M., Endries, A.Y., Ermakov, S.P., Eshrati, B., Farid, T.A., Khan, A.R., Farinha, C.S.E.S., Faro, A., Feigin, V.L., Te Ao, B.J., Kwan, G.F., Felson, D.T., Fernandes, J.G., Fernandes, J.C., Fischer, F., Shiue, I., Fowkes, F.G.R., Franklin, R.C., Fürst, T., Iyer, V.J., Gankpé, F.G., Gebre, T., Geleijnse, J.M., Gessner, B.D., Ginawi, I.A., Giroud, M., Gishu, M.D., Tura, A.K., Glaser, E., Halasa, Y.A., Shepard, D.S., Undurraga, E.A., Gona, P., Goodridge, A., Gopalani, S. V., Gotay, C.C., Kissoon, N., Kopec, J.A., Pourmalek, F., Goto, A., Inoue, M., Grainger, R., Gupta, R., Gupta, R., Gupta, V., Gutiérrez, R.A., Knudsen, A.K., Norheim, O.F., Hamadeh, R.R., Hamidi, S., Hammami, M., Handal, A.J., Hankey, G.J., Hao, Y., Harikrishnan, S., Haro, J.M., Hoek, H.W., Skirbekk, V., Horino, M., Horita, N., Hosgood, H.D., Hoy, D.G., Huang, H., Iburg, K.M., Innos, K., Kawakami, N., Shibuya, K., Jacobsen, K.H., Jakovljevic, M.B., Javanbakht, M., Jayaraman, S.P., Jayatilleke, A.U., Jee, S.H., Prabhakaran, D., Jiang, Y., Jimenez-Corona, A., Jimenez-Corona, A., Jonas, J.B., Kabir, Z., Kalkonde, Y., Kamal, R., Kesavachandran, C.N., Kan, H., Karch, A., Karimkhani, C., Kaul, A., Keiyoro, P.N., Lyons, R.A., Keren, A., Khader, Y.S., Khan, E.A., Khang, Y.H., Won, S., Khera, S., Tavakkoli, M., Khoja, T.A.M., Khubchandani, J., Kim, C., Kim, D.,

Kim, Y.J., Skogen, J.C., Savic, M., Kokubo, Y., Kolte, D., McGarvey, S.T., Kosen, S., Koul, P.A., Koyanagi, A., Kravchenko, M., Varakin, Y.Y., Kuate Defo, B., Kucuk Bicer, B., Kudom, A.A., Polinder, S., Kuipers, E.J., Lallukka, T., Shiri, R., Meretoja, T.J., Lam, H., Lam, J.O., Nachega, J.B., Tran, B.X., Langan, S.M., McKee, M., Lavados, P.M., Leasher, J.L., Leung, R., Levi, M., Li, Y., Liang, J., Liu, Y., Phillips, M.R., Lloyd, B.K., Logroscino, G., Looker, K.J., Lunevicius, R., Mackay, M.T., Magdy Abd El Razek, M., Mahdavi, M., Marcenes, W., Meaney, P.A., Margolis, D.J., Martinez-Raga, J., McMahon, B.J., Mehari, A., Tedla, B.A., Memiah, P., Memish, Z.A., Mendoza, W., Mhimbira, F.A., Miller, T.R., Mills, E.J., Mohammadi, A., Monasta, L., Montico, M., Ronfani, L., Morawska, L., Norman, R.E., Werdecker, A., Mueller, U.O., Westerman, R., Paternina Caicedo, A.J., Murdoch, M.E., Seedat, S., Wiysonge, C.S., Nagel, G., Rothenbacher, D., Naheed, A., Naldi, L., Nangia, V., Ngalesoni, F.N., Nguyen, Q.L., Nkamedjie Pete, P.M., Nolla, J.M., Nunes, B.P., Ogbo, F.A., Oh, I., Ohkubo, T., Olivares, P.R., Olusanya, B.O., Olusanya, J.O., Ortiz, A., Ota, E., Park, E., Passos, V.M.D.A., Patten, S.B., Tonelli, M., Pereira, D.M., Perez-Padilla, R., Pesudovs, K., Pillay, J.D., Plass, D., Platts-Mills, J.A., Pond, C.D., Prasad, N.M., Qorbani, M., Radfar, A., Rafay, A., Rahman, M., Rahman, S.U., Rai, R.K., Rajsic, S., Refaat, A.H., Ribeiro, A.L., Rojas-Rueda, D., Roy, A., Sagar, R., Satpathy, M., Tandon, N., Sahathevan, R., Sanabria, J.R., Sanchez-Niño, M.D., Sarmiento-Suarez, R., Sartorius, B., Sawhney, M., Schaub, M.P., Schneider, I.J.C., Silva, D.A.S., Schöttker, B., Schwebel, D.C., Singh, J.A., Shaheen, A., Shaikh, M.A., Sharma, R., Sharma, U., Shin, M., Yoon, S., Sigfusdottir, I.D., Silveira, D.G.A., Singh, O.P., Singh, P.K., Søreide, K., Sliwa, K., Stein, D.J., Soriano, J.B., Sposato, L.A., Sreeramareddy, C.T., Stathopoulou, V., Stovner, L.J., Steinke, S., Stroumpoulis, K., Sunguya, B.F., Swaminathan, S., Sykes, B.L., Tabarés-Seisdedos, R., Takala, J.S., Tanne, D., Terkawi, A.S., Tuzcu, E.M., Thomson, A.J., Thurston, G.D., Tobe-Gai, R., Topor-Madry, R., Topouzis, F., Truelsen, T., Tsala Dimbuene, Z., Tsilimbaris, M., Tyrovolas, S., Ukwaja, K.N., Uneke, C.J., Uthman, O.A., van Gool, C.H., Vasankari, T., Venketasubramanian, N., Violante, F.S., Vladimirov, S.K., Vlassov, V. V., Waller, S.G., Weichenthal, S., White, R.A., Williams, H.C., Wubshet, M., Xavier, D., Xu, G., Yan, L.L., Yano, Y., Yip, P., Yonemoto, N., Younis, M.Z., Yu, C., Zaidi, Z., Zaki, M.E., Zeeb, H., Zuhlke, L.J., 2016. Global, regional, and national incidence, prevalence, and years lived with disability for 310 diseases and injuries, 1990–2015: a systematic analysis for the Global Burden of Disease Study 2015. Lancet 388, 1545–1602. https://doi.org/10.1016/S0140-6736(16)31678-6

Wang, X., Yue, T., Lee, T. ching, 2015. Development of Pleurocidin-poly(vinyl alcohol) electrospun antimicrobial nanofibers to retain antimicrobial activity in food system application. Food Control 54, 150–157. https://doi.org/10.1016/j.foodcont.2015.02.001

Wang, X., Zhao, H., Turng, L.S., Li, Q., 2013. Crystalline morphology of electrospun poly(ε-caprolactone) (PCL) nanofibers. Ind. Eng. Chem. Res. 52, 4939–4949. https://doi.org/10.1021/IE302185E/SUPPL_FILE/IE302185E_SI_001.PDF

Weller, R.B., Hunter, H.J., W. Mann, M., 2015. Clinical Dermatology.

White, R., Cooper, R., 2005. Silver sulphadiazine: a review of the evidence. Wounds UK 1, 51–61.

Wiegand, I., Hilpert, K., Hancock, R.E.W., 2008. Agar and broth dilution methods to determine the minimal inhibitory concentration (MIC) of antimicrobial substances. Nat. Protoc. 3, 163–175. https://doi.org/10.1038/nprot.2007.521

Williamson, D.A., Carter, G.P., Howden, B.P., 2017. Current and Emerging Topical Antibacterials and Antiseptics: Agents, Action, and Resistance Patterns. Clin. Microbiol. Rev. 30, 827–860.

Wolcott, R.D., Rumbaugh, K.P., James, G., Schultz, G., Phillips, P., Yang, Q., Waiters, C., Stewart, P.S., Dowd, S.E., 2010. Biofilm maturity studies indicate sharp debridement opens a timedependent therapeutic window. J. Wound Care 19, 320–328. https://doi.org/10.12968/jowc.2010.19.8.77709

Wolf, K., te Lindert, M., Krause, M., Alexander, S., te Riet, J., Willis, A.L., Hoffman, R.M., Figdor, C.G., Weiss, S.J., Friedl, P., 2013. Physical limits of cell migration: Control by ECM space and nuclear deformation and tuning by proteolysis and traction force. J. Cell Biol. 201, 1069–1084. https://doi.org/10.1083/JCB.201210152/VIDEO-4

Woodruff, M.A., Hutmacher, D.W., 2010. The return of a forgotten polymer - Polycaprolactone in the 21st century. Prog. Polym. Sci. 35, 1217–1256. https://doi.org/10.1016/j.progpolymsci.2010.04.002

World Health Organization, 2017. WHO publishes list of bacteria for which new antibiotics are urgently needed [WWW Document]. URL https://www.who.int/news/item/27-02-2017-who-publishes-list-of-bacteria-for-which-new-antibiotics-are-urgently-needed (accessed 8.25.23).

Wu, T., Xue, J., Xia, Y., 2020. Engraving the Surface of Electrospun Microfibers with Nanoscale Promotes the Outgrowth of Neurites and the Migration of Schwann Cells. Angew. Chemie Int. 59, 15626–15632. https://doi.org/10.1002/anie.202002593

Xia, Y., Tang, X., Wu, X., Li, Y., Xu, C., Chen, S., Wu, P., 2023. Electrospun chitosan-based nanofibers loading tea tree oil for fresh salmon fillet shelf-life extension. J. Food Sci. 88, 3075–3089. https://doi.org/10.1111/1750-3841.16666

Xie, Z., Buschle-Diller, G., 2010. Electrospun poly(D,L-lactide) fibers for drug delivery: The influence of cosolvent and the mechanism of drug release. J. Appl. Polym. Sci. 115, 1–8. https://doi.org/10.1002/APP.31026

Yan, B., Zhang, Y., Li, Z., Zhou, P., Mao, Y., 2022. Electrospun nanofibrous membrane for biomedical application. SN Appl. Sci. 4, 172. https://doi.org/10.1007/s42452-022-05056-2

Yang, T.B., Sun, X.L., Ren, Z.J., Li, H.H., Yan, S.K., 2014. Crystallizability of poly(ε-caprolactone) blends with poly(vinylphenol) under different conditions. Chinese J. Polym. Sci. 32, 1119–1127. https://doi.org/10.1007/S10118-014-1492-Z

Yang, Y., Chen, W., Wang, M., Shen, J., Tang, Z., Qin, Y., Yu, D.G., 2023. Engineered Shellac Beads-on-the-String Fibers Using Triaxial Electrospinning for Improved Colon-Targeted Drug Delivery. Polymers (Basel). 15, 2237. https://doi.org/10.3390/polym15102237

Yarin, A.L., 2011. Coaxial electrospinning and emulsion electrospinning of core-shell fibers. Polym. Adv. Technol. 22, 310–317. https://doi.org/10.1002/pat.1781

Yaru, W., Lan, X., Jianhua, S., Chenxu, F., 2018. Preparation, Characterization and Drug Release of Salicylic Acid Loaded Porous Electrospun Nanofibers. Recent Pat. Nanotechnol. 12, 208–217. https://doi.org/10.2174/1872210512666181029154908

Yohe, S.T., Colson, Y.L., Grinstaff, M.W., 2012. Superhydrophobic materials for tunable drug release: Using displacement of air to control delivery rates. J. Am. Chem. Soc. 134, 2016–2019. https://doi.org/10.1021/JA211148A/SUPPL_FILE/JA211148A_SI_001.PDF

Yoshino, Y., Hashimoto, A., Ikegami, R., Irisawa, R., Kanoh, H., Sakurai, E., Nakanishi, T., Maekawa, T., Tachibana, T., Amano, M., Hayashi, M., Ishii, T., Iwata, Y., Kawakami, T., Sarayama, Y., Hasegawa, M., Matsuo, K., Ihn, H., Omoto, Y.,

Madokoro, N., Isei, T., Otsuka, M., Kukino, R., Shintani, Y., Hirosaki, K., Motegi, S., Kawaguchi, M., Asai, J., Isogai, Z., Kato, H., Kono, T., Tanioka, M., Fujita, H., Yatsushiro, H., Sakai, K., Asano, Y., Ito, T., Kadono, T., Koga, M., Tanizaki, H., Fujimoto, M., Yamasaki, O., Doi, N., Abe, M., Inoue, Y., Kaneko, S., Kodera, M., Tsujita, J., Fujiwara, H., Le Pavoux, A., 2020. Wound, pressure ulcer and burn guidelines – 6: Guidelines for the management of burns, second edition. J. Dermatol. 47, 1207–1235. https://doi.org/10.1111/1346-8138.15335

Yu, D.G., Zhu, L.M., Bligh, S.W.A., Branford-White, C., White, K.N., 2011. Coaxial electrospinning with organic solvent for controlling the size of self-assembled nanoparticles. Chem. Commun. 47, 1216–1218. https://doi.org/10.1039/c0cc03521a

Yuan, Y., Choi, K., Choi, S.O., Kim, J., 2018. Early stage release control of an anticancer drug by drug-polymer miscibility in a hydrophobic fiber-based drug delivery system. RSC Adv. 8, 19791–19803. https://doi.org/10.1039/C8RA01467A

Yunis, A.A., 1988. Chloramphenicol: Relation of structure to activity and toxicity. Annu. Rev. Pharmacol. Toxicol. 28, 83–100. https://doi.org/10.1146/annurev.pa.28.040188.000503

Zamora, J.L., 1986. Chemical and microbiologic characteristics and toxicity of povidone-iodine solutions. Am. J. Surg. 151, 400–406. https://doi.org/10.1016/0002-9610(86)90477-0

Zhang, H.J., Sellaiyan, S., Kakizaki, T., Uedono, A., Taniguchi, Y., Hayashi, K., 2017. Effect of Free-Volume Holes on Dynamic Mechanical Properties of Epoxy Resins for Carbon-Fiber-Reinforced Polymers. Macromolecules 50, 3933–3942. https://doi.org/10.1021/ACS.MACROMOL.7B00472/ASSET/IMAGES/MEDIUM/MA-2017-00472P_0013.GIF

Zupančič, Š., Preem, L., Kristl, J., Putrinš, M., Tenson, T., Kocbek, P., Kogermann, K., 2018. Impact of PCL nanofiber mat structural properties on hydrophilic drug release and antibacterial activity on periodontal pathogens. Eur. J. Pharm. Sci. 122, 347–358. https://doi.org/10.1016/J.EJPS.2018.07.024

9. SUMMARY IN ESTONIAN

Antimikroobsete elektrospinnitud maatriksite valmistamine ja hindamine haavaravis rakendamiseks

Sissejuhatus

Ägedate ja krooniliste haavade esinemissagedus on kõrge ja kasvab igal aastal (Martinengo et al., 2019). Elu mitte-paranevate haavadega on oluline koorem nii patsientidele kui ka tervele tervishoiusüsteemile, mis vajavad palju rahalisi vahendeid nende ravikulude katmiseks (Lindholm and Searle, 2016).

Halvasti paranevad haavad on tänapäeval suur probleem. Haava põhjalik puhastamine on haavaravi oluline nurgakivi, see hõlmab haavapõhja korralikku puhastamist ja selle ettevalmistamist paiksete ravimite manustamiseks (Anghel et al., 2016). Traditsiooniline haavaravi on aga tihtipeale ebatõhus. Näiteks paiksed haavaravimid ja neis kasutatavad ravimvormid (kreemid, geelid, lahused jne) omavad lühikest toimeaaega haavas ning haavaeksudaadi olemasolu võib veelgi nende toimet vähendada. Süsteemsed antibiootikumpreparaadid on endiselt kasutusel, aga nende puhul esineb probleeme toksilisusega, mis omakorda piirab nende kasutamist (Eriksson et al., 2022). Lisaks sellele on haavaravi väljakutseks ka antimikroobse resistentsuse (AMR) teke. Tõenäoliselt on haavaravi üks peamine alustugi nakkuse kontroll, kuna naha kaitsva barjääri lõhkumise järgselt vajab organism nakkuste vastu täiendavat kaitset. Viimastel aastatel on antimikroobsete ravimite kättesaadavus vähenenud, kuna AMR kasvab eksponentsiaalselt. Käesolevas doktoritöös otsiti lahendusi nii paiksete ravimvormide, kui ka raviaine antimikroobse resistentsuse probleemide jaoks.

Antibiootikum klooramfenikool (CAM) ja erinevad antimikroobsed peptiidid (AMP-d) valiti uurimiseks nende erineva toimespektri ja -mehhanismi tõttu kasutamiseks erinevate haavapatogeenide vastu. Lisaks uuriti ka AMP-de kombinatsioone laialdaselt haavaravis kasutatavate biotsiididega. Pleurotsidiin valiti suhteliselt uudse AMP-na, mis oma laia toimespektri ja erinevate toimemehhanismide tõttu omab suurt potentsiaali haavanakkuse ravis kasutamiseks. Antud juhul on pleurotsidiin hea alternatiiv antibiootikumidele multiresistentsete bakterite vastu võitlemiseks ning aitab pidurdada AMR-i arengut.

Käesolevas doktoritöös paigutati CAM ja pleurotsidiin uudsesse paiksesse elektrospinnitud ravimkandursüsteemi (elektrospinnitud haavakattesse), et parandada ravi efektiivsust ja vähendada süsteemset toksilisust. Need uudsed haavakatted on valmistatud elektrospinnimise tehnoloogial, mis võimaldab saada nanotehnoloogilisi maatrikseid, kus nanoskaalas kiud kogutakse kokku mittekootud maatriksisse. See valmistamismeetod võimaldab lisada haavakatete koostisesse raviaineid, parandades nende stabiilsust ja kontrollides nende vabanemist (Yarin, 2011). Lisaks elektrospinnitud maatriksite headele füsikokeemilistele omadustele, nagu nende suur pindala ja mahu suhe, suur poorus ja soovitud mehaanilised omadused, aitavad ja toetavad nad niiskuse tasakaalu, ja

parandavad gaasivahetust haavas soodustades selle paranemist (Leaper et al., 2014; Muthukrishnan, 2022).

Neid arendatud antimikroobseid maatrikseid on põhjalikult iseloomustatud *in vitro* eksperimentide abil testides nende antibakteriaalset efektiivsust erinevate oluliste haavapatogeenide vastu. Käesolev doktoritöö on toonud esile mõningaid piiranguid, kuid see on avanud ka uue strateegia, mida edasi uurida, lootes jõuda lõppeesmärgini: nende haavakatete lisamine uue terapeutilise võimalusena haavaravisse.

Uurimise eesmärgid

Käesoleva doktoritöö üldiseks eesmärgiks oli arendada ja iseloomustada uudseid antimikroobseid raviaineid sisaldavaid elektrospinnitud maatrikseid haavaravis kasutamise eesmärgil. Lisaks uuriti potentsiaalset sünergiat antimikroobse peptiidi (AMP) ja biotsiidide vahel lahuses oluliste haavapatogeenide vastu. Nende eesmärkide saavutamiseks jagati töö konkreetseteks eesmärkideks, mis olid:

1. Valmistada poorseid kiude. Erinevate polümeeride, lahustisüsteemide ja elektrospinnimise parameetrite testimine ja protsessi optimeerimine poorsete kiudude saamiseks (I, II).
2. Arendada antibiootikum CAM-ni sisaldavaid maatrikseid (I, II) ja pleurotsidiini sisaldavaid maatrikseid (III). CAM ja pleurotsidiin valiti antimikroobsete molekulidena, mis on kasulikud haavanakkuse ravi jaoks. Elektrospinnimise parameetrite testimine ja kontrollimine protsessi optimeerimiseks.
3. Iseloomustada elektrospinnitud maatrikseid: morfoloogia ja raviaine sisalduse analüüsi (I, II, III) abil.
4. Iseloomustada elektrospinnitud maatrikseid tahke faasi analüüsi (I), mehaaniliste omaduste katsete (II), märgumise (I) ja raviaine vabanemiskatsete (I, III) abil.
5. Hinnata CAM-i sisaldavate maatriksite ohutust ja biosobivust (II).
6. Hinnata raviainet sisaldavate maatriksite antimikroobset toimet (II, III).
7. Mõista pleurotsidiini ja erinevate biotsiidide toimet erinevatele antibiootikumresistentsetele haavapatogeenidele (III) ja uurida nende vahel tekkivate fenotüübiliste mõjude (sünergism, antagonism või koosmõju puudumine) teket (III) potentsiaalse kombinatsioonravi jaoks haavade paranemiseks.

Materjalid ja meetodid

Maatriksid valmistati elektrospinnimise tehnoloogia abil. Kandjapolümeeridena kasutati polükaprolaktooni (PCL) ja polüvinüülalkoholi (PVA). Antimikroobsete ainetena kasutati klooramfenikooli (CAM) ja pleurotsidiini, mida lisati elektrospinnitud maatriksidesse. Kiuliste maatriksite morfoloogiat analüüsiti skaneeriva elektronmikroskoobi (SEM) abil. Poorsust uuriti gaasadsorptsioonimeetodil (BET) ja SEM-i abil. Mehhaanilist käitumist uuriti tekstuurianalüsaatori abil.

Maatriksite hüdrofiilsust /hüdrofoobsust ja nende märgumisomadusi iseloomustati kontaktnurga, paisumisnäitaja ja massikao hindamise teel. Tahke faasi omadusi hinnati röntgendifraktsiooni (XRD), summutatud täispeegeldusega Fourier'i transformeeritud infrapuna spektroskoopiat (ATR-FTIR) ja diferentsiaalset skaneerivat kalorimeetrit (DSC) kasutades. Raviaine sisaldust maatriksites ja raviaine vabanemist uuriti kõrgefektiivse vedelikkromatograafia (HPLC) abil. Beebi hamstri neeru (BHK-21) fibroblastid valiti elektrospinnitud maatriksite biosobivuse uurimiseks, kasutades MTS katset ja konfokaalset mikroskoopiat (CFM). Elektrospinnitud maatriksite potentsiaalset antimikroobset aktiivsust uuriti järgmisi olulisi multiresistentseid baktereid kasutades: *Acinetobacter baumannii* AYE, *A. baumannii* ATCC 17978, *Pseudomonas aeruginosa* PAO1, *P. aeruginosa* NCTC 13437, *P. aeruginosa* DSM 1117, *Staphylococcus aureus* EMRSA-15, *Klebsiella pneumoniae* M6, *K. pneumoniae* NCTC 13368 ja *Escherichia coli* NCTC 12923 ning *E. coli* DSM 1103. Testiti erinevaid antibakteriaalsete ja antibiofilm-omaduste uurimise meetodeid nagu agardifusiooni meetod ja antibiofilm test. Lisaks uuriti järgmisi biotsiide: kloorheksidiin diglukonaat, bensalkooniumkloriid, hõbenitraat, hõbesulfadiasiin, oktenidiindikloriid ja povidoon-jood (PVP-jood) üksi ja koos pleurotsidiiniga mainitud haavapatogeenide vastu.

Tulemused ja arutelu

Antimikroobseid raviaineid sisaldavaid elektrospinnitud maatrikseid oli võimalik edukalt valmistada monoaksiaalse ja koaksiaalse elektrospinnimise meetodi abil. Poorsete mikrokiudude moodustumine õnnestus ainult siis, kui polümeerina kasutati polükaprolaktooni (PCL), lahustisüsteemina kloroform-DMSO-d (CF:DMSO) või tetrahüdrofuraan-DMSO-d (THF:DMSO) ning elektrospinnimine viidi läbi kõrge suhtelise õhuniiskuse (RH; 65%) juures. Viimane oli neist kriitilise tähtsusega parameeter poorsuse saavutamisel.

Kasutatud polümeeri kontsentratsioon mõjutas kiudude läbimõõtu, suuremaid kiude oli võimalik tekitada suurima PCL kontsentratsiooni korral (PCL 15%). See tulemus on kooskõlas varasemalt kirjanduses tooduga (Luraghi et al., 2021). Lisaks mõjutas valitud lahustisüsteem oluliselt kiudude läbimõõtu. Mikrokiud saadi, kui kasutati THF:DMSO-d, CF:DMSO-d ja atsetoon-diklorometaani (ACE:DCM), ning nanokiud, kui kasutati lahusti süsteemina äädikhape-sipelghapet (AA:FA).

Kuigi raviaine lisamine maatriksisse muutis kiudude läbimõõtu, puudub usaldusväärne ja ühtne korrelatsioon kiu läbimõõdu ja raviaine kius juuresoleku vahel. CAM-ga laetud PCL-maatriksite kiu läbimõõt oli suurem kui ilma raviaineta PCL-kiu läbimõõt, samal ajal kui pleurotsidiini lisamine PVA-maatriksitesse viis väiksema kiu läbimõõdu tekkimiseni (0,60 ± 0,17 µm ilma raviaineta PVA kiudude puhul võrreldes 0,54 ± 0,09 µm pleurotsidiiniga laetud kiudude puhul). Lisaks vähendas CAM-i lisamine kiu pinnal esinevate pooride suurust.

Suuremate pooride moodustumist on täheldatud maatriksi pinnal sel juhul, kui üksikud kiud olid suurema läbimõõduga (Pham et al., 2006). Käesolevas töös

tekkisid elektrospinnimise käigus mikrokiudmaatriksid (PCL THF:DMSO), kus pooride läbimõõdud olid vahemikus 13,24 ± 4,78 µm kuni 21,87 ± 7,30 µm, samas kui nanopoorsete maatriksite (PCL AA:FA) poorid olid vahemikus 2,88 ± 1,22 µm kuni 3,65 ± 1,55 µm. Hoolimata suuremate pooride esinemisest mikrokiudmaatriksites, näitasid nanokiudmaatriksid suurimat eripinda, mida mõõdeti BET analüüsi ja N_2 adsorptsioonisotermide abil. Seda on ka varasemates töödes näidatud nano- ja mikrokiudmaatriksite võrdlemisel (Huang et al., 2003).

PCL elektrospinnitud maatriksite mehaanilisi omadusi mõjutasid kiudude poorus, kiudude läbimõõt ja kasutatud lahustisüsteem. Mittepoorsed mikrokiud olid kõige vastupidavamad ja neil oli kõige suurem tõmbetugevus ja Youngi moodul. See võib olla seletatav asjaoluga, et pooride esinemine vähendab kiudude tõmbetugevust (D'Amato et al., 2018). Teiselt poolt suurendas pooride olemasolu kiudude elastsust, seega purunemist oli võimalik esile kutsuda ainult suuremate jõudude rakendamisega. Leidis kinnitust, et suurem katkevenivus saavutati suurema läbimõõduga kiudude jaoks (Tan et al., 2005). Vähemelastne käitumine saadi PCL AA:FA maatriksitega võrreldes PCL THF:DMSO maatriksitega, kinnitades veelgi kasutatud lahustisüsteemide mõju maatriksite mehaanilistele omadustele. AA kasutamisel elektrospinnimise lahustina on varem kirjeldatud haprate nanokiudude tekkimist (Kanani and Bahrami, 2011). Mingeid olulisi muutusi maatriksite mehaanilistes omadustes ei täheldatud, kui need olid biorelevantses puhvris 3 minutit või 24 tundi. Viimane test on eriti oluline imiteerimaks reaalses haavas etappi, kui maatriksid on kontaktis haavaeksudaadiga. Valmistatud PCL maatriksite mehaanilised omadused simuleerisid edukalt naha enda omadusi (Chen et al., 2017; Pailler-Mattei et al., 2008; Shevchenko et al., 2010).

Hüdrofiilse CAM-i olemasolu kiu koostises põhjustas paisumisnäitaja ja massikao suurenemise ning kontaktnurga vähenemise kõigis maatriksites. CAM-i olemasolu kiududes põhjustas maatriksite hüdrofiilsemat käitumist, kuna raviaine molekul lahustub ja võimaldab puhvri tungimist kiududesse.

Tahke faasi analüüs kinnitas, et kui raviaine molekul oli kiududesse lisatud, muutus CAM kristalsest amorfseks vormiks. ATR-FTIR spekter näitas jooni, mis kinnitasid CAM amorfset vormi, lisaks puudus tipp 1560 cm^{-1} juures, mis on iseloomulik ainult CAM-i kristalsele vormile (Preem et al., 2017). XRD abil ei tuvastatud difraktogrammil kristalsele vormile omistatavaid teravaid peegeldusi. DSC analüüsid kinnitasid CAM-i olemasolu amorfses olekus, kuna termogrammil ei täheldatud kristallvormi sulamist. Vastupidi, PCL säilitas oma poolkristalsuse ja täheldati lahustisüsteemi mõju PCL kristalliinsusele. THF:DMSO-ga valmistatud PCL maatriksid näitasid suuremat kristalliinsust võrreldes AA:FA-ga valmistatud PCL maatriksitega.

Efektiivne raviaine kiududesse sisseviimine saavutati mõlemate arendatud elektrospinnitud maatriksite puhul – CAM viidi PCL kiududesse ja pleurotsidiin PVA kiududesse. Tulemused näitasid, et üle 80% CAM-ist oli võimalik edukalt inkorporeerida PCL kiududesse. Samuti kogu pleurotsidiin viidi sisse PVA kiulistesse maatriksitesse, mis kinnitab suurepärast peptiidi stabiilsust elektrospinnimisprotsessi ajal ja koaksiaalse elektrospinnimise kaitsvat toimet. Täiendavad

6-kuulised stabiilsusuuringud elektrospinnitud maatriksitega kinnitasid, et ka säilitamise ajal püsis peptiid suhteliselt stabiilsena.

Kõik elektrospinnitud PCL maatriksid näitasid algul kiiret CAM-i vabanemist, millele järgnes aeglasem vabanemine sõltumata nende kiudude morfoloogiast. Olulised erinevused olid täheldatavad just vabanenud raviaine kogustes ning vastavalt disaini erinevustele puudus raviaine vabanemine peaaegu üldse ilma pooridetta kiudude puhul. Mittepoorsed mikrokiud vabastasid ainult 20% sisse viidud CAM-ist. Raviaine vabanemist mõjutas oluliselt ka elektrospinnitud maatriksite hüdrofiilsus. Sel juhul vabanes tõenäoliselt ainult maatriksi pinnale paigutatud raviaine ja ülejäänud CAM jäi maatriksi sisse kinni. Nanokiudude maatriksite suur eripind ja kasutatud lahustisüsteem (AA:FA) parandas nendest maatriksitest raviaine vabanemist, näidates kõige suuremat vabanenud CAM-i hulka (lõplik vabanemine 72,6 ± 7,7%), ületades mikrokiudude maatriksite poorsuse mõju (lõplik vabanemine 59,2 ± 3,2%). Siin näitasid poorsed mikrokiud märkimisväärselt kiiremat vabanemist võrreldes mittepoorsete mikrokiududega. Seda võib seletada asjaoluga, et poorsete kiudude olemasolu suurendab vabanemiskeskkonna tungimist nendesse PCL-hüdrofoobsetesse maatriksitesse, mille ravimi vabanemist on kirjeldatud difusiooniprotsessina (McInnes et al., 2018; Preem et al., 2017).

Kasutatud lahustisüsteem võis mõjutada ka nende maatriksite raviaine vabanemiskäitumist, kuna lahustid võivad oluliselt muuta polümeeri omadusi ja elektrospinnimise protsessi (erinevate aurustumiskiiruste kaudu) (D'Amato et al., 2017). Keemiline interaktsioon PCL-i ja AA:FA lahustisüsteemi vahel võib tekkida sellises happelises ja hüdrofiilsemas keskkonnas (võrreldes THF:DMSO-ga), põhjustades PCL pinnaomaduste muutumise ja viies CAM-i kiudude pinnale ning tekitades nõrgemaid sidemeid raviaine ja polümeeri vahele, mis võimaldab kiiremat raviaine vabanemist (Pok et al., 2010; Širc et al., 2012). Difusioon on peamine raviaine vabanemise mehhanism poorsetest PCL mikrokiududest ja PCL nanokiududest. Mittepoorsete mikrokiudude raviaine vabanemise kineetikat ei õnnestunud sobitada ühegi testitud võrrandiga, mis viitab difusiooni puudumisele. Seda vabanemist võib seostada raviaine adsorptsiooniprotsessiga kiudude pinnale või nanopooridesse (mida ei tuvastatud) (Srikar et al., 2009). PVA maatriksite uurimisel ei olnud võimalik raviaine vabanemiskäitumisest selgeid järeldusi teha, kuna tulemused näitasid pleurotsidiini kontsentratsioonides suuri varieeruvusi. Seda võib selgitada katioonse AMP pleurotsidiini füsikokeemiliste omadustega, mis võivad interakteeruda anumatega või moodustada suuremaid agregaate (Clark et al., 2021; Wiegand et al., 2008). Järgmised uuringud on planeeritud, et töötada välja sobivamad analüüsimudelid ja testida AMP vabanemiskäitumist põhjalikumalt.

Elektrospinnitud maatriksite interaktsioone eukarüootsete rakkudega uuriti ohutusetestides. Fibroblastid kinnitusid maatriksitele ja paljunesid ühtlaselt kõigil PCL maatriksitel, kinnitades nende ohutust ja biosobivust. Poorsetel maatriksitel saavutati parem rakkude infiltreerumine, mida on ka varem kirjanduses näidatud (Farooque et al., 2014). Lisaks täheldati, et rakud kinnitusid ja tungisid

sügavamale just hüdrofiilsematesse poorsetesse kiududesse. Vastupidi, nanokiudmaatriksite puhul kinnitusid rakud peamiselt ainult pinnale.

Kõik testitud antimikroobsed raviained ja biotsiidid takistasid edukalt valitud haavapatogeenide kasvu. Ainult CAM ei suutnud tappa *P. aeruginosa* bakterit ning see patogeen näitas suurt resistentsust kõigi testitud raviaine molekulide suhtes.

Kõik CAM-iga laetud PCL-maatriksid olid efektiivsed planktoonilise *E. coli* kasvu inhibeerimisel ilma oluliste erinevusteta aktiivsuses maatrikside vahel. Siiski mõjutas elektrospinnitud maatriksite morfoloogia bakteriaalse biofilmi moodustumist erinevalt. Poorsetel mikrokiududel oli suurem antibiofilmi efekt kui mittepoorsetel mikrokiududel, mis on tugevalt seotud nende mainitud hüdrofiilsuse ja raviaine vabanemise käitumisega. Lisaks häirivad mikrokiudmaatriksid biofilmi teket suuremas ulatuses kui nanokiudmaatriksid. Seletuseks on see, et nanokiudmaatriksitest vabaneb raviaine kiiremini, mis viib selleni, et maatriksisse endasse jääb vähem raviainet.

Agardifusioonimeetodit ei olnud võimalik AMP-de antibakteriaalse aktiivsuse uurimisel kasutada kuna AMP difusioon agarisse oli takistatud nende molekulide katioonsete osade ja agaropektiini negatiivselt laetud sulfaadi- ja suhkrukomponentide vaheliste molekulaarsete interaktsioonide tõttu (Lehrer et al., 1991). PVA maatriksid kutsusid esile bakterite kasvu inhibeerimise, mis viitab sellele, et maatriksitest vabanenud funktsionaalne pleurotsidiini kontsentratsioon on üle minimaalse inhibeeriva kontsentratsiooni. Siiski mõjutas nende maatriksite kaal ja seega keskkonda vabanenud pleurotsidiini kogus oluliselt raviaine võimet takistada resistentsete bakterite, nagu *P. aeruginosa* NCTC 13437, kasvu, mida saab ainult 500 µg kaaluv maatriks pidurdada (sisaldab raviainet 3.5µg). Huvitaval kombel selgus, et pleurotsidiiniga laetud maatriksite abil saavutatud bakterite kasvu inhibeerimine ületas oluliselt seda, mida saavutati värskelt valmistatud pleurotsidiini lahusega. Seda mõju on varem näidanud ka Wang jt (Wang et al., 2015). Võimalikud seletused sellisele nähtusele on järgmised: (i) koaksiaalselt elektrospinnitud kiududes on peptiidil täiendav kaitse keskkonna tingimuste eest ja (ii) patogeenide ning maatriksite vahel tekib täiendav interaktsioon, mis mõjub soodsalt bakterite kasvu inhibeerimisele.

Pleurotsidiini kasutamisel biotsiididega tuvastati erinevaid koostoimeid. Pleurotsidiini saab ohutult kasutada koos hõbenitraadi, hõbesulfadiasiini, oktenidiini ja PVP-joodiga, kus leiti koosmõju puudumist või sünergilist käitumist kõigi testitud bakterite vastu. Siiski tuleb arvestada, et pleurotsidiini ja bensalkooniumkloriidi ning pleurotsidiini ja kloorheksidiini kombinatsioonide kasutamisel leiti antagonistlikku käitumist. Lisaks täheldati *P. aeruginosa* jaoks erinevaid fenotüüpilisi mõjusid, kuna sama raviainete kombinatsioon (pleurotsidiin ja bensalkooniumkloriid) andis vastupidiseid tulemusi (mõõdukas sünergia *P. aeruginosa* NCTC 13437 ja antagonism *P. aeruginosa* PAO1 vastu). Seda varieeruvust on selle bakteri puhul varem kirjeldatud, ka teiste raviainete kombinatsioone korral (Barnham and Kerby, 1980; Markowska et al., 2014; Pietsch et al., 2021). Laia valiku *P. aeruginosa* tüvede edasine analüüs on oluline nende interaktsioonide ja nende raviainete koosmanustamise piirangute mõistmiseks.

Kokkuvõte

Kasutades kandjapolümeere (PCL ja PVA) ja antibakteriaalseid raviaineid (klooramfenikool ja pleurotsidiin), oli võimalik valmistada erineva koostise ja struktuuriga nano- ja mikrokiulisi maatrikseid monoaksiaalse ja koaksiaalse elektrospinnimismeetodite abil. Kasutades kõrgemat õhuniiskuse taset ja valides sobiv lahustisüsteem (THF:DMSO), valmistati edukalt poorsete mikrokiududega maatrikseid. Saadud elektrospinnitud maatriksid imiteerivad naha mehaanilisi omadusi isegi niisketes tingimustes ja seetõttu saab neid kasutada haavasidemetena eksudaadi juuresolekul. Töö käigus leiti, et kiudude poorsus ja läbimõõt mõjutavad maatriksite mehaanilisi omadusi ning pooride olemasolu suurendas kiudude elastsust.

Klooramfenikooli (CAM) lisamine maatriksitele suurendas paisumisindeksit ja kaalukadu vesikeskkonnas. Lisaks leiti, et klooramfenikool oli kiududes amorfses vormis ja seda kõigis elektrospinnitud PCL-maatriksites. Tõhus raviaine inkorporeerimine saavutati kõigis välja töötatud elektrospinnitud maatriksites. Raviaine vabanemiskäitumist mõjutas suuresti elektrospinnitud maatriksite hüdrofiilsus. Uurides kiudude läbimõõdu mõju maatriksite käitumisele selgus, et suurenenud pindala ja mahu suhtarvuga nanokiududest oli CAM-i vabanemine kõige kiirem, järgnesid poorsed mikrokiud ja siis mittepoorsed mikrokiud, kust vabanes ainult 20% raviainest. Viimasel juhul ei täheldatud prolongeeritud vabanemist, tõenäoliselt vabanes raviaine ainult maatriksi kiudude pinnalt.

Elektrospinnitud CAM-iga laetud maatriksid on ohutud ja biosobivad. Poorsed mikrokiulised maatriksid võimaldasid suuremat rakkude infiltratsiooni. Samuti tuvastati, et rakud kinnitusid ja tungisid sügavamale poorsetesse hüdrofiilsematesse kiududesse. Vastupidiselt eelnevale, nanokiudmaatriksite puhul kinnitusid rakud peamiselt ainult pinnale.

Kõik testitud antimikroobsed raviained ja biotsiidid takistasid edukalt valitud haavapatogeenide kasvu. Ainult CAM ei suutnud tappa *P. aeruginosa* bakterit ning see patogeen näitas üles suurt resistentsust kõigi testitud raviaine molekulide suhtes. Poorsetel CAM sisaldavatel mikrokiududel oli suurem antibiofilmi toime kui mittepoorsetel CAM sisaldavatel mikrokiududel ja nanokiududel. Viimane vaatlus on tugevalt seotud nende kiudude hüdrofiilsuse ja võimega vabastada raviainet. Pleurotsidiini õnnestus edukalt inkorporeerida PVA maatriksitesse koaksiaalse elektrospinnimise ajal. Kuigi nende valimistatud maatriksite puhul raviaine vabanemist ei õnnestunud mõõta, tõestati nende AMP sisaldavate maatriksite tõhusus haavapatogeenide vastu. Need analüüsid näitasid, et antibakteriaalne tõhusus oli äärmiselt sõltuv maatriksite kaalust just resistentsete *P. aeruginosa* tüvede jaoks. Pleurotsidiini sisaldavate maatriksite toimed ületasid oluliselt seda toimet, mis saavutati värskelt valmistatud pleurotsidiini lahusega. Pleurotsidiini kooskasutamine traditsiooniliste biotsiididega võimaldab saavutada erinevaid koostoimeid. Pleurotsidiini kombinatsioonid hõbenitraadi, hõbesulfadiasiini, oktenidiini ja PVP-joodiga võimaldasid saavutada koostoime

puudumist või sünergilist toimet kõigi testitud bakterite vastu. Samas pleurotsidiini samaaegse kasutamise ajal bensalkooniumkloriidi või kloorheksidiiniga täheldati antagonistlikke koostoimeid.

Kokkuvõtvalt võib öelda, et elektrospinnitud haavakatete valmistamisel tuleb arvesse võtta mitmeid erinevaid ja olulisi parameetreid. Doktoritöö käigus kasutati nii mono- kui koaksiaalsete elektrospinnimise tehnoloogiat, mille käigus saadi täiendavaid teadmisi tegurite kohta, mis mõjutavad pooride teket fiibrite pinnal. Lisaks uuriti seoseid haavakatete morfoloogia, mehaaniliste omaduse ning raviaine vabanemise vahel. Doktoritöös kirjeldatud haavakatteid on plaan edasi uurida juba *ex vivo* ja *in vivo* mudelites, et selgitada välja nende toime biorelevantsetes tingimustes ning jõuda lõpliku eesmärgini, et kasutada neid tulevikus ka patsientide ravis.

ACKNOWLEDGEMENTS

This work was carried out at the Institue of Pharmacy (Faculty of Medicine, University of Tartu, Estonia), the Institue of Technology (Faculty of Technology and Science, University of Tartu, Estonia), the Institute of Pharmaceutical Science (School of Cancer and Pharmaceutical Sciences, King's College London, London, United Kingdom) and English National Infection Service (Public Health England, Salisbury, United Kingdom) during the years 2018-2022.

The research has been financially supported by grants from the Estonian Research Council (PUT1088, PRG726, and PRG1507). Additional funding has been provided through the European Regional Development Fund via the Centre of Excellence for Molecular Cell Technology. Gratitude is extended to the Estonian Ministry of Education and Research, the European Regional Development Fund (specifically through the Kristjan Jaak Scholarship, Dora Pluss Programme and University of Tartu ASTRA project PER ASPERA), NordicPOP (supported by NordFosk) and the European Commission (Erasmus +) for their contribution to research and mobility funding. L'ORÉAL Baltic "For Women In Science" fellowship 2018 (K. Kogermann) with the support of the Estonian National Comission for UNESCO and the Estonian Academy of Sciences and the L'ORÉAL-UNESCO international program "For Women In Science" is acknowledged.

These years pursuing my PhD have been among the most exciting yet exhausting of my life. I would not have been able to embark on and successfully complete this journey if it were not for the unconditional help of numerous kind people around me during this time.

I wish to thank everyone involved in this study at the University of Tartu, King's College London, and Public Health England. I am profoundly grateful to all my Estonian supervisors: Prof. Karin Kogermann, Dr. Marta Putrinš, Prof. Tanel Tenson and Associate Prof. Ivo Laidmäe, whose guidance and expertise were instrumental to the success of my research. Additionally, I extend my appreciation to Prof. James Mason, PhD Charlotte Hind and Prof. Mark Sutton, who supervised my work while I was in London and whose invaluable insights greatly contributed to the advancement of my work. Special recognition is due to Professor Karin Kogermann and Professor James Mason for their dedicated guidance throughout these years. I am very thankful to my reviewers Professor Angela Ivask and Professor Reet Mändar for generously dedicating their time and offering feedback to enhance the quality of my thesis.

My sincere gratitude to my friends and colleagues in Tartu and London for their invaluable help. I extend my appreciation to everyone I have worked with in Madrid, at Complutense University and at AEMPS, for their unconditional understanding and generous support.

I am deeply grateful to my parents and family for encouraging me to step out of my comfort zone, leave my hometown, and pursue my academic aspirations.

Their continuous support has been essential in guiding me towards achieving my goals.

I wish to thank all my friends, with whom I have shared worries and achievements throughout all these years. They have always patiently listened to me and comforted me, even from a distance. To Ana, Elena, Sara, Raquel, Elena, Amaru, Silvia, María, Pablo and Jor: gracias.

Ale, I want to express my most sincere gratitude for your unwavering love and patience. I genuinely believe that a significant portion of this thesis belongs to you. Having you by my side has meant everything to me, and I will forever cherish your presence in my life.

PUBLICATIONS

CURRICULUM VITAE

Name:	Celia Teresa Pozo Ramos
Date of birth:	October 14, 1994
Address:	Institute of Pharmacy, University of Tartu. Nooruse 1, 50411, Tartu, Estonia
Email:	celia.pozo@ut.ee

Education:

1998–2012	Cabrini School. Madrid, Spain.
2012–2018	Complutense University (Pharmacy Degree). EQF level 7. Madrid, Spain.
2018–…	University of Tartu, Faculty of Medicine, Institute of Pharmacy, PhD studies
2019–2022	Visiting PhD student at King's College London, Prof. James Mason laboratory, United Kingdom

Professional employment:

09.2017–11.2017	Hospital Pharmacist Trainee. La Paz University Hospital
11.2017–02.2018	Community Pharmacist Trainee. Mateo Vic Pharmacy
2022–2023	Research Pharmacist. Microbiology and Parasitology Department. Faculty of Pharmacy. Complutense University.
2023–…	Quality Assurance Specialist. Biological Products, Advanced Therapies and Biotechnology Division. Spanish Agency of Medicines and Medical Devices.

Research fields:
Development, characterization and analysis of nanotechnological drug delivery systems, antimicrobial activity studies (CERCS classification: B740 Pharmacological sciences, pharmacognosy, pharmacy, toxicology, T410 Pharmaceuticals and related technologies; T490 Biotechnology, B230 Microbiology, bacteriology). Study of metformin as an antifungal drug (B230 Microbiology, mycology).

Research projects:

2018–2019	PUT1088: Design and development of multicomponent antibacterial nanofibrous dressings for advanced wound care.
2020–2021	PRG726: Development of multifunctional antimicrobial peptides releasing drug delivery systems for the prevention and treatment of skin and wound infections.

2022–… PRG1507: Development of biorelevant assays for the analyses of multifunctional antimicrobial wound dressings for the treatment of wound infections.

List of publications on international peer-reviewed journals:

I. **Celia Ramos***, Georg-Marten* Lanno, Ivo Laidmäe, Andres Meos, Riinu Härmas and Karin Kogermann. 2020. High humidity electrospinning of porous fibers for tuning the release of drug delivery systems. *International Journal of Polymeric Materials and Polymeric Biomaterials*. 70, 880-892.
https://doi.org/10.1080/00914037.2020.1765361
*Equal contribution to this publication.

II. Georg-Marten Lanno, **Celia Ramos**, Liis Preem, Marta Putrinš, Ivo Laidmäe, Tanel Tenson and Karin Kogermann. 2020. Antibacterial Porous Electrospun Fiber as Skin Scaffolds for Wound Healing Applications. *ACS Omega* 5, 30011–30022.
https://doi.org/10.1021/acsomega.0c04402

III. **Celia Ramos**, Kairi Lorenz, Marta Putrinš, Charlotte K. Hind, Andres Meos, Ivo Laidmäe, Tanel Tenson, J. Mark Sutton, A. James Mason and Karin Kogermann. 2024. Fibrous matrices facilitate pleurocidin killing of wound associated bacterial pathogens. *European Journal of Pharmaceutical Sciences*. 192, 106648.
https://doi.org/10.1016/j.ejps.2023.106648.

In addition, 1 oral presentation and 3 poster presentations have been presented at international scientific conferences.

ELULOOKIRJELDUS

Nimi:	Celia Teresa Pozo Ramos
Sünniaeg:	Oktoober 14, 1994
Address:	Farmaatsia instituut, Tartu Ülikool. Nooruse 1, 50411, Tartu, Eesti
E-post:	celia.pozo@ut.ee

Haridus:

1998–2012	Cabrini keskkool. Madrid, Hispaania.
2012–2018	Complutense Ülikool (farmaatsia eriala). EQF tase 7. Madrid, Hispaania.
2018–…	Tartu Ülikool, Meditsiiniteaduste valdkond, farmaatsia instituut, doktorant farmaatsia erialal
2019–2022	Külalis-doktorant Prof. James Mason laboris, King´s College London, Ühendkuningriik

Erialane teenistuskäik:

09.2017–11.2017	Haiglaapteekri praktikant. La Pazi Ülikooli Haigla.
11.2017–02.2018	Kogukonna apteekri praktikant. Apteek Mateo Vic.
2022–2023	Teadur-proviisor. Mikrobioloogia ja parasitoloogia osakond. Farmaatsia teaduskond. Complutense Ülikool.
2023– …	Kvaliteedispetsialist. Bioloogilised tooted, täiustatud teraapiad ja biotehnoloogia osakond. Hispaania Ravimite ja Meditsiiniseadmete Agentuur.

Teadustöö suunad:

Nanotehnoloogiliste ravimkandursüsteemide arendamine, iseloomustamine ja analüüs, antimikroobse aktiivsuse uuringud (CERCS klassifikatsioon: B740 Farmakoloogilised teadused, farmakognoosia, farmaatsia, toksikoloogia, T410 Ravimid ja sellega seotud tehnoloogiad; T490 Biotehnoloogia, B230 Mikrobioloogia, bakterioloogia). Metformiini uurimine seenevastase ravimina (B230 Mikrobioloogia, mütsoloogia).

Teadusprojektid:

2018–2019	PUT1088: Haavaravis kasutatavate mitmeosaliste antibakteriaalsete nanofiiberkatete disain ja valmistamine
2020–2021	PRG726: Naha- ja haavainfektsioonide ennetuseks ja raviks kasutatavate antimikroobseid peptiide vabastavate ravimkandursüsteemide väljatöötamine
2022–…	PRG1507: Biorelevantsete mudelite arendamine haavainfektsioonide ravis kasutatavate multifunktsionaalsete antimikroobsete haavakatete uurimiseks

Publikatsioonid:

I. **Celia Ramos***, Georg-Marten* Lanno, Ivo Laidmäe, Andres Meos, Riinu Härmas and Karin Kogermann. 2020. High humidity electrospinning of porous fibers for tuning the release of drug delivery systems. *International Journal of Polymeric Materials and Polymeric Biomaterials*. 70, 880–892.
https://doi.org/10.1080/00914037.2020.1765361
*Equal contribution to this publication.

II. Georg-Marten Lanno, **Celia Ramos**, Liis Preem, Marta Putrinš, Ivo Laidmäe, Tanel Tenson and Karin Kogermann. 2020. Antibacterial Porous Electrospun Fiber as Skin Scaffolds for Wound Healing Applications. *ACS Omega* 5, 30011–30022.
https://doi.org/10.1021/acsomega.0c04402

III. **Celia Ramos**, Kairi Lorenz, Marta Putrinš, Charlotte K. Hind, Andres Meos, Ivo Laidmäe, Tanel Tenson, J. Mark Sutton, A. James Mason and Karin Kogermann. 2024. Fibrous matrices facilitate pleurocidin killing of wound associated bacterial pathogens. *European Journal of Pharmaceutical Sciences*. 192, 106648.
https://doi.org/10.1016/j.ejps.2023.106648.

Lisaks on esitatud 1 suuline ettekanne ja 3 posterettekannet rahvusvahelistel teaduskonverentsidel.

DISSERTATIONES MEDICINAE UNIVERSITATIS TARTUENSIS

1. **Heidi-Ingrid Maaroos**. The natural course of gastric ulcer in connection with chronic gastritis and *Helicobacter pylori*. Tartu, 1991.
2. **Mihkel Zilmer**. Na-pump in normal and tumorous brain tissues: Structural, functional and tumorigenesis aspects. Tartu, 1991.
3. **Eero Vasar**. Role of cholecystokinin receptors in the regulation of behaviour and in the action of haloperidol and diazepam. Tartu, 1992.
4. **Tiina Talvik**. Hypoxic-ischaemic brain damage in neonates (clinical, biochemical and brain computed tomographical investigation). Tartu, 1992.
5. **Ants Peetsalu**. Vagotomy in duodenal ulcer disease: A study of gastric acidity, serum pepsinogen I, gastric mucosal histology and *Helicobacter pylori*. Tartu, 1992.
6. **Marika Mikelsaar**. Evaluation of the gastrointestinal microbial ecosystem in health and disease. Tartu, 1992.
7. **Hele Everaus**. Immuno-hormonal interactions in chronic lymphocytic leukaemia and multiple myeloma. Tartu, 1993.
8. **Ruth Mikelsaar**. Etiological factors of diseases in genetically consulted children and newborn screening: dissertation for the commencement of the degree of doctor of medical sciences. Tartu, 1993.
9. **Agu Tamm**. On metabolic action of intestinal microflora: clinical aspects. Tartu, 1993.
10. **Katrin Gross**. Multiple sclerosis in South-Estonia (epidemiological and computed tomographical investigations). Tartu, 1993.
11. **Oivi Uibo**. Childhood coeliac disease in Estonia: occurrence, screening, diagnosis and clinical characterization. Tartu, 1994.
12. **Viiu Tuulik**. The functional disorders of central nervous system of chemistry workers. Tartu, 1994.
13. **Margus Viigimaa**. Primary haemostasis, antiaggregative and anticoagulant treatment of acute myocardial infarction. Tartu, 1994.
14. **Rein Kolk**. Atrial versus ventricular pacing in patients with sick sinus syndrome. Tartu, 1994.
15. **Toomas Podar**. Incidence of childhood onset type 1 diabetes mellitus in Estonia. Tartu, 1994.
16. **Kiira Subi**. The laboratory surveillance of the acute respiratory viral infections in Estonia. Tartu, 1995.
17. **Irja Lutsar**. Infections of the central nervous system in children (epidemiologic, diagnostic and therapeutic aspects, long term outcome). Tartu, 1995.
18. **Aavo Lang**. The role of dopamine, 5-hydroxytryptamine, sigma and NMDA receptors in the action of antipsychotic drugs. Tartu, 1995.
19. **Andrus Arak**. Factors influencing the survival of patients after radical surgery for gastric cancer. Tartu, 1996.

20. **Tõnis Karki**. Quantitative composition of the human lactoflora and method for its examination. Tartu, 1996.
21. **Reet Mändar**. Vaginal microflora during pregnancy and its transmission to newborn. Tartu, 1996.
22. **Triin Remmel**. Primary biliary cirrhosis in Estonia: epidemiology, clinical characterization and prognostication of the course of the disease. Tartu, 1996.
23. **Toomas Kivastik**. Mechanisms of drug addiction: focus on positive reinforcing properties of morphine. Tartu, 1996.
24. **Paavo Pokk**. Stress due to sleep deprivation: focus on $GABA_A$ receptor-chloride ionophore complex. Tartu, 1996.
25. **Kristina Allikmets**. Renin system activity in essential hypertension. Associations with atherothrombogenic cardiovascular risk factors and with the efficacy of calcium antagonist treatment. Tartu, 1996.
26. **Triin Parik**. Oxidative stress in essential hypertension: Associations with metabolic disturbances and the effects of calcium antagonist treatment. Tartu, 1996.
27. **Svetlana Päi**. Factors promoting heterogeneity of the course of rheumatoid arthritis. Tartu, 1997.
28. **Maarike Sallo**. Studies on habitual physical activity and aerobic fitness in 4 to 10 years old children. Tartu, 1997.
29. **Paul Naaber**. *Clostridium difficile* infection and intestinal microbial ecology. Tartu, 1997.
30. **Rein Pähkla**. Studies in pinoline pharmacology. Tartu, 1997.
31. **Andrus Juhan Voitk**. Outpatient laparoscopic cholecystectomy. Tartu, 1997.
32. **Joel Starkopf**. Oxidative stress and ischaemia-reperfusion of the heart. Tartu, 1997.
33. **Janika Kõrv**. Incidence, case-fatality and outcome of stroke. Tartu, 1998.
34. **Ülla Linnamägi**. Changes in local cerebral blood flow and lipid peroxidation following lead exposure in experiment. Tartu, 1998.
35. **Ave Minajeva**. Sarcoplasmic reticulum function: comparison of atrial and ventricular myocardium. Tartu, 1998.
36. **Oleg Milenin**. Reconstruction of cervical part of esophagus by revascularised ileal autografts in dogs. A new complex multistage method. Tartu, 1998.
37. **Sergei Pakriev**. Prevalence of depression, harmful use of alcohol and alcohol dependence among rural population in Udmurtia. Tartu, 1998.
38. **Allen Kaasik**. Thyroid hormone control over β-adrenergic signalling system in rat atria. Tartu, 1998.
39. **Vallo Matto**. Pharmacological studies on anxiogenic and antiaggressive properties of antidepressants. Tartu, 1998.
40. **Maire Vasar**. Allergic diseases and bronchial hyperreactivity in Estonian children in relation to environmental influences. Tartu, 1998.
41. **Kaja Julge**. Humoral immune responses to allergens in early childhood. Tartu, 1998.

42. **Heli Grünberg**. The cardiovascular risk of Estonian schoolchildren. A cross-sectional study of 9-, 12- and 15-year-old children. Tartu, 1998.
43. **Epp Sepp**. Formation of intestinal microbial ecosystem in children. Tartu, 1998.
44. **Mai Ots**. Characteristics of the progression of human and experimental glomerulopathies. Tartu, 1998.
45. **Tiina Ristimäe**. Heart rate variability in patients with coronary artery disease. Tartu, 1998.
46. **Leho Kõiv**. Reaction of the sympatho-adrenal and hypothalamo-pituitary-adrenocortical system in the acute stage of head injury. Tartu, 1998.
47. **Bela Adojaan**. Immune and genetic factors of childhood onset IDDM in Estonia. An epidemiological study. Tartu, 1999.
48. **Jakov Shlik**. Psychophysiological effects of cholecystokinin in humans. Tartu, 1999.
49. **Kai Kisand**. Autoantibodies against dehydrogenases of α-ketoacids. Tartu, 1999.
50. **Toomas Marandi**. Drug treatment of depression in Estonia. Tartu, 1999.
51. **Ants Kask**. Behavioural studies on neuropeptide Y. Tartu, 1999.
52. **Ello-Rahel Karelson**. Modulation of adenylate cyclase activity in the rat hippocampus by neuropeptide galanin and its chimeric analogs. Tartu, 1999.
53. **Tanel Laisaar**. Treatment of pleural empyema — special reference to intrapleural therapy with streptokinase and surgical treatment modalities. Tartu, 1999.
54. **Eve Pihl**. Cardiovascular risk factors in middle-aged former athletes. Tartu, 1999.
55. **Katrin Õunap**. Phenylketonuria in Estonia: incidence, newborn screening, diagnosis, clinical characterization and genotype/phenotype correlation. Tartu, 1999.
56. **Siiri Kõljalg**. *Acinetobacter* – an important nosocomial pathogen. Tartu, 1999.
57. **Helle Karro**. Reproductive health and pregnancy outcome in Estonia: association with different factors. Tartu, 1999.
58. **Heili Varendi**. Behavioral effects observed in human newborns during exposure to naturally occurring odors. Tartu, 1999.
59. **Anneli Beilmann**. Epidemiology of epilepsy in children and adolescents in Estonia. Prevalence, incidence, and clinical characteristics. Tartu, 1999.
60. **Vallo Volke**. Pharmacological and biochemical studies on nitric oxide in the regulation of behaviour. Tartu, 1999.
61. **Pilvi Ilves**. Hypoxic-ischaemic encephalopathy in asphyxiated term infants. A prospective clinical, biochemical, ultrasonographical study. Tartu, 1999.
62. **Anti Kalda**. Oxygen-glucose deprivation-induced neuronal death and its pharmacological prevention in cerebellar granule cells. Tartu, 1999.
63. **Eve-Irene Lepist**. Oral peptide prodrugs – studies on stability and absorption. Tartu, 2000.

64. **Jana Kivastik**. Lung function in Estonian schoolchildren: relationship with anthropometric indices and respiratory symptomas, reference values for dynamic spirometry. Tartu, 2000.
65. **Karin Kull**. Inflammatory bowel disease: an immunogenetic study. Tartu, 2000.
66. **Kaire Innos**. Epidemiological resources in Estonia: data sources, their quality and feasibility of cohort studies. Tartu, 2000.
67. **Tamara Vorobjova**. Immune response to *Helicobacter pylori* and its association with dynamics of chronic gastritis and epithelial cell turnover in antrum and corpus. Tartu, 2001.
68. **Ruth Kalda**. Structure and outcome of family practice quality in the changing health care system of Estonia. Tartu, 2001.
69. **Annika Krüüner**. *Mycobacterium tuberculosis* – spread and drug resistance in Estonia. Tartu, 2001.
70. **Marlit Veldi**. Obstructive Sleep Apnoea: Computerized Endopharyngeal Myotonometry of the Soft Palate and Lingual Musculature. Tartu, 2001.
71. **Anneli Uusküla**. Epidemiology of sexually transmitted diseases in Estonia in 1990–2000. Tartu, 2001.
72. **Ade Kallas**. Characterization of antibodies to coagulation factor VIII. Tartu, 2002.
73. **Heidi Annuk**. Selection of medicinal plants and intestinal lactobacilli as antimicrobil components for functional foods. Tartu, 2002.
74. **Aet Lukmann**. Early rehabilitation of patients with ischaemic heart disease after surgical revascularization of the myocardium: assessment of health-related quality of life, cardiopulmonary reserve and oxidative stress. A clinical study. Tartu, 2002.
75. **Maigi Eisen**. Pathogenesis of Contact Dermatitis: participation of Oxidative Stress. A clinical – biochemical study. Tartu, 2002.
76. **Piret Hussar**. Histology of the post-traumatic bone repair in rats. Elaboration and use of a new standardized experimental model – bicortical perforation of tibia compared to internal fracture and resection osteotomy. Tartu, 2002.
77. **Tõnu Rätsep**. Aneurysmal subarachnoid haemorrhage: Noninvasive monitoring of cerebral haemodynamics. Tartu, 2002.
78. **Marju Herodes**. Quality of life of people with epilepsy in Estonia. Tartu, 2003.
79. **Katre Maasalu**. Changes in bone quality due to age and genetic disorders and their clinical expressions in Estonia. Tartu, 2003.
80. **Toomas Sillakivi**. Perforated peptic ulcer in Estonia: epidemiology, risk factors and relations with *Helicobacter pylori*. Tartu, 2003.
81. **Leena Puksa**. Late responses in motor nerve conduction studies. F and A waves in normal subjects and patients with neuropathies. Tartu, 2003.
82. **Krista Lõivukene**. *Helicobacter pylori* in gastric microbial ecology and its antimicrobial susceptibility pattern. Tartu, 2003.

83. **Helgi Kolk**. Dyspepsia and *Helicobacter pylori* infection: the diagnostic value of symptoms, treatment and follow-up of patients referred for upper gastrointestinal endoscopy by family physicians. Tartu, 2003.
84. **Helena Soomer**. Validation of identification and age estimation methods in forensic odontology. Tartu, 2003.
85. **Kersti Oselin**. Studies on the human MDR1, MRP1, and MRP2 ABC transporters: functional relevance of the genetic polymorphisms in the *MDR1* and *MRP1* gene. Tartu, 2003.
86. **Jaan Soplepmann**. Peptic ulcer haemorrhage in Estonia: epidemiology, prognostic factors, treatment and outcome. Tartu, 2003.
87. **Margot Peetsalu**. Long-term follow-up after vagotomy in duodenal ulcer disease: recurrent ulcer, changes in the function, morphology and *Helicobacter pylori* colonisation of the gastric mucosa. Tartu, 2003.
88. **Kersti Klaamas**. Humoral immune response to *Helicobacter pylori* a study of host-dependent and microbial factors. Tartu, 2003.
89. **Pille Taba**. Epidemiology of Parkinson's disease in Tartu, Estonia. Prevalence, incidence, clinical characteristics, and pharmacoepidemiology. Tartu, 2003.
90. **Alar Veraksitš**. Characterization of behavioural and biochemical phenotype of cholecystokinin-2 receptor deficient mice: changes in the function of the dopamine and endopioidergic system. Tartu, 2003.
91. **Ingrid Kalev**. CC-chemokine receptor 5 (CCR5) gene polymorphism in Estonians and in patients with Type I and Type II diabetes mellitus. Tartu, 2003.
92. **Lumme Kadaja**. Molecular approach to the regulation of mitochondrial function in oxidative muscle cells. Tartu, 2003.
93. **Aive Liigant**. Epidemiology of primary central nervous system tumours in Estonia from 1986 to 1996. Clinical characteristics, incidence, survival and prognostic factors. Tartu, 2004.
94. **Andres, Kulla**. Molecular characteristics of mesenchymal stroma in human astrocytic gliomas. Tartu, 2004.
95. **Mari Järvelaid**. Health damaging risk behaviours in adolescence. Tartu, 2004.
96. **Ülle Pechter**. Progression prevention strategies in chronic renal failure and hypertension. An experimental and clinical study. Tartu, 2004.
97. **Gunnar Tasa**. Polymorphic glutathione S-transferases – biology and role in modifying genetic susceptibility to senile cataract and primary open angle glaucoma. Tartu, 2004.
98. **Tuuli Käämbre**. Intracellular energetic unit: structural and functional aspects. Tartu, 2004.
99. **Vitali Vassiljev**. Influence of nitric oxide syntase inhibitors on the effects of ethanol after acute and chronic ethanol administration and withdrawal. Tartu, 2004.

100. **Aune Rehema**. Assessment of nonhaem ferrous iron and glutathione redox ratio as markers of pathogeneticity of oxidative stress in different clinical groups. Tartu, 2004.
101. **Evelin Seppet**. Interaction of mitochondria and ATPases in oxidative muscle cells in normal and pathological conditions. Tartu, 2004.
102. **Eduard Maron**. Serotonin function in panic disorder: from clinical experiments to brain imaging and genetics. Tartu, 2004.
103. **Marje Oona**. *Helicobacter pylori* infection in children: epidemiological and therapeutic aspects. Tartu, 2004.
104. **Kersti Kokk**. Regulation of active and passive molecular transport in the testis. Tartu, 2005.
105. **Vladimir Järv**. Cross-sectional imaging for pretreatment evaluation and follow-up of pelvic malignant tumours. Tartu, 2005.
106. **Andre Õun**. Epidemiology of adult epilepsy in Tartu, Estonia. Incidence, prevalence and medical treatment. Tartu, 2005.
107. **Piibe Muda**. Homocysteine and hypertension: associations between homocysteine and essential hypertension in treated and untreated hypertensive patients with and without coronary artery disease. Tartu, 2005.
108. **Külli Kingo**. The interleukin-10 family cytokines gene polymorphisms in plaque psoriasis. Tartu, 2005.
109. **Mati Merila**. Anatomy and clinical relevance of the glenohumeral joint capsule and ligaments. Tartu, 2005.
110. **Epp Songisepp**. Evaluation of technological and functional properties of the new probiotic *Lactobacillus fermentum* ME-3. Tartu, 2005.
111. **Tiia Ainla**. Acute myocardial infarction in Estonia: clinical characteristics, management and outcome. Tartu, 2005.
112. **Andres Sell**. Determining the minimum local anaesthetic requirements for hip replacement surgery under spinal anaesthesia – a study employing a spinal catheter. Tartu, 2005.
113. **Tiia Tamme**. Epidemiology of odontogenic tumours in Estonia. Pathogenesis and clinical behaviour of ameloblastoma. Tartu, 2005.
114. **Triine Annus**. Allergy in Estonian schoolchildren: time trends and characteristics. Tartu, 2005.
115. **Tiia Voor**. Microorganisms in infancy and development of allergy: comparison of Estonian and Swedish children. Tartu, 2005.
116. **Priit Kasenõmm**. Indicators for tonsillectomy in adults with recurrent tonsillitis – clinical, microbiological and pathomorphological investigations. Tartu, 2005.
117. **Eva Zusinaite**. Hepatitis C virus: genotype identification and interactions between viral proteases. Tartu, 2005.
118. **Piret Kõll**. Oral lactoflora in chronic periodontitis and periodontal health. Tartu, 2006.
119. **Tiina Stelmach**. Epidemiology of cerebral palsy and unfavourable neurodevelopmental outcome in child population of Tartu city and county, Estonia Prevalence, clinical features and risk factors. Tartu, 2006.

120. **Katrin Pudersell**. Tropane alkaloid production and riboflavine excretion in the field and tissue cultures of henbane (*Hyoscyamus niger* L.). Tartu, 2006.
121. **Külli Jaako**. Studies on the role of neurogenesis in brain plasticity. Tartu, 2006.
122. **Aare Märtson**. Lower limb lengthening: experimental studies of bone regeneration and long-term clinical results. Tartu, 2006.
123. **Heli Tähepõld**. Patient consultation in family medicine. Tartu, 2006.
124. **Stanislav Liskmann**. Peri-implant disease: pathogenesis, diagnosis and treatment in view of both inflammation and oxidative stress profiling. Tartu, 2006.
125. **Ruth Rudissaar**. Neuropharmacology of atypical antipsychotics and an animal model of psychosis. Tartu, 2006.
126. **Helena Andreson**. Diversity of *Helicobacter pylori* genotypes in Estonian patients with chronic inflammatory gastric diseases. Tartu, 2006.
127. **Katrin Pruus**. Mechanism of action of antidepressants: aspects of serotoninergic system and its interaction with glutamate. Tartu, 2006.
128. **Priit Põder**. Clinical and experimental investigation: relationship of ischaemia/reperfusion injury with oxidative stress in abdominal aortic aneurysm repair and in extracranial brain artery endarterectomy and possibilities of protection against ischaemia using a glutathione analogue in a rat model of global brain ischaemia. Tartu, 2006.
129. **Marika Tammaru**. Patient-reported outcome measurement in rheumatoid arthritis. Tartu, 2006.
130. **Tiia Reimand**. Down syndrome in Estonia. Tartu, 2006.
131. **Diva Eensoo**. Risk-taking in traffic and Markers of Risk-Taking Behaviour in Schoolchildren and Car Drivers. Tartu, 2007.
132. **Riina Vibo**. The third stroke registry in Tartu, Estonia from 2001 to 2003: incidence, case-fatality, risk factors and long-term outcome. Tartu, 2007.
133. **Chris Pruunsild**. Juvenile idiopathic arthritis in children in Estonia. Tartu, 2007.
134. **Eve Õiglane-Šlik**. Angelman and Prader-Willi syndromes in Estonia. Tartu, 2007.
135. **Kadri Haller**. Antibodies to follicle stimulating hormone. Significance in female infertility. Tartu, 2007.
136. **Pille Ööpik**. Management of depression in family medicine. Tartu, 2007.
137. **Jaak Kals**. Endothelial function and arterial stiffness in patients with atherosclerosis and in healthy subjects. Tartu, 2007.
138. **Priit Kampus**. Impact of inflammation, oxidative stress and age on arterial stiffness and carotid artery intima-media thickness. Tartu, 2007.
139. **Margus Punab**. Male fertility and its risk factors in Estonia. Tartu, 2007.
140. **Alar Toom**. Heterotopic ossification after total hip arthroplasty: clinical and pathogenetic investigation. Tartu, 2007.

141. **Lea Pehme**. Epidemiology of tuberculosis in Estonia 1991–2003 with special regard to extrapulmonary tuberculosis and delay in diagnosis of pulmonary tuberculosis. Tartu, 2007.
142. **Juri Karjagin**. The pharmacokinetics of metronidazole and meropenem in septic shock. Tartu, 2007.
143. **Inga Talvik**. Inflicted traumatic brain injury shaken baby syndrome in Estonia – epidemiology and outcome. Tartu, 2007.
144. **Tarvo Rajasalu**. Autoimmune diabetes: an immunological study of type 1 diabetes in humans and in a model of experimental diabetes (in RIP-B7.1 mice). Tartu, 2007.
145. **Inga Karu**. Ischaemia-reperfusion injury of the heart during coronary surgery: a clinical study investigating the effect of hyperoxia. Tartu, 2007.
146. **Peeter Padrik**. Renal cell carcinoma: Changes in natural history and treatment of metastatic disease. Tartu, 2007.
147. **Neve Vendt**. Iron deficiency and iron deficiency anaemia in infants aged 9 to 12 months in Estonia. Tartu, 2008.
148. **Lenne-Triin Heidmets**. The effects of neurotoxins on brain plasticity: focus on neural Cell Adhesion Molecule. Tartu, 2008.
149. **Paul Korrovits**. Asymptomatic inflammatory prostatitis: prevalence, etiological factors, diagnostic tools. Tartu, 2008.
150. **Annika Reintam**. Gastrointestinal failure in intensive care patients. Tartu, 2008.
151. **Kristiina Roots**. Cationic regulation of Na-pump in the normal, Alzheimer's and CCK_2 receptor-deficient brain. Tartu, 2008.
152. **Helen Puusepp**. The genetic causes of mental retardation in Estonia: fragile X syndrome and creatine transporter defect. Tartu, 2009.
153. **Kristiina Rull**. Human chorionic gonadotropin beta genes and recurrent miscarriage: expression and variation study. Tartu, 2009.
154. **Margus Eimre**. Organization of energy transfer and feedback regulation in oxidative muscle cells. Tartu, 2009.
155. **Maire Link**. Transcription factors FoxP3 and AIRE: autoantibody associations. Tartu, 2009.
156. **Kai Haldre**. Sexual health and behaviour of young women in Estonia. Tartu, 2009.
157. **Kaur Liivak**. Classical form of congenital adrenal hyperplasia due to 21-hydroxylase deficiency in Estonia: incidence, genotype and phenotype with special attention to short-term growth and 24-hour blood pressure. Tartu, 2009.
158. **Kersti Ehrlich**. Antioxidative glutathione analogues (UPF peptides) – molecular design, structure-activity relationships and testing the protective properties. Tartu, 2009.
159. **Anneli Rätsep**. Type 2 diabetes care in family medicine. Tartu, 2009.
160. **Silver Türk**. Etiopathogenetic aspects of chronic prostatitis: role of mycoplasmas, coryneform bacteria and oxidative stress. Tartu, 2009.

161. **Kaire Heilman**. Risk markers for cardiovascular disease and low bone mineral density in children with type 1 diabetes. Tartu, 2009.
162. **Kristi Rüütel**. HIV-epidemic in Estonia: injecting drug use and quality of life of people living with HIV. Tartu, 2009.
163. **Triin Eller**. Immune markers in major depression and in antidepressive treatment. Tartu, 2009.
164. **Siim Suutre**. The role of TGF-β isoforms and osteoprogenitor cells in the pathogenesis of heterotopic ossification. An experimental and clinical study of hip arthroplasty. Tartu, 2010.
165. **Kai Kliiman**. Highly drug-resistant tuberculosis in Estonia: Risk factors and predictors of poor treatment outcome. Tartu, 2010.
166. **Inga Villa**. Cardiovascular health-related nutrition, physical activity and fitness in Estonia. Tartu, 2010.
167. **Tõnis Org**. Molecular function of the first PHD finger domain of Autoimmune Regulator protein. Tartu, 2010.
168. **Tuuli Metsvaht**. Optimal antibacterial therapy of neonates at risk of early onset sepsis. Tartu, 2010.
169. **Jaanus Kahu**. Kidney transplantation: Studies on donor risk factors and mycophenolate mofetil. Tartu, 2010.
170. **Koit Reimand**. Autoimmunity in reproductive failure: A study on associated autoantibodies and autoantigens. Tartu, 2010.
171. **Mart Kull**. Impact of vitamin D and hypolactasia on bone mineral density: a population based study in Estonia. Tartu, 2010.
172. **Rael Laugesaar**. Stroke in children – epidemiology and risk factors. Tartu, 2010.
173. **Mark Braschinsky**. Epidemiology and quality of life issues of hereditary spastic paraplegia in Estonia and implemention of genetic analysis in everyday neurologic practice. Tartu, 2010.
174. **Kadri Suija**. Major depression in family medicine: associated factors, recurrence and possible intervention. Tartu, 2010.
175. **Jarno Habicht**. Health care utilisation in Estonia: socioeconomic determinants and financial burden of out-of-pocket payments. Tartu, 2010.
176. **Kristi Abram**. The prevalence and risk factors of rosacea. Subjective disease perception of rosacea patients. Tartu, 2010.
177. **Malle Kuum**. Mitochondrial and endoplasmic reticulum cation fluxes: Novel roles in cellular physiology. Tartu, 2010.
178. **Rita Teek**. The genetic causes of early onset hearing loss in Estonian children. Tartu, 2010.
179. **Daisy Volmer**. The development of community pharmacy services in Estonia – public and professional perceptions 1993–2006. Tartu, 2010.
180. **Jelena Lissitsina**. Cytogenetic causes in male infertility. Tartu, 2011.
181. **Delia Lepik**. Comparison of gunshot injuries caused from Tokarev, Makarov and Glock 19 pistols at different firing distances. Tartu, 2011.
182. **Ene-Renate Pähkla**. Factors related to the efficiency of treatment of advanced periodontitis. Tartu, 2011.

183. **Maarja Krass**. L-Arginine pathways and antidepressant action. Tartu, 2011.
184. **Taavi Lai**. Population health measures to support evidence-based health policy in Estonia. Tartu, 2011.
185. **Tiit Salum**. Similarity and difference of temperature-dependence of the brain sodium pump in normal, different neuropathological, and aberrant conditions and its possible reasons. Tartu, 2011.
186. **Tõnu Vooder**. Molecular differences and similarities between histological subtypes of non-small cell lung cancer. Tartu, 2011.
187. **Jelena Štšepetova**. The characterisation of intestinal lactic acid bacteria using bacteriological, biochemical and molecular approaches. Tartu, 2011.
188. **Radko Avi**. Natural polymorphisms and transmitted drug resistance in Estonian HIV-1 CRF06_cpx and its recombinant viruses. Tartu, 2011, 116 p.
189. **Edward Laane**. Multiparameter flow cytometry in haematological malignancies. Tartu, 2011, 152 p.
190. **Triin Jagomägi**. A study of the genetic etiology of nonsyndromic cleft lip and palate. Tartu, 2011, 158 p.
191. **Ivo Laidmäe**. Fibrin glue of fish (*Salmo salar*) origin: immunological study and development of new pharmaceutical preparation. Tartu, 2012, 150 p.
192. **Ülle Parm**. Early mucosal colonisation and its role in prediction of invasive infection in neonates at risk of early onset sepsis. Tartu, 2012, 168 p.
193. **Kaupo Teesalu**. Autoantibodies against desmin and transglutaminase 2 in celiac disease: diagnostic and functional significance. Tartu, 2012, 142 p.
194. **Maksim Zagura**. Biochemical, functional and structural profiling of arterial damage in atherosclerosis. Tartu, 2012, 162 p.
195. **Vivian Kont**. Autoimmune regulator: characterization of thymic gene regulation and promoter methylation. Tartu, 2012, 134 p.
196. **Pirje Hütt**. Functional properties, persistence, safety and efficacy of potential probiotic lactobacilli. Tartu, 2012, 246 p.
197. **Innar Tõru**. Serotonergic modulation of CCK-4- induced panic. Tartu, 2012, 132 p.
198. **Sigrid Vorobjov**. Drug use, related risk behaviour and harm reduction interventions utilization among injecting drug users in Estonia: implications for drug policy. Tartu, 2012, 120 p.
199. **Martin Serg**. Therapeutic aspects of central haemodynamics, arterial stiffness and oxidative stress in hypertension. Tartu, 2012, 156 p.
200. **Jaanika Kumm**. Molecular markers of articular tissues in early knee osteoarthritis: a population-based longitudinal study in middle-aged subjects. Tartu, 2012, 159 p.
201. **Kertu Rünkorg**. Functional changes of dopamine, endopioid and endocannabinoid systems in CCK2 receptor deficient mice. Tartu, 2012, 125 p.
202. **Mai Blöndal**. Changes in the baseline characteristics, management and outcomes of acute myocardial infarction in Estonia. Tartu, 2012, 127 p.

203. **Jana Lass**. Epidemiological and clinical aspects of medicines use in children in Estonia. Tartu, 2012, 170 p.
204. **Kai Truusalu**. Probiotic lactobacilli in experimental persistent *Salmonella* infection. Tartu, 2013, 139 p.
205. **Oksana Jagur**. Temporomandibular joint diagnostic imaging in relation to pain and bone characteristics. Long-term results of arthroscopic treatment. Tartu, 2013, 126 p.
206. **Katrin Sikk**. Manganese-ephedrone intoxication – pathogenesis of neurological damage and clinical symptomatology. Tartu, 2013, 125 p.
207. **Kai Blöndal**. Tuberculosis in Estonia with special emphasis on drug-resistant tuberculosis: Notification rate, disease recurrence and mortality. Tartu, 2013, 151 p.
208. **Marju Puurand**. Oxidative phosphorylation in different diseases of gastric mucosa. Tartu, 2013, 123 p.
209. **Aili Tagoma**. Immune activation in female infertility: Significance of autoantibodies and inflammatory mediators. Tartu, 2013, 135 p.
210. **Liis Sabre**. Epidemiology of traumatic spinal cord injury in Estonia. Brain activation in the acute phase of traumatic spinal cord injury. Tartu, 2013, 135 p.
211. **Merit Lamp**. Genetic susceptibility factors in endometriosis. Tartu, 2013, 125 p.
212. **Erik Salum**. Beneficial effects of vitamin D and angiotensin II receptor blocker on arterial damage. Tartu, 2013, 167 p.
213. **Maire Karelson**. Vitiligo: clinical aspects, quality of life and the role of melanocortin system in pathogenesis. Tartu, 2013, 153 p.
214. **Kuldar Kaljurand**. Prevalence of exfoliation syndrome in Estonia and its clinical significance. Tartu, 2013, 113 p.
215. **Raido Paasma**. Clinical study of methanol poisoning: handling large outbreaks, treatment with antidotes, and long-term outcomes. Tartu, 2013, 96 p.
216. **Anne Kleinberg**. Major depression in Estonia: prevalence, associated factors, and use of health services. Tartu, 2013, 129 p.
217. **Triin Eglit**. Obesity, impaired glucose regulation, metabolic syndrome and their associations with high-molecular-weight adiponectin levels. Tartu, 2014, 115 p.
218. **Kristo Ausmees**. Reproductive function in middle-aged males: Associations with prostate, lifestyle and couple infertility status. Tartu, 2014, 125 p.
219. **Kristi Huik**. The influence of host genetic factors on the susceptibility to HIV and HCV infections among intravenous drug users. Tartu, 2014, 144 p.
220. **Liina Tserel**. Epigenetic profiles of monocytes, monocyte-derived macrophages and dendritic cells. Tartu, 2014, 143 p.
221. **Irina Kerna**. The contribution of *ADAM12* and *CILP* genes to the development of knee osteoarthritis. Tartu, 2014, 152 p.

222. **Ingrid Liiv**. Autoimmune regulator protein interaction with DNA-dependent protein kinase and its role in apoptosis. Tartu, 2014, 143 p.
223. **Liivi Maddison**. Tissue perfusion and metabolism during intra-abdominal hypertension. Tartu, 2014, 103 p.
224. **Krista Ress**. Childhood coeliac disease in Estonia, prevalence in atopic dermatitis and immunological characterisation of coexistence. Tartu, 2014, 124 p.
225. **Kai Muru**. Prenatal screening strategies, long-term outcome of children with marked changes in maternal screening tests and the most common syndromic heart anomalies in Estonia. Tartu, 2014, 189 p.
226. **Kaja Rahu**. Morbidity and mortality among Baltic Chernobyl cleanup workers: a register-based cohort study. Tartu, 2014, 155 p.
227. **Klari Noormets**. The development of diabetes mellitus, fertility and energy metabolism disturbances in a Wfs1-deficient mouse model of Wolfram syndrome. Tartu, 2014, 132 p.
228. **Liis Toome**. Very low gestational age infants in Estonia. Tartu, 2014, 183 p.
229. **Ceith Nikkolo**. Impact of different mesh parameters on chronic pain and foreign body feeling after open inguinal hernia repair. Tartu, 2014, 132 p.
230. **Vadim Brjalin**. Chronic hepatitis C: predictors of treatment response in Estonian patients. Tartu, 2014, 122 p.
231. **Vahur Metsna**. Anterior knee pain in patients following total knee arthroplasty: the prevalence, correlation with patellar cartilage impairment and aspects of patellofemoral congruence. Tartu, 2014, 130 p.
232. **Marju Kase**. Glioblastoma multiforme: possibilities to improve treatment efficacy. Tartu, 2015, 137 p.
233. **Riina Runnel**. Oral health among elementary school children and the effects of polyol candies on the prevention of dental caries. Tartu, 2015, 112 p.
234. **Made Laanpere**. Factors influencing women's sexual health and reproductive choices in Estonia. Tartu, 2015, 176 p.
235. **Andres Lust**. Water mediated solid state transformations of a polymorphic drug – effect on pharmaceutical product performance. Tartu, 2015, 134 p.
236. **Anna Klugman**. Functionality related characterization of pretreated wood lignin, cellulose and polyvinylpyrrolidone for pharmaceutical applications. Tartu, 2015, 156 p.
237. **Triin Laisk-Podar**. Genetic variation as a modulator of susceptibility to female infertility and a source for potential biomarkers. Tartu, 2015, 155 p.
238. **Mailis Tõnisson**. Clinical picture and biochemical changes in blood in children with acute alcohol intoxication. Tartu, 2015, 100 p.
239. **Kadri Tamme**. High volume haemodiafiltration in treatment of severe sepsis – impact on pharmacokinetics of antibiotics and inflammatory response. Tartu, 2015, 133 p.

240. **Kai Part**. Sexual health of young people in Estonia in a social context: the role of school-based sexuality education and youth-friendly counseling services. Tartu, 2015, 203 p.
241. **Urve Paaver**. New perspectives for the amorphization and physical stabilization of poorly water-soluble drugs and understanding their dissolution behavior. Tartu, 2015, 139 p.
242. **Aleksandr Peet**. Intrauterine and postnatal growth in children with HLA-conferred susceptibility to type 1 diabetes. Tartu. 2015, 146 p.
243. **Piret Mitt**. Healthcare-associated infections in Estonia – epidemiology and surveillance of bloodstream and surgical site infections. Tartu, 2015, 145 p.
244. **Merli Saare**. Molecular Profiling of Endometriotic Lesions and Endometria of Endometriosis Patients. Tartu, 2016, 129 p.
245. **Kaja-Triin Laisaar**. People living with HIV in Estonia: Engagement in medical care and methods of increasing adherence to antiretroviral therapy and safe sexual behavior. Tartu, 2016, 132 p.
246. **Eero Merilind**. Primary health care performance: impact of payment and practice-based characteristics. Tartu, 2016, 120 p.
247. **Jaanika Kärner**. Cytokine-specific autoantibodies in AIRE deficiency. Tartu, 2016, 182 p.
248. **Kaido Paapstel**. Metabolomic profile of arterial stiffness and early biomarkers of renal damage in atherosclerosis. Tartu, 2016, 173 p.
249. **Liidia Kiisk**. Long-term nutritional study: anthropometrical and clinico-laboratory assessments in renal replacement therapy patients after intensive nutritional counselling. Tartu, 2016, 207 p.
250. **Georgi Nellis**. The use of excipients in medicines administered to neonates in Europe. Tartu, 2017, 159 p.
251. **Aleksei Rakitin**. Metabolic effects of acute and chronic treatment with valproic acid in people with epilepsy. Tartu, 2017, 125 p.
252. **Eveli Kallas**. The influence of immunological markers to susceptibility to HIV, HBV, and HCV infections among persons who inject drugs. Tartu, 2017, 138 p.
253. **Tiina Freimann**. Musculoskeletal pain among nurses: prevalence, risk factors, and intervention. Tartu, 2017, 125 p.
254. **Evelyn Aaviksoo**. Sickness absence in Estonia: determinants and influence of the sick-pay cut reform. Tartu, 2017, 121 p.
255. **Kalev Nõupuu**. Autosomal-recessive Stargardt disease: phenotypic heterogeneity and genotype-phenotype associations. Tartu, 2017, 131 p.
256. **Ho Duy Binh**. Osteogenesis imperfecta in Vietnam. Tartu, 2017, 125 p.
257. **Uku Haljasorg**. Transcriptional mechanisms in thymic central tolerance. Tartu, 2017, 147 p.
258. **Živile Riispere**. IgA Nephropathy study according to the Oxford Classification: IgA Nephropathy clinical-morphological correlations, disease progression and the effect of renoprotective therapy. Tartu, 2017, 129 p.

259. **Hiie Soeorg**. Coagulase-negative staphylococci in gut of preterm neonates and in breast milk of their mothers. Tartu, 2017, 216 p.
260. **Anne-Mari Anton Willmore**. Silver nanoparticles for cancer research. Tartu, 2017, 132 p.
261. **Ott Laius**. Utilization of osteoporosis medicines, medication adherence and the trend in osteoporosis related hip fractures in Estonia. Tartu, 2017, 134 p.
262. **Alar Aab**. Insights into molecular mechanisms of asthma and atopic dermatitis. Tartu, 2017, 164 p.
263. **Sander Pajusalu**. Genome-wide diagnostics of Mendelian disorders: from chromosomal microarrays to next-generation sequencing. Tartu, 2017, 146 p.
264. **Mikk Jürisson**. Health and economic impact of hip fracture in Estonia. Tartu, 2017, 164 p.
265. **Kaspar Tootsi**. Cardiovascular and metabolomic profiling of osteoarthritis. Tartu, 2017, 150 p.
266. **Mario Saare**. The influence of AIRE on gene expression – studies of transcriptional regulatory mechanisms in cell culture systems. Tartu, 2017, 172 p.
267. **Piia Jõgi**. Epidemiological and clinical characteristics of pertussis in Estonia. Tartu, 2018, 168 p.
268. **Elle Põldoja**. Structure and blood supply of the superior part of the shoulder joint capsule. Tartu, 2018, 116 p.
269. **Minh Son Nguyen**. Oral health status and prevalence of temporomandibular disorders in 65–74-year-olds in Vietnam. Tartu, 2018, 182 p.
270. **Kristian Semjonov**. Development of pharmaceutical quench-cooled molten and melt-electrospun solid dispersions for poorly water-soluble indomethacin. Tartu, 2018, 125 p.
271. **Janne Tiigimäe-Saar**. Botulinum neurotoxin type A treatment for sialorrhea in central nervous system diseases. Tartu, 2018, 109 p.
272. **Veiko Vengerfeldt**. Apical periodontitis: prevalence and etiopathogenetic aspects. Tartu, 2018, 150 p.
273. **Rudolf Bichele**. TNF superfamily and AIRE at the crossroads of thymic differentiation and host protection against *Candida albicans* infection. Tartu, 2018, 153 p.
274. **Olga Tšuiko**. Unravelling Chromosomal Instability in Mammalian Preimplantation Embryos Using Single-Cell Genomics. Tartu, 2018, 169 p.
275. **Kärt Kriisa**. Profile of acylcarnitines, inflammation and oxidative stress in first-episode psychosis before and after antipsychotic treatment. Tartu, 2018, 145 p.
276. **Xuan Dung Ho**. Characterization of the genomic profile of osteosarcoma. Tartu, 2018, 144 p.
277. **Karit Reinson**. New Diagnostic Methods for Early Detection of Inborn Errors of Metabolism in Estonia. Tartu, 2018, 201 p.

278. **Mari-Anne Vals**. Congenital N-glycosylation Disorders in Estonia. Tartu, 2019, 148 p.
279. **Liis Kadastik-Eerme**. Parkinson's disease in Estonia: epidemiology, quality of life, clinical characteristics and pharmacotherapy. Tartu, 2019, 202 p.
280. **Hedi Hunt**. Precision targeting of intraperitoneal tumors with peptide-guided nanocarriers. Tartu, 2019, 179 p.
281. **Rando Porosk**. The role of oxidative stress in Wolfram syndrome 1 and hypothermia. Tartu, 2019, 123 p.
282. **Ene-Ly Jõgeda**. The influence of coinfections and host genetic factor on the susceptibility to HIV infection among people who inject drugs. Tartu, 2019, 126 p.
283. **Kristel Ehala-Aleksejev**. The associations between body composition, obesity and obesity-related health and lifestyle conditions with male reproductive function. Tartu, 2019, 138 p.
284. **Aigar Ottas**. The metabolomic profiling of psoriasis, atopic dermatitis and atherosclerosis. Tartu, 2019, 136 p.
285. **Elmira Gurbanova**. Specific characteristics of tuberculosis in low default, but high multidrug–resistance prison setting. Tartu, 2019, 129 p.
286. **Van Thai Nguyeni**. The first study of the treatment outcomes of patients with cleft lip and palate in Central Vietnam. Tartu, 2019, 144 p.
287. **Maria Yakoreva**. Imprinting Disorders in Estonia. Tartu, 2019, 187 p.
288. **Kadri Rekker**. The putative role of microRNAs in endometriosis pathogenesis and potential in diagnostics. Tartu, 2019, 140 p.
289. **Ülle Võhma**. Association between personality traits, clinical characteristics and pharmacological treatment response in panic disorder. Tartu, 2019, 121 p.
290. **Aet Saar**. Acute myocardial infarction in Estonia 2001–2014: towards risk-based prevention and management. Tartu, 2019, 124 p.
291. **Toomas Toomsoo**. Transcranial brain sonography in the Estonian cohort of Parkinson's disease. Tartu, 2019, 114 p.
292. **Lidiia Zhytnik**. Inter- and intrafamilial diversity based on genotype and phenotype correlations of Osteogenesis Imperfecta. Tartu, 2019, 224 p.
293. **Pilleriin Soodla**. Newly HIV-infected people in Estonia: estimation of incidence and transmitted drug resistance. Tartu, 2019, 194 p.
294. **Kristiina Ojamaa**. Epidemiology of gynecological cancer in Estonia. Tartu, 2020, 133 p.
295. **Marianne Saard**. Modern Cognitive and Social Intervention Techniques in Paediatric Neurorehabilitation for Children with Acquired Brain Injury. Tartu, 2020, 168 p.
296. **Julia Maslovskaja**. The importance of DNA binding and DNA breaks for AIRE-mediated transcriptional activation. Tartu, 2020, 162 p.
297. **Natalia Lobanovskaya**. The role of PSA-NCAM in the survival of retinal ganglion cells. Tartu, 2020, 105 p.

298. **Madis Rahu**. Structure and blood supply of the postero-superior part of the shoulder joint capsule with implementation of surgical treatment after anterior traumatic dislocation. Tartu, 2020, 104 p.
299. **Helen Zirnask**. Luteinizing hormone (LH) receptor expression in the penis and its possible role in pathogenesis of erectile disturbances. Tartu, 2020, 87 p.
300. **Kadri Toome**. Homing peptides for targeting of brain diseases. Tartu, 2020, 152 p.
301. **Maarja Hallik**. Pharmacokinetics and pharmacodynamics of inotropic drugs in neonates. Tartu, 2020, 172 p.
302. **Raili Müller**. Cardiometabolic risk profile and body composition in early rheumatoid arthritis. Tartu, 2020, 133 p.
303. **Sergo Kasvandik**. The role of proteomic changes in endometrial cells – from the perspective of fertility and endometriosis. Tartu, 2020, 191 p.
304. **Epp Kaleviste**. Genetic variants revealing the role of STAT1/STAT3 signaling cytokines in immune protection and pathology. Tartu, 2020, 189 p.
305. **Sten Saar**. Epidemiology of severe injuries in Estonia. Tartu, 2020, 104 p.
306. **Kati Braschinsky**. Epidemiology of primary headaches in Estonia and applicability of web-based solutions in headache epidemiology research. Tartu, 2020, 129 p.
307. **Helen Vaher**. MicroRNAs in the regulation of keratinocyte responses in *psoriasis vulgaris* and atopic dermatitis. Tartu, 2020, 242 p.
308. **Liisi Raam**. Molecular Alterations in the Pathogenesis of Two Chronic Dermatoses – Vitiligo and Psoriasis. Tartu, 2020, 164 p.
309. **Artur Vetkas**. Long-term quality of life, emotional health, and associated factors in patients after aneurysmal subarachnoid haemorrhage. Tartu, 2020, 127 p.
310. **Teele Kasepalu**. Effects of remote ischaemic preconditioning on organ damage and acylcarnitines' metabolism in vascular surgery. Tartu, 2020, 130 p.
311. **Prakash Lingasamy**. Development of multitargeted tumor penetrating peptides. Tartu, 2020, 246 p.
312. **Lille Kurvits.** Parkinson's disease as a multisystem disorder: whole transcriptome study in Parkinson's disease patients' skin and blood. Tartu, 2021, 142 p.
313. **Mariliis Põld.** Smoking, attitudes towards smoking behaviour, and nicotine dependence among physicians in Estonia: cross-sectional surveys 1982–2014. Tartu, 2021, 172 p.
314. **Triin Kikas**. Single nucleotide variants affecting placental gene expression and pregnancy outcome. Tartu, 2021, 160 p.
315. **Hedda Lippus-Metsaots**. Interpersonal violence in Estonia: prevalence, impact on health and health behaviour. Tartu, 2021, 172 p.

316. **Georgi Dzaparidze.** Quantification and evaluation of the diagnostic significance of adenocarcinoma-associated microenvironmental changes in the prostate using modern digital pathology solutions. Tartu, 2021, 132 p.
317. **Tuuli Sedman.** New avenues for GLP1 receptor agonists in the treatment of diabetes. Tartu, 2021, 118 p.
318. **Martin Padar.** Enteral nutrition, gastrointestinal dysfunction and intestinal biomarkers in critically ill patients. Tartu, 2021, 189 p.
319. **Siim Schneider.** Risk factors, etiology and long-term outcome in young ischemic stroke patients in Estonia. Tartu, 2021, 131 p.
320. **Konstantin Ridnõi.** Implementation and effectiveness of new prenatal diagnostic strategies in Estonia. Tartu, 2021, 191 p.
321. **Risto Vaikjärv.** Etiopathogenetic and clinical aspects of peritonsillar abscess. Tartu, 2021, 115 p.
322. **Liis Preem.** Design and characterization of antibacterial electrospun drug delivery systems for wound infections. Tartu, 2022, 220 p.
323. **Keerthie Dissanayake.** Preimplantation embryo-derived extracellular vesicles: potential as an embryo quality marker and their role during the embryo-maternal communication. Tartu, 2022, 203 p.
324. **Laura Viidik.** 3D printing in pharmaceutics: a new avenue for fabricating therapeutic drug delivery systems. Tartu, 2022, 139 p.
325. **Kasun Godakumara.** Extracellular vesicle mediated embryo-maternal communication – A tool for evaluating functional competency of preimplantation embryos. Tartu, 2022, 176 p.
326. **Hindrek Teder.** Developing computational methods and workflows for targeted and whole-genome sequencing based non-invasive prenatal testing. Tartu, 2022, 138 p.
327. **Jana Tuusov.** Deaths caused by alcohol, psychotropic and other substances in Estonia: evidence based on forensic autopsies. Tartu, 2022, 157 p.
328. **Heigo Reima.** Colorectal cancer care and outcomes – evaluation and possibilities for improvement in Estonia. Tartu, 2022, 146 p.
329. **Liisa Kuhi.** A contribution of biomarker collagen type II neoepitope C2C in urine to the diagnosis and prognosis of knee osteoarthritis. Tartu, 2022, 157 p.
330. **Reeli Tamme.** Associations between pubertal hormones and physical activity levels, and subsequent bone mineral characteristics: a longitudinal study of boys aged 12–18. Tartu, 2022, 118 p.
331. **Deniss Sõritsa.** The impact of endometriosis and physical activity on female reproduction. Tartu, 2022, 152 p.
332. **Mohammad Mehedi Hasan.** Characterization of follicular fluid-derived extracellular vesicles and their contribution to periconception environment. Tartu, 2022, 194 p.
333. **Priya Kulkarni.** Osteoarthritis pathogenesis: an immunological passage through synovium-synovial fluid axis. Tartu, 2022, 268 p.

334. **Nigul Ilves.** Brain plasticity and network reorganization in children with perinatal stroke: a functional magnetic resonance imaging study. Tartu, 2022, 169 p.
335. **Marko Murruste.** Short- and long-term outcomes of surgical management of chronic pancreatitis. Tartu, 2022, 180 p.
336. **Marilin Ivask.** Transcriptomic and metabolic changes in the WFS1-deficient mouse model. Tartu, 2022, 158 p.
337. **Jüri Lieberg.** Results of surgical treatment and role of biomarkers in pathogenesis and risk prediction in patients with abdominal aortic aneurysm and peripheral artery disease. Tartu, 2022, 160 p.
338. **Sanna Puusepp.** Comparison of molecular genetics and morphological findings of childhood-onset neuromuscular disorders. Tartu, 2022, 216 p.
339. **Khan Nguyen Viet.** Chemical composition and bioactivity of extracts and constituents isolated from the medicinal plants in Vietnam and their nanotechnology-based delivery systems. Tartu, 2023, 172 p.
340. **Getnet Balcha Midekessa.** Towards understanding the colloidal stability and detection of Extracellular Vesicles. Tartu, 2023, 172 p.
341. **Kristiina Sepp.** Competency-based and person-centred community pharmacy practice – development and implementation in Estonia. Tartu, 2023, 242 p.
342. **Linda Sõber.** Impact of thyroid disease and surgery on patient's quality of voice and swallowing. Tartu, 2023, 114 p.
343. **Anni Lepland.** Precision targeting of tumour-associated macrophages in triple negative breast cancer. Tartu, 2023, 160 p.
344. **Sirje Sammul.** Prevalence and risk factors of arterial hypertension and cardiovascular mortality: 13-year longitudinal study among 35- and 55-year-old adults in Estonia and Sweden. Tartu, 2023, 158 p.
345. **Maarjaliis Paavo**. Short-Wavelength and Near-Infrared Autofluorescence Imaging in Recessive Stargardt Disease, Choroideremia, *PROM1*-Macular Dystrophy and Ocular Albinism. Tartu, 2023, 202 p.
346. **Kaspar Ratnik.** development of predictive multimarker test for preeclampsia in early and late pregnancy. Tartu, 2023, 134 p.
347. **Kärt Simre.** Development of coeliac disease in two populations with different environmental backgrounds. Tartu, 2023, 161 p.
348. **Qurat Ul Ain Reshi.** Characterization of the maternal reproductive tract and spermatozoa communication during periconception period via extracellular vesicles. Tartu, 2023, 182 p.
349. **Stanislav Tjagur.** *Mycoplasma genitalium* and other sexually transmitted infections causing urethritis – their prevalence, impact on male fertility parameters and prostate health. Tartu, 2023, 225 p.
350. **Lagle Lehes.** The first study of voice and resonance related treatment outcomes of Estonian cleft palate children. Tartu, 2023, 126 p.
351. **Liis Ilves.** Metabolomic profiling of chronic inflammatory skin diseases. Tartu, 2023, 146 p.

352. **Marina Šunina**. Flow cytometric analysis of T and B cell properties in healthy donors and subjects with vitiligo. Tartu, 2023, 164 p.
353. **Jaanus Suumann.** Gastric biomarkers and their dynamics as a less invasive method to evaluate stomach health in bariatric surgery patients. Tartu, 2023, 122 p.
354. **Ele Hanson.** Clinical and biochemical markers for the prediction and early diagnosis of pregnancy related complications. Tartu, 2023, 145 p.
355. **Priit Pauklin.** Hemodynamic and biochemical characteristics of patients with atrial fibrillation and anticoagulation of ≥65-year-old patients with atrial fibrillation in Estonia. Tartu, 2023, 144 p.
356. **Triinu Keskpaik.** Quality Indicators and Non-Ischemic Myocardial Injury in Emergency Medicine. Tartu, 2023, 121 p.
357. **Laura Roht.** Hereditary colorectal cancer syndromes in Estonia. Tartu, 2023, 178 p.
358. **Norman Ilves.** Risk factors and onset time of periventricular hemorrhagic infarction in preterm born children and periventricular venous infarction in term born children. Tartu, 2024, 177 p.
359. **Edgar Lipping.** Postoperative antibacterial therapy in complicated appendicitis and appendectomy in pregnancy. Tartu, 2024, 121 p.